Announcing Publication of the Third Edition of
The Chemistry of the Actinide and Transactinide Elements

A team of international experts was invited to co-author the third edition of a classic text, *The Chemistry of the Actinide and Transactinide Elements*. Edited by Lester Morss, Norman Edelstein, and Jean Fuger, the book will be released in early 2006 by Springer Publishers. The five-volume set is critically acclaimed as the most authoritative and comprehensive compilation of the chemical properties of the actinide and transactinide elements to date and is anticipated to be the definitive work on actinides for the next twenty-five years.
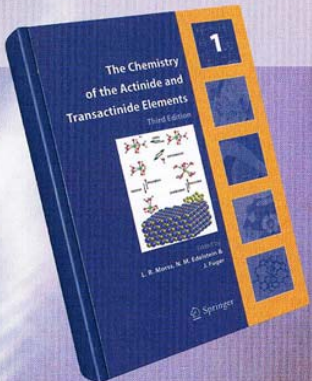
The first edition of *The Chemistry of the Actinide Elements*, edited by Joseph Katz and Glenn Seaborg, was published in 1957 before the discovery of nobelium and lawrencium and the transactinide elements. The second edition of *The Chemistry of the Actinide Elements*, edited by Katz, Seaborg, and Morss, was published in 1986 by Chapman and Hall, London and New York. The third edition, containing thirty-one chapters, will include a contemporary and definitive compilation of the chemical properties of the elements from actinium (atomic number 89) to hassium (atomic number 108). Also included are authoritative review chapters on specialized topics such as thermodynamics, electronic theory, spectroscopy, magnetic properties organoactinide chemistry, coordination chemistry, solution chemistry separations science and technology, environmental science, analysis, and future element predictions. The book editors assembled teams of authors who are active practitioners and recognized experts in their specialty to write each chapter. The editors and authors have endeavored to provide a thorough, balanced, and perceptive treatment of the fascinating elements at the frontier of the Periodic Table.

THE CHEMISTRY OF THE ACTINIDE AND TRANSACTINIDE ELEMENTS

For the complete table of contents and author listing, see the web site at:
http://www.springeronline.com

LA-UR-06-1234

Actinides Research Capabilities at the Lujan Neutron Scattering Center at LANSCE.

A.J. Hurd[*]

[*]Los Alamos National Laboratory, Los Alamos NM 87545 USA

NATIONAL SECURITY AND ACADEMIC RESEARCH

The Lujan Center has a new set of tools for users in neutron scattering and nuclear physics research. These tools further the Center's unique position for performing national security research including actinide science.

Since 2000, four new scattering instruments have been commissioned and three scattering instruments were substantially upgraded. For nuclear physics and nuclear chemistry, two new instruments have been built; these complement the Isotope Production Facility at LANSCE commissioned in 2004. This new suite of tools, along with user-support facilities in chemistry, x-ray scattering, and Raman scattering, plus new sample-environments in extreme pressure, magnetic fields, and temperature, provide the research community a superb environment to address both academic and national security issues.

The ability to perform research requiring special security is a key unique factor at the Lujan Center. Alliances with Theory Division, the Center for Integrated Nanotechnologies (LANL and SNL), the National High Magnetic Field Laboratory (LANL), and the Molecular Foundry (LBNL) expand the possibilities for applying unique tools to the most challenging problems.

Figure 1 The Lujan Center's 11-Tesla superconducting magnet has an internal sample goniometer (±15° about the neutron

Plutonium and other *f*-Element Complexes With 'soft' Donor Ligands

Andrew J. Gaunt, Sean D. Reilly, Alejandro E. Enriquez, Brian L. Scott, Mary P. Neu

*Los Alamos National Laboratory, Los Alamos, NM 87545, USA

There are fundamental unanswered and intensely debated questions in the coordination chemistry of the early actinides (Th-Cm). For example, to what extent and generality is covalent bonding important? What are the limits of 'hard-soft' interactions? And, expressed in a way to illustrate the role of coordination chemistry in industrial processes, do relativistic effects impact f-element coordination chemistry such that bonding differences between An(III) and Ln(III) ions of similar ionic radii,[1] can be exploited to minimize the cost and environmental impact of waste in advanced nuclear fuel cycles? The prevailing thesis is that An(III) complexes display greater covalency than corresponding Ln(III) complexes and this difference in covalency decreases across the actinide series, and is thought to be negligible for actinides beyond Bk. However, systematic studies are needed to understand and support or dispel the thesis. Towards addressing these questions and discerning differences that may be developed into separations processes, we are preparing actinide and Ln(III) complexes with N, S, Se and Te donor ligands. We have prepared trivalent Pu, U, La and Ce complexes with $[N(EPR_2)_2]^-$ ligands (E = S, Se, Te; R = Ph, *i*Pr) allowing systematic variation of the 'softness' of the donor atom in isostructural compounds. Most directly related to the Cyanex agents that have shown great promise for An/Ln separations, low-valent *f*-element complexes with dithiophosphinates and diselenophosphinates have also been prepared. In addition, thiolates and selenolates have been synthesized by oxidation of actinide metal with dichalcogenides.
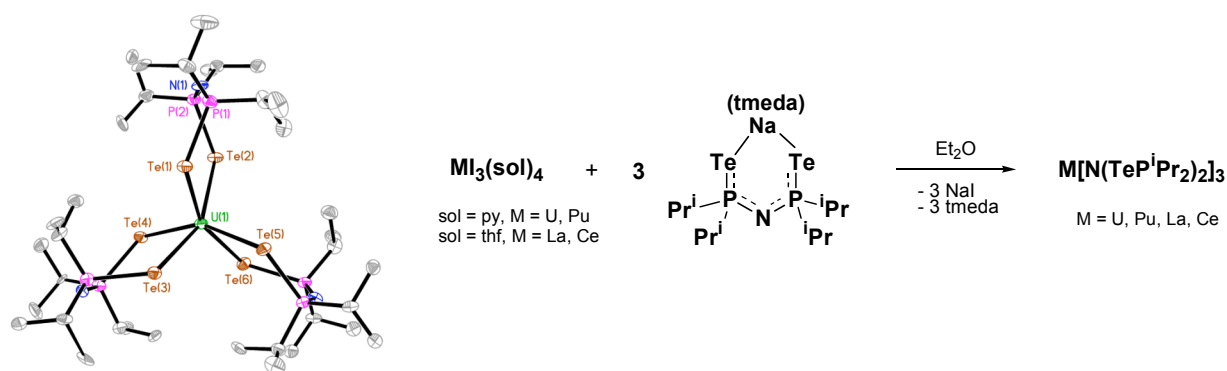
Fig. 1: ORTEP (left) and synthetic scheme (right) of trivalent f-element imidodiphosphinotellurido complexes.

The synthesis, structural analysis by single crystal X-ray diffraction, and traditional spectroscopic characterization (multi-nuclear NMR, IR, UV/vis/nIR) have been completed. From these studies, we find stronger bonding in U(III) 'soft' donor complexes compared to La(III), reflected by shorter U-E than La-E bonds, and that the difference is greater the 'softer' the donor atom. Collaborative studies have been initiated to more directly characterize the bonding in these molecules using X-ray spectroscopy and photoemission methods. Comparable theoretical analyses, using density functional theory, are also in progress.

References:

1   M. P. Jensen and A. H. Bond, J. Am. Chem. Soc. **124(33)**, 9870, (2002).

Structural Studies of Pu(VII) Under Extreme Alkaline Solution Conditions

D. L. Clark*, S. D. Conradson*, P. L. Gordon†, D. W. Keogh†, C. D. Tait†
*Los Alamos National Laboratory, Los Alamos, NM 87545
†present address: Applied Marine Technology, Inc., Virginia Beach, VA 23452

BACKGROUND

Light actinide ions (U, Np, Pu, Am, Cm) in their higher oxidation states (V) and (VI) form a unique series of linear trans dioxo ions (AnO_2^{n+}; n = 1, 2) that pervade the chemistry of these elements in aqueous, nonaqueous and solid-state media. Over the last 60 years, a great deal of effort has gone into study of this inorganic functional group, and to understand its physico-chemical properties. These cations are remarkably stable, showing a high degree of covalency and chemical inertness with respect to the axial An=O bonds that can be traced to the ability to use a combination of valence 5f, and 6d, and semi-core 6p atomic orbitals in chemical bonding.[1] The ability of the $6p_z$ orbital to hybridize with $5f_{z3}$ can lead to unusually strong σ-bonding, and this type of σ-hybridization was shown to be a predominant contributor to the strong covalent bonds in linear hexavalent AnO_2^{2+} ions (An = U, Np, Pu).[2] For transuranium elements, even higher oxidation states are possible. For the heptavalent (VII) state for Np and Pu, it is known that other highly unusual, polyoxo units can form. In general, very little is known about these functional groups in comparison to the linear trans dioxo unit. In alkaline aqueous solutions between 1-10 M NaOH, An(VII) ions form unusual square planar tetra-oxo units of general formula $AnO_4(OH_2)_2^-$, and $AnO_4(OH)_2^{3-}$ that have gained recent attention and study.[3,4] At even higher alkalinity, between 10-18 M NaOH, it is thought that penta- or hexa-oxo units $AnO_5(OH)^{4-}$ and AnO_6^{5-} of unknown structure can form.[5] For plutonium, Tananaev reported that between hydroxide concentrations of 10-17 M, the Pu(VII) ion displays profound changes in the electronic absorption spectra, and the results were interpreted as evidence for the formation of either $PuO_5(OH)^{4-}$ or PuO_6^{5-}.[5] These unusual inorganic ions are exceedingly rare in actinide chemistry, and little is known about their molecular and electronic structure. The present study aims to examine the molecular structure of the Pu(VII) species formed under these extreme alkaline solution conditions.

RESULTS AND DISCUSSION

Heptavalent plutonium solutions are only stable for about 12 hours, making it impossible to prepared them in a radiological laboratory and ship them to a synchrotron facility over 1000 miles away for XAS study. Due to this inherent instability of Pu(VII) solutions, we developed an electrochemical XAFS cell for *in situ* preparation of samples based on the seminal work of Antonio and co-workers,[6] and tested it's utility on Np(VII) under moderate hydroxide conditions. The *in situ* electrochemical cell was made of polyethylene, and consisted of working and counter compartments approximately $25 \times 10 \times 6$ mm, separated by a Nafion membrane. The working compartment held a Pt mesh electrode, a Ag/AgCl reference electrode, a magnetic stir bar, and the sample. The counter compartment contained a Pt mesh electrode with a surface area greater than that of the working electrode and an electrochemical buffer solution consisting of 0.05 M $Na_3Fe(CN)_6$ in 18 M NaOH. The plutonium sample contained 0.008 M Pu(VI) and 18 M NaOH.

The high NaOH concentration was chosen to shift the Pu(VII/VI) couple below that of H_2O oxidation and inhibit O_2 generation in the cell for use at a synchrotron radiation source.

The *in situ* cell was tested using the transformation from Np(VI) to Np(VII) in 3M NaOH. Using XANES spectroscopy at the Np L_{III} edge, we observed the clear transformation of dioxo to tetraoxo forms upon oxidation of Np(VI) to Np(VII), similar to that reported by Williams and coworkers,[3] and shown in Fig. **1a**. We found a rather small 0.4 eV shift in the edge between Np(VI) and Np(VII) hydroxide complexes and a double "white line" peak of the tetraoxo species, as observed previously.[3] These spectral changes were reversible when the electrochemical potential was changed to promote reduction of Np(VII) back to Np(VI). In these experiments the reversible oxidation, concomitant transformation to the tetraoxo geometry, the energy shift, and change in

Figure 1. (a) XANES spectra of a Np solution as a function of electrolysis time, showing the reversible transformation from dioxo Np(VI) to tetraoxo Np(VII). **(b)** XANES spectra showing the reversible transformation of Pu(VI) to Pu(VII) in 18 M NaOH.

the shape of the XANES are all observed in real time (Fig. **1a**), demonstrating the effectiveness of the *in situ* cell. EXAFS analysis of the resulting Np(VII) species produces four Np=O units at 1.88 Å, and two Np-OH units at 2.32 Å consistent with the formulation of $NpO_4(OH)_2^{3-}$ (shown in **1**) as reported previously.[3,4]

1 **2** **3**
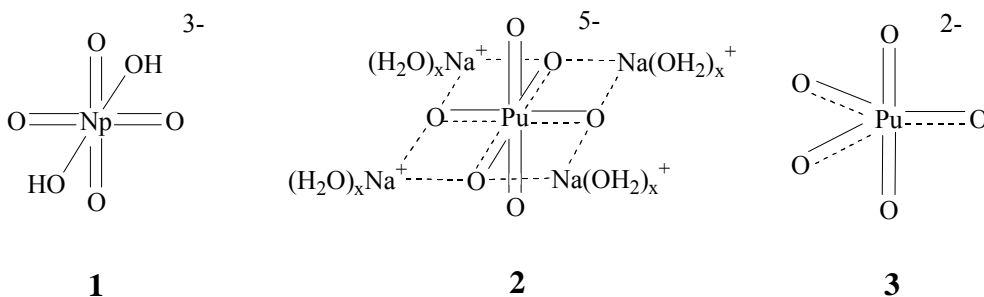
Using the same cell setup, we recorded Pu L_{III} XANES spectra during the oxidation of Pu(VI) to Pu(VII) in highly concentrated 18 M NaOH in search of evidence for either $PuO_5(OH)^{4-}$ or PuO_6^{5-} as shown in Fig. **1b**. A 1.0 eV edge energy shift was observed similar what we found in Np(VII), yet the characteristic double "white line" and first EXAFS oscillation (Fig. **1a**) did not develop as for the Np(VII) series. EXAFS data analysis for the Pu(VII) species under these highly alkaline conditions indicate that the two inner shells of Pu-O bonds are both contracted, in contrast to $NpO_4(OH)_2^{3-}$ (**1**) where both shells lengthened relative to the Np(VI) starting compound. For Pu(VII) under these extreme alkaline conditions, EXAFS analysis reveals two O atoms at 1.83 Å, and 4 O atoms at 2.29Å, thus the ion is clearly not the tetraoxo $PuO_4(OH)_2^{3-}$ ion, consistent with Tananaev's proposal for a species of formulation $PuO_5(OH)^{4-}$ or PuO_6^{5-} under these conditions. In interpreting our data, we recognize that 18M NaOH is

2

essentially NaOH·2H$_2$O, and therefore there is no free water in the "solution". Therefore, even the Na ions must be highly coordinatively unsaturated. We postulate therefore, that under these conditions, a PuO$_5$(OH)$^{4-}$ or PuO$_6^{5-}$ ion is likely to have interactions with Na ions, and we propose the structural motif indicated in **2**. At first the result of a trans dioxo unit seems puzzling, but we note that Straka and coworkers recently reported DFT calculations on the related hypothetical octavalent PuO$_5^{2-}$ ion, and found, remarkably, that the most stable configuration is to convert back to a trigonal bipyramidal trans dioxo form as shown in **3**,[7] with calculated axial and equatorial Pu-O bond lengths of 1.84 and 1.95 Å, respectively. Experimental details and interpretation of data leading to these conclusions will be discussed.

REFERENCES

(1)   Denning, R. G. *Structure and Bonding (Berlin, Germany)* **1992**, *79*, 215-276.

(2)   Denning, R. G.; Green, J. C.; Hutchings, T. E.; Dallera, C.; Tagliaferri, A.; Giarda, K.; Brookes, N. B.; Braicovich, L. *Journal of Chemical Physics* **2002**, *117*, 8008-8020.

(3)   Williams, C. W.; Blaudeau, J. P.; Sullivan, J. C.; Antonio, M. R.; Bursten, B.; Soderholm, L. *J. Am. Chem. Soc.* **2001**, *123*, 4346-4347.

(4)   Bolvin, H.; Wahlgren, U.; Moll, H.; Reich, T.; Geipel, G.; Fanghaenel, T.; Grenthe, I. *Journal of Physical Chemistry A* **2001**, *105*, 11441-11445.

(5)   Tananaev, I. G.; Rozov, S. P.; Mironov, V. S. *Radiokhimiya* **1992**, *34*, 88-92.

(6)   Antonio, M. R.; Soderholm, L.; Williams, C. W.; Blaudeau, J.-P.; Bursten, B. E. *Radiochim. Acta* **2001**, *89*, 17-25.

(7)   Straka, M.; Dyall, K. G.; Pyykko, P. *Theoretical Chemistry Accounts* **2001**, *106*, 393-403.

Quantum Mechanical studies of the Cation Cation interaction.

H.M. Steele, R.J. Taylor and M Sarsfield.

Nexia Solutions, Hinton House, Warrington WA3 5AS

INTRODUCTION

The tendency for pentavalent actinides to form so-called cation cation (CC) complexes is clearly a ubiquitous feature of actinyl chemistry and although first reported by Sullivan[1] in the 1960's their potential role within separation processes is still not fully quantified. There is now substantial evidence, including crystal structures of solid Np(V) compounds, that a CC complex contains at least one actinyl molecule acting as a ligand through its actinyl oxygens to another 'active cation', which can be either another actinyl or other positively charged metals.

Experimentally, the presence of a CC complex is typically characterized by short An-An separations and considerable change in the UV and IR spectra's of the actinyl group. The ability of the CC complex to perturb the IR and UV spectra, the dominance of Np CC complexes with respect to U and Pu actinides, the type of 'bonding' which exists within the CC complex and the roles played by ligands and solvation, are still not fully understood[2]. We have used quantum mechanical (QM) approach to start to address some of these key questions.
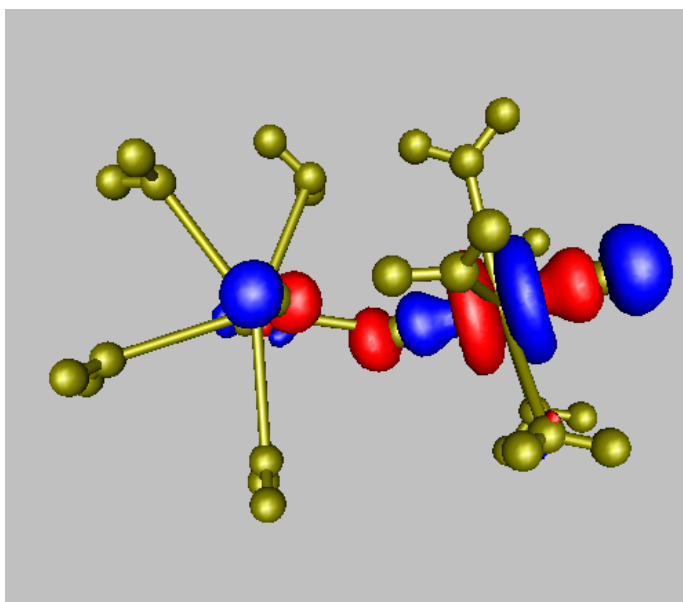
COMPUTATIONAL APPROACH

Initial atomic co-ordinates were taken from experimentally determined crystal structures and optimised.[3,4] The affects of interchanging actinide species in both donator and acceptor sites, altering the actinide oxidation state between V and VI, changing the complexing ligands, adjusting the electronic structure of the actinyl species and changing the dielectric of the solvation were all studied. All calculations were performed using Gaussian '03 employing the Hartree-Fock, Moller-Plesset and Density Functional levels of theory, relativistic pseudopotentials and a range of basis sets were employed.

KEY OBSERVATIONS

By following the orbital occupancy, it was shown that when the actinyl acts as a ligand its symmetry is reduced from $D_{\infty h}$ to C_v. This leads to orbital rearrangement which enables the oxygen on the actinyl donator molecule to carry significantly more electron density than usual for actinyl oxygen atoms, this is shown in the figure above. A much stronger electrostatic interaction can then occur between the donator actinyl oxygen and the cation centre. Further, the strength of the CC interaction is specific to the actinides involved, their oxidation state and whether they occupy the donor or acceptor sites.

From our calculations of the vibrational frequencies we obtained similar values for the asymmetric stretching vibrations to those observed experimentally. It is well known that CC complexation causes shifts in O=An=O vibrational frequencies compared to those normally expected for the actinyl group[2]. However, the calculations also showed that each of these lower energy bands has a higher energy partner. Hence we conclude that this is not a shift in the vibrational frequency as usually suggested but a splitting due to the broken symmetry of the actinyl group.

Finally, the affect of altering the solvent surrounding the CC complex was studied and initial calculations have shown that increasing the solvent dielectric constant decreased the stability of the CC complex.

1   J.C. Sullivan, *et al.,* J. Am. Chem. Soc. **82,** 5288, (1960).
2   N.N. Krot and M.S. Grigoriev Russ. Chem. Rev. **73,** 89, (2004).
3   M.S. Grigoriev, *et al.,* Radiokhimiya **37,** 15, (1995).
4   M.S. Grigoriev, *et al.,* Radiokhimiya **33,** 46, (1991).

Heteropolyanion Ligand Sensitised Uranyl Luminescence

Caytie Talbot-Eckelaers, Simon Pope and Iain May[*]

*Centre for Radiochemistry Research, School of Chemistry,
University of Manchester, Oxford Road, Manchester, M13 9PL, UK

INTRODUCTION

A systematic analysis of the photophysical properties of uranyl containing tri-lacunary heteropolyanions (HPA) is presented. HPA stimulated emission of lanthanide and actinide complexes, is well documented, as is the emissive nature of the uranyl moiety.[1-4] However, no studies to date have explored the photophysics of uranyl complexed HPAs. We report the effects of heteroatom, cluster type, counter-cation, solvent and concentration on the lifetime, intensity, excitation and emission wavelengths observed for these clusters in solution.

Both A- and B-type tri-lacunary heteropolyanion ligands (of general formula $[A-X^m W_9 O_{34}]^{n-}$, X = As^V, P^V, Ge^{IV}, Si^{IV}; n = m −14 or $[B-Y^P W_9 O_{33}]^{q-}$, Y = As^{III}, Bi^{III}, Sb^{III} and Te^{IV}; q = p – 12) are observed to sequester $\{UO_2\}^{2+}$ ions forming 2:2 sandwich clusters in solution and in the solid state.[5-8] Complexes with A-type ligands, such as the $[(UO_2)_2 Na_2(A-PW_9 O_{34})_2]^{12-}$ anion form closed-type structures containing encapsulated Na^+ ions (Fig. 1).[5] B-type ligands are unable to form this type of complex due to the presence of a lone-pair of electrons located on the heteroatom and form an open-type structure such as observed in $[(UO_2)_2(H_2O)_2(B-SbW_9 O_{33})_2]^{16-}$ (Fig.2).[8]
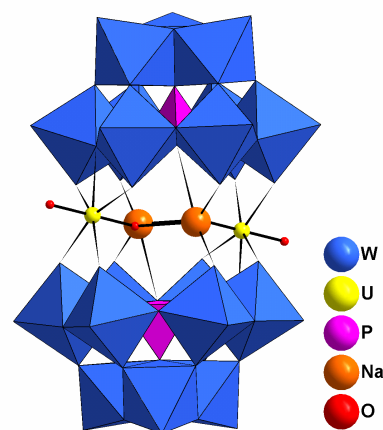
Fig. 1: Polyhedral representation of the $[(UO_2)_2 Na_2(A-PW_9 O_{34})_2]^{12-}$ anion
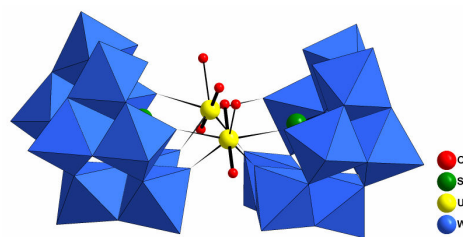
Fig. 2: Polyhedral representation of the $[(UO_2)_2(H_2O)_2(B-SbW_9 O_{33})_2]^{16-}$ anion

RESULTS

Emission from tri-lacunary heteropolyoxotungstate uranyl complexes is observed between 500 and 600 nm, the typical region for uranyl complexes (Fig. 3). The corresponding excitation wavelengths show two bands, at ~350 nm and ~ 440 nm. The former relates to the O→W LMCT and the latter to the O→U LMCT in the absorption spectra. Variation in heteroatom, for a given complex type, leads to subtle differences in excitation frequency. Luminescence life-times

(ranging from 0.05 ms to 0.5 ms) and degree of vibronic fine structure are similarly determined by choice of heteroatom and ionic strength of the solution.
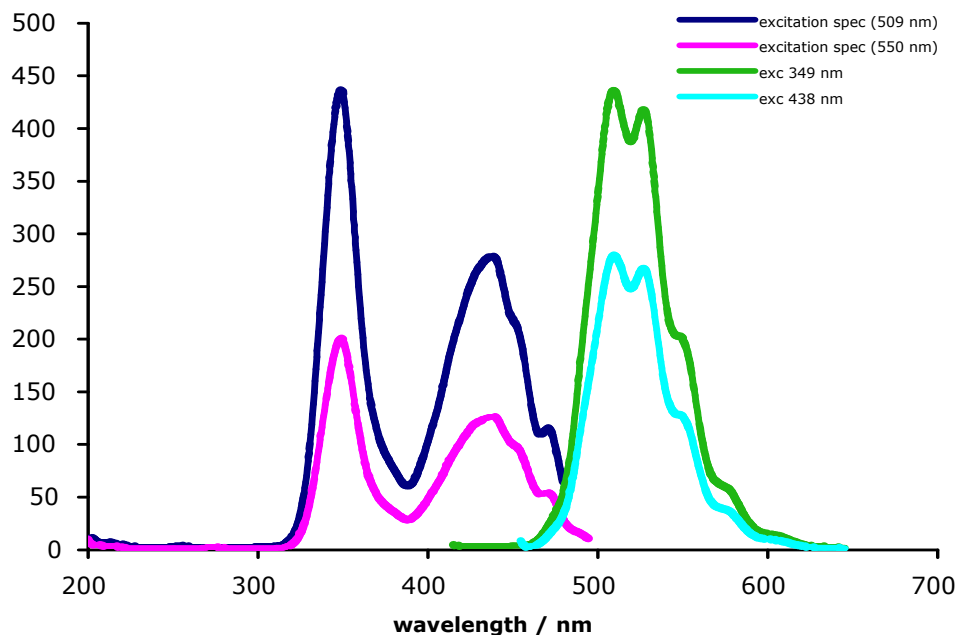
Fig. 3: Excitation and emission spectra of the $[(UO_2)_2Na_2(A\text{-}PW_9O_{34})_2]^{12-}$ anion in 1M NaCl

References

1 T. Yamase, H. Naruke, and Y. Sasaki, *J. Chem. Soc., Dalton Trans*, (1990), 1687.

2 A. B. Yusov and V.P. Shilov, *Radiochemistry*, **41**, (1999), 3.

3 S. Lis and S. But, *J. Alloys and Compounds*, **300-301**, (2000), 370.

4 S. Lis, S. But, R. Van Deun, T. N. Parac-Vogt, C. Görller-Walrand, K. Binnemans*, Spectrochimica Acta Part A,* **62**, (2005), 478.

5 K. C. Kim and M. T. Pope, *J. Am. Chem. Soc.,* **121**, (1999), 8512.

6 K. C. Kim, A. J. Gaunt and M. T. Pope, *J. Cluster. Sci.,* **13**, (2002), 423.

7 A. J. Gaunt, I. May, R. Copping, A. I. Bhatt, D. Collison, O. D. Fox, T. Holman and M. T. Pope, *Dalton Trans*, (2003), 3009.

8 Roy Copping, PhD thesis, University of Manchester, 2006

Uranium complexes with newly designed tetraketones
for active materials of redox flow battery

K. Shirasaki, T. Yamamura, S. Ohta, Y. Shiokawa

Institute for Materials Research, Tohoku University, Sendai, Miyagi 980-8577, Japan

The light actinide such as uranium and neptunium are known to show two couples of reversible or quasi-reversible electrode reactions as seen in Np(III)/Np(IV) and Np(V)/Np(VI) [1]. By utilizing these two couples of fast reactions suppressing the overvoltage at electrodes, a redox-flow battery using the light actinide as an active material with the high efficiency has been proposed [2]. Though redox flow batteries befit the battery for the electric power storage, the energy efficiency of the existing battery with vanadium ions for positive and negative electrolytes is rather high [3]. However, because of the slow kinetics especially for the positive reaction (VO^{2+}/VO_2^+), the large reaction overvoltage lowers the energy efficiency.

Active materials of the uranium battery require several conditions to be satisfied for the high-energy efficiency. At the first, the materials for both positive and negative electrolytes should dissolve in an aprotic solution at a high concentration, in order to avoid the disproportionation reaction of U(V) from degrading to U(IV) and U(VI) in the presence of the proton [4, 5]. Since uranium β-diketone complexes show relatively high solubility in the aprotic solution, they have been investigated for the active material [6]. Recently, we reported that a quantitative electrolysis of the dimethyl sulfoxide (DMSO) solution of U(VI) to give the U(V) solution which was r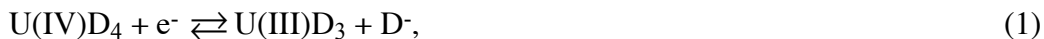elatively stable as the half-life of 2 days at 16ºC [7, 8]. In the course of the electrochemical investigation of U(VI) and U(IV) β-diketones, both complexes were found to display the ligand dissociation and association reactions during the electrode reactions as

$$U(IV)D_4 + e^- \rightleftarrows U(III)D_3 + D^-, \tag{1}$$
$$U(VI)O_2D_2 + e^- \rightleftarrows U(V)O_2D + D^-, \tag{2}$$

where D- denotes the β-diketone ligands. These side reactions would be originated from the instability of U(V) and U(III) complexes compared with U(IV) and U(VI) complexes, respectively, and this consideration agrees with the general tendency of the stability of uranium complexes; U(IV) > U(VI) > U(III) > U(V). With an aim in the development of the high-energy efficiency battery, these side reactions are not desired because of the rearrangement makes the kinetics slower and also the change in the redox potential results in the energy loss [6]. The simple redox reaction without these side reactions would be realized by stabilizing the U(V) and U(III) complexes by using long-chained or macrocyclic ligands, which utilizes the entropy effect as can be seen in crown ethers capable of complexation even with alkaline metal ions. Previous study, two tetraketones with two units of acetylacetone ligand in their molecule,

8-oxo-2,4,12,14-teraoxapentadecane (**1**; keto-form in Fig. 1) and *m*-bis(2,4-dioxo-1-pentyl)benzene (**2**; keto-form in Fig. 1) were synthesized [9]. Detailed NMR measurements were conducted to reveal the keto-enol tautomerism of the tetraketones in CDCl$_3$ and titration measurements were carried out in water-dioxane (1:1 (v/v)) solutions to evaluate formation constants with metal ions at III-VI valences. Although the first acid dissociation constants for **1** and **2** were close to that for the acetylacetone, the formation constants of them at large coordination numbers are larger than those of acetylacetone. On the basis of these formation constants, the thermodynamic distributions of tetraketone complexes are evaluated in the solution to
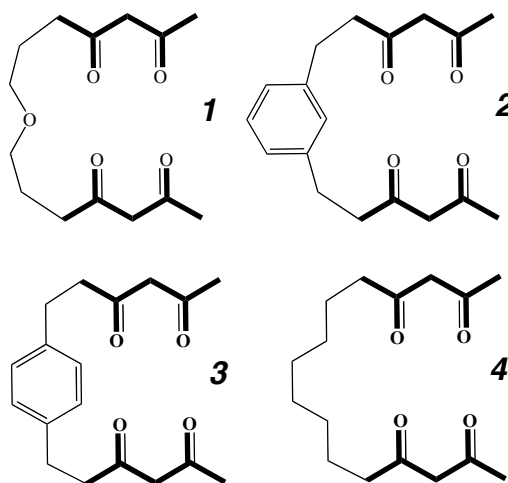
Fig 1: Tetraketone ligands prepared according to A.H. Alberts and D.J. Cram (**1**, **2**) and newly designed (**3**, **4**)

demonstrate that the change in the coordination number is not expected during the redox reactions contrary to the case of the acetylacetone. Recently, we observed dimer formation with uranyl(VI) was observed for **2** in single crystal x-ray crystallography. This could mean that cavity radius of these ligands (1 and 2) is larger than ionic radius of uranium and it is not desirable for active materials of the battery.

In the present study, new tetraketones, *m*-bis(3,5-dioxohexyl)benzene (**3**; keto-form in Fig. 1) and 1,6-bis(2,4-dioxo-1-hexyl)hexane (**4**; keto-form in Fig. 1), which is expected to form monomer complex with uranium, were synthesized. Uranium(V) and uranium(IIII) complexes with these new tetraketones were characterized by electrode reaction and also by electrolytic reduction.

[1]   T. Yamamura, N. Watanabe, T. Yano, Y. Shiokawa, J. Electrochem. Soc., 152 (2005) A830.
[2]   Y. Shiokawa, H. Yamana, H. Moriyama, J. Nucl. Sci. Tech., 37 (2000) 253.
[3]   M. Skyllas-Kazacos, M. Rychcik, R.G. Robins, A.G. Fane, M.A. Green, J. Electrochem. Soc., 133 (1986) 1057.
[4]   G. Gritzner, J. Selbin, J. Inorg. Nucl. Chem., 30 (1968) 1799.
[5]   A. Ekstrom, Inorg. Chem., 13 (1974) 2237.
[6]   T. Yamamura, Y. Shiokawa, H. Yamana, H. Moriyama, Electrochim. Acta, 48 (2002) 43.
[7]   K. Shirasaki, T. Yamamura, Y. Shiokawa, J. Alloys Compds., 408-412C (2006) 1296.
[8]   K. Shirasaki, T. Yamamura, Y. Monden, Y. Shiokawa, Royal Soc. Chem., (in press).
[9]   A.H. Alberts, D.J. Cram, J. Am. Chem. Soc., 99 (1977) 3880.

Studies of Gluconate Complexation with U(VI) and Np(V)

In Acidic to Neutral Solutions

Z. Zhang,[a,b] S. B. Clark,[a] G. Tian,[b] L. Rao[b]

a. Washington State University, Pullman, WA 99164
b. Lawrence Berkeley National Lab, Berkeley, CA 94720

INTRODUCTION

The complexation of actinide cations by gluconate is of interest due to their existence in the Hanford high-level radioactive waste tanks. Gluconic acid, a polyhydroxycarboxylic ligand, has strong complexation ability with metal cations.[1] To develop effective treatment strategies for high-level radioactive wastes, the interaction of gluconate with actinides must be understood.

While this ligand has been investigated for many years, the majority of the studies have been focused on systems involving transition metals, with very few reports relating to complexation with lanthanides and actinides.[2,3] Furthermore, molecular-level interactions between actinide cations and gluconate are not well defined. In this work, multiple techniques have been used to study the complexation of gluconate with U(VI) and Np(V) as dioxo cations, e.g. $Np^VO_2^+$ and $U^{VI}O_2^{2+}$ in acidic to neutral solutions. The uranyl and neptunyl cations serve as analogs for the $Pu^VO_2^+$ and $Pu^{VI}O_2^{2+}$ cations, respectively.

$$^1COOH$$
$$^2HCOH$$
$$^3HOCH$$
$$^4HCOH$$
$$^5HCOH$$
$$^6H_2COH$$

Gluconic acid
(HGH_4)
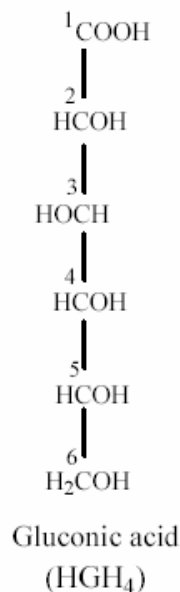
COMPLEXATION WITH NEPTUNYL

The thermodynamic parameters of gluconate complexation with NpO_2^+ have been measured by spectrophotometric titrations and calorimetry under the conditions: t = 25 °C, I = 1.0 M and $pH{\sim}6.0$.[4] As indicated in Figure 1 (next page), near-IR data collected during titrations of the Np(V) cation with gluconate yield two species, NpO_2GH_4 and $NpO_2(GH_4)_2^-$. The formation constants and enthalpies of complexation are: log β_1 = (1.48 ± 0.03) and ΔH_1 = -(7.42 ± 0.13) kJ·mol^{-1} for $NpO_2(GH_4)$, log β_2 = (2.14 ± 0.09) and ΔH_2 = -(12.08 ± 0.45) kJ·mol^{-1} for $NpO_2(GH_4)_2^-$. Comparison of those parameters to the thermodynamic data for complexation of NpO_2^+ with other carboxylic ligands, it is observed that gluconic acid, like α-hydroxycarboxylic acids, forms stronger complexes than simple monocarboxylic acids. It is therefore suggested that α-hydroxyl group of the gluconate probably participates in coordination to the NpO_2^+ cation. Analysis of extended x-ray absorption fine structure (EXAFS) state also supports this observation.

COMPLEXATION WITH URANYL

For the uranyl-gluconate system, we have used potentiometry and calorimetry to measure the thermodynamic properties under the conditions: t = 25 °C, I = 1.0 M and pH 2.0 – 3.5. In this case, ^{13}C NMR was employed to determine coordination sites for the uranyl cation to the gluconate ligand (Figure 2). With addition of uranyl into gluconate solutions, significant line

broadening of the peaks corresponding to the first (data not shown) and second carbons of the gluconate indicates that both the carboxylic group and α-hydroxyl group most probably take part in complexation. In combination with the structural information obtained by ^{13}C NMR, the structural characteristics of those complexes has been analyzed by EXAFS.

SUMMARY

In this presentation, our results will be described and discussed in terms of the impact of effective cationic charge on the metal cation and steric effects for the ligand and the dioxo cations. Comparison to other systems of similar ligands will also be made.
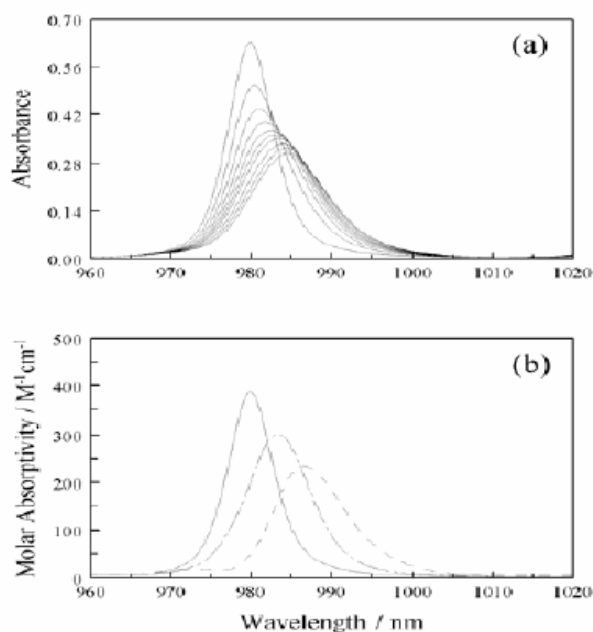
Fig 1: Spectrophotometric titration of Neptunyl – gluconate. $t = 25°C$, $I = 1.0$ M, pH~6.0. (a) Raw spectra for one titration. (b) Resolved molar abs spectra of Np(V) species: NpO_2^+ (solid line), $NpO_2GH_4(aq)$ (dotted-dash), $NpO_2(GH_4)_2^-$ (dash)
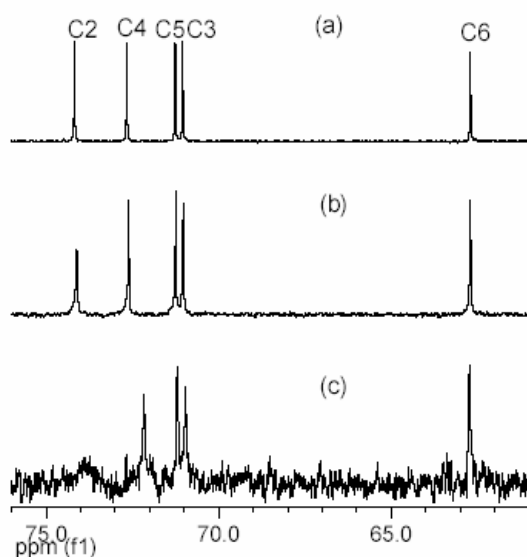
Fig 2: ^{13}C NMR of uranyl – gluconate. $t = 22$ °C, $[NaGH_4]_0 = 25$ mM. (a) U/NaGH$_4$ = 0/25, $pH = 6.0$; (b) U/NaGH$_4$ = 1/25, pH = 4.0; (c)U/NaGH$_4$ = 8/25, $pH = 3.2$.

1. D. T. Sawyer, Chem. Rev. **64**, 633 (1964)
2. S. Giroux, P. Rubini, B. Henry, S. Aury, Polyhedron, **19**, 1567 (2000).
3. D. T. Sawyer, R. J.Kula, Inorg. Chem. **1**, 303 (1962).
4. Z. Zhang, et al., accepted in: Radiochim. Acta, (2005).

ENVIRONMENTAL CONSIDERATIONS IN THE WEST SINAI AND ROSSETTA BEACH ON THE MEDITERRANEAN

Dr.ASHRAF EL SAYED MOHAMED MOHAMED

ENS/IMANUF/GNS.

SOUF SHAMAA-TALON-STREET#1-HOUSE#28-ALEXANDRIA,21351-EGYPT.

amohamed@loftmail.com

amohamed@hushmail.com

ABSTRACT

THE NUCLEAR MATERIALS AUTHORITY IS TAKING OVER THE RESPONSIBILITY FOR EXPLOITATION OF
THE BLACK SAND DEPOSITS AT THE ROSSETTA BEACH ON THE MEDITERRANEAN COAST AND AT THE
WEST SINAI AREA WHERE THE REMAINING PROSPECTING DRILL HOLES OFFER SUITABLE SITES FOR HYDROGEOLOGICAL AND GEOCHEMICAL STUDIES.THESE DEPOSITS CONTAIN MONAZITE,ZIRCON AND RUTILE AS WELL AS ILMENITE AND MAGNETITE.A RESEARCH PROGRAMME ON RADIONUCLIDE TRANSPORT ANALOGY CONTINUES IN THE SURROUNDINGS OF THE ROSSETTA AND WEST SINAI DEPOSIT. IN THIS PAPER WE DETERMINE AND STUDY THE PROCEDURES THAT UNDERTAKE AT THE SITES.ALSO,WE ,AS INDEPENDANT SPECIALISTS,WILL DESCRIBE THE GOVERNMANTAL POLICY OF THE
NUCLEAR WASTE AND OUR FEARS.

Plutonium Uptake by Brucite and Periclase

J. D. Farr[*], M. P. Neu*, Roland K. Schulze and B. D. Honeyman[†]

*Los Alamos National Laboratory, Los Alamos, NM 87545 USA
†Colorado School of Mines, Golden, CO 80401 USA

Batch adsorption experiments and spectroscopic investigations consistently show that aqueous Pu(IV) is quickly removed from solution and becomes incorporated in a brucite or hydroxylated MgO surface to a depth of at least 50 nm, primarily as Pu(IV) within a pH range of 8.5 to 12.5. This *ab*sorption behavior is unaffected by the presence of the organic ligand, citrate.[1]

Further studies on colloidal brucite, natural crystalline brucite and MgO crystals that were exposed for longer times (70 hours) to solutions containing Pu(IV) confirmed the presence of subsurface Pu and demonstrated a continuation of the Pu uptake behavior previously observed. X-ray photoelectron spectroscopy (XPS), x-ray absorption fine structure (XAFS), Rutherford backscattering spectroscopy (RBS) and x-ray diffraction (XRD) were used to estimate Pu penetration depth and provide information about its chemical state.

Fig. 1. XPS spectra for Pu 4f and O 1s regions of the MgO and brucite crystals that were exposed to 1 x 10^{-5} M Pu(IV) for 70 hours. Pu intensities are less than those seen for crystals exposed for only 7 hours, but alpha activity is much greater, indicating more subsurface Pu oxides and hydroxides.

Periclase (MgO) and brucite (Mg(OH)$_2$ are not commonly used as substrates in batch adsorption experiments because they dissolve readily and are highly basic. A large body of research involving metal adsorption from solution has been performed on less soluble oxides such as silica or hematite. At first, it was not clear to us how plutonium could be removed from solution by a substrate that so rapidly dissolves. Another mystery was how Pu got so deep in the crystal so rapidly. The 50 nm penetration depth of Pu in such a short time precludes solid state diffusion as a mechanism.

The initial adsorption of Pu(IV) is expected to occur rapidly due the easy availability of sorption sites on the hydroxylated MgO and brucite surfaces. In most systems, sorption of cations will commence at the pH of initial hydrolysis. The first hydrolysis constant for Pu+4 is 0.6[2], so hydrolysis and adsorption occur below pH 1. Under the solution conditions of these experiments, Pu will exist primarily as the neutral tetra hydroxide.[2]   The MgO and brucite

Fig. 2. Rutherford backscattering spectroscopy. Pu was detected 60 – 100 nm below the surface of the hydroxylated MgO(100) crystal. The sample holder is the source of the Fe signal.

surfaces will be hydroxylated and have a hydration layer that extends from the solid into the solution. MgO dissolution is believed to occur by first converting to brucite[3, 4]. A flocculent, gel-like adherent film was observed on MgO crystals that were exposed to water for several months at a time. The observed film is assumed to be composed of disordered and extended polynuclear Mg oxide and hydroxide moieties and water, much like a gel. This film was not observed on MgO crystals that were exposed to water for shorter periods, or even the crystals that were exposed for 70 hours, but it was likely still forming and had not yet become visible. After dehydration, the hydroxylated surface layer is at least 50 Å thick on the MgO crystals exposed to water for 7 hours, according to the XPS and RBS data. The thickness of the hydroxylated layers on crystals exposed for longer periods is expected to be greater.

Pu(IV) will diffuse through the gel-like layer and may become incorporated in the active crystal surface. Pu hydroxides are much less soluble than Mg hydroxides so remain with the solid. Upon dehydration the gel-like layer re-solidifies with the incorporated Pu.

The research presented here strengthens the technical basis for our stewardship of actinide materials, particularly Pu oxide or materials contaminated with Pu. These investigations directly support TRU waste disposal practices at the WIPP and enhance our ability to predict Pu behaviour in other environmental settings. Pu ions adsorbed from water on brucite and hydroxylated MgO form compounds on the surface that share many of the same spectral features that have been observed on water-exposed Pu oxide [5], suggesting that Pu adsorbed on mineral surfaces will behave similarly.

1.   Farr, J.D., R.K. Schulze, and B.D. Honeyman, Radiochimica Acta, 2000. **88**(9-11): p. 675-679.
2.   Runde, W., et al.,. Applied Geochemistry, 2002. **17**(6): p. 837-853.
3.   Wogelius, R.A., et al.,. Geochimica et Cosmochimica Acta, 1995. **59**(9): p. 1875-1881.
4.   Jordan, G., S. Higgins, and C. Eggleston,. American Mineralogist, 1999. **84**(1-2): p. 144-151.
5.   Farr, J.D., R.K. Schulze, and M.P. Neu,. Journal of Nuclear Materials, 2004. **328**(2-3): p. pp. 124-136

Actinide Interactions with Iron Oxide/Oxyhydroxide

S. A. Stout, E. Bauer, S.D. Reilly, P. Lichtner, J. D. Farr, and M. P. Neu

Los Alamos National Laboratory, Los Alamos, NM 87544

INTRODUCTION

Actinides (An) are commonly found as contaminants at sites performing nuclear material production, processing, and storage. The fate and transport of these radionuclides is largely controlled by interactions occurring at the solid-solution interface of vadose zone minerals. Thermodynamic adsorption data is needed to accurately model behavior and to produce reliable risk assessments. Adsorption experiments were conducted to determine the affect of pH (2 –10) and concentration (10^{-6}-10^{-4} M An) on the adsorption of U(VI), Np(V), and Pu(VI) onto hematite (Fe_2O_3) and goethite (FeOOH). Spectroscopic data show that Pu(VI) was reduced in solution to Pu(V) by goethite, while no reduction of Np(V) was observed.

RESULTS

Hematite and goethite have very similar binding sites and points of zero charge (PZC); therefore, it is not unexpected that the actinide adsorption isotherms for a given actinide have very similar pH-dependence and edge positions. Although the surface areas of the mineral suspensions were normalized, the adsorption edges for like actinides were not identical. The adsorption edges for actinides reacted with goethite occurred at slightly lower pH than those reacted with hematite under similar concentrations. Figure 1 shows the pH-dependent adsorption isotherm for U(VI) adsorption onto the iron minerals after a 24 h reaction time. Decreasing the initial concentration of actinide reacted with the mineral phases also decreased the pH where the adsorption edge occurred. Figure 2a shows the adsorption of U(VI), Np(V), and Pu(VI) onto goethite. The shape and position of the Pu adsorption edge was more similar to that of the Np(V) than to U(VI) suggesting that the Pu was bound as Pu(V).

Figure 1. pH-dependent adsorption of U(VI) onto Fe_2O_3 and FeOOH. $[U(VI)]_{initial} = 10^{-6}$ M.
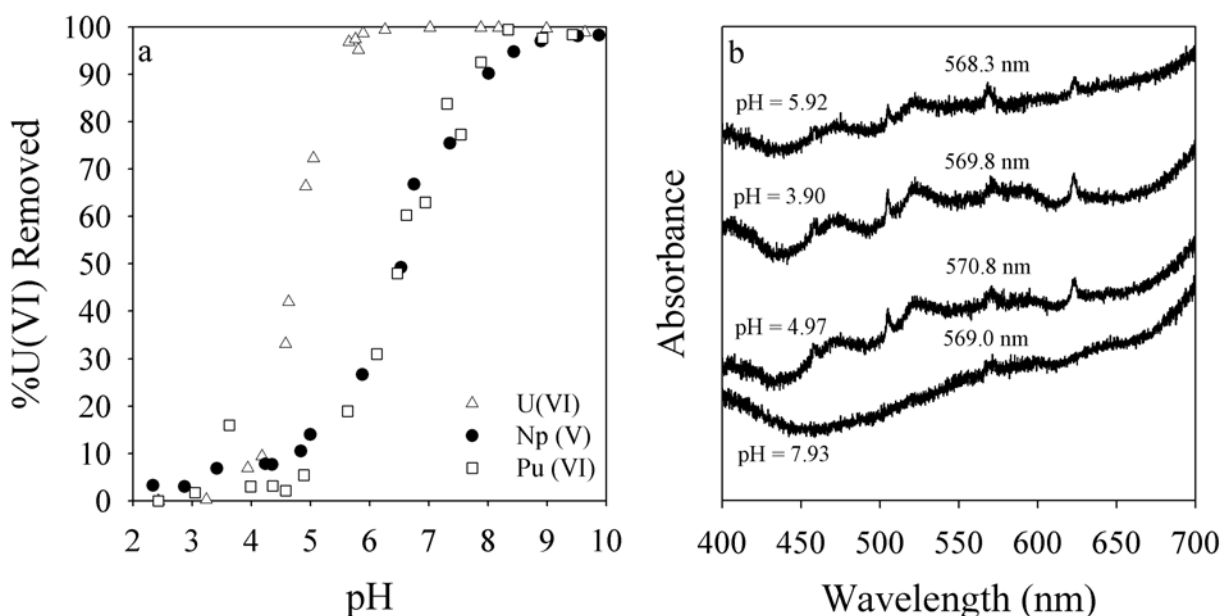
Figure 2. a.) pH dependent adsorption of U(VI), Np(V), and Pu(VI) onto FeOOH. $[An]_{initial}$ $= 10^{-5}$ M. b.) UV/Vis spectra of Pu(VI) solution in contact with FeOOH. $[Pu(VI)]_{initial} = 10^{-4}$ M and time = 24 h.

To test this hypothesis, Pu(VI) (initially 10^{-4} M) was reacted with goethite for 24 hr. The solution phase contained Pu(V) as was evident by the presence of a characteristic Pu(V) adsorption band at $\sim$ 569 nm indicating that Pu(VI) was reduced in solution by the FeOOH; however, no Pu(IV) absorption bands were observed (Figure 2b). These results contrast those observed previously when studying Pu(V) interactions with δ-MnO$_2$. In the presence of δ-MnO$_2$, Pu(V) was completely oxidized to Pu(VI) and bound to the manganese oxide as a Pu(VI) inner-sphere surface complex. The goethite solids were filtered from the reaction solutions, washed, and air-dried for $\sim$ 1 month in a glovebox prior to analysis with x-ray photoelectron spectroscopy (XPS). The XPS results indicted that at near neutral pH Pu was bound to the mineral surface primarily as Pu(IV) with a small percentage of Pu(V) also present. These experiments were conducted under CO$_2$ free conditions and even at high pH no carbonate species were detected by XPS. As expected, under similar experimental conditions no reduction of Np(V) was observed in solution by UV-Vis or on the goethite solid by XPS.

DISCUSSION

The oxidation states of U(VI) and Np(V) are stable under our experimental parameters, and we are attempting to fit this data using hexavalent and pentavalent surface complexes, respectively. These fits will then be compared to those for Pu(VI). Initial surface complexation modeling efforts for Pu(VI) interaction with hematite required the use of both Pu(VI) and Pu(IV) surface complexes to accurately fit our experimental data. These predictive geochemical models will enhance our ability to produce more accurate risk assessments and support the use of monitored natural attenuation.

Speciation of Plutonium in Aqueous Systems

N. L. Banik[*], R. A. Buda[*], S. Bürger[**], J. V. Kratz[*], N. Trautmann[*]

* Institut für Kernchemie, Johannes Gutenberg-Universität, D-55099 Mainz, Germany
** Chemical & Isotope Mass Spectrometry Group, Oak Ridge National Laboratory, Oak Ridge, TN 37831, USA

To assist the safety assessment of high-level nuclear waste repositories, a profound knowledge about the speciation of plutonium in aqueous systems is necessary. The knowledge of physical and chemical processes responsible for the behavior of plutonium in a geogenic system enables to predict the migration of plutonium and thus advances the long term safety assessments of nuclear waste repositories or facilitates the development of new remediation strategies for contaminated sites.

Capillary electrophoresis (CE) coupled online to ICP-MS has been developed as a method for the speciation of plutonium oxidation states [1]. The detection limit is 20 ppb (10^{-12} – 10^{-13} g) for one oxidation state. To improve the sensitivity further, the coupling of CE to resonance ionization mass spectrometry (RIMS) has been explored. The detection limit of RIMS [2] enables to decrease the concentration of plutonium by 2 to 3 orders of magnitude compared to the CE-ICP-MS. Thus, the speciation of the oxidation states of plutonium at ultra trace levels of 10^{-9} to 10^{-10} mol/L appears to be possible [3].

For the speciation of plutonium in aqueous systems, the (I) redox kinetics, (II) complexation, and (III) sorption behavior of plutonium under environmental conditions have to be studied.

(I) Redox kinetics: Ubiquitous humic substances (HS) play an essential role in the migration of plutonium due to their complexation and reducing abilities. The redox speciation of plutonium in contact with HS has been investigated by CE-ICP-MS. A reduction of Pu(VI) by Aldrich humic acid (HA) and Gorleben fulvic acid (FA) to Pu(IV) and Pu(III) occurs within a couple of days or weeks, a short time on the scale of nuclear waste disposal in a deep geological formation. Therefore, the speciation of trivalent and tetravalent plutonium in aqueous solution was mainly studied. The reduction of Pu(VI) with FA shows an approximately linear behavior (in half-logarithmic scaling) and a significant dependence on the pH value, similar to the behavior of HA. The enhanced reduction of Pu(VI) by increasing the pH may be explained by the increased fraction of dissociated groups of the HA [4].

(II) Compexation: The time dependence of the plutonium(IV) complexation with Aldrich humic acid has been investigated and the complex formation constants ($\log\beta_{LC}$) of Pu(III) and Pu(IV) at different pH values have been determined using the ultrafiltration method. Different concentrations of plutonium (10^{-6} to 10^{-8} M) and Aldrich humic acid (0.01 to 25 mg/l) were applied.

(III) Sorption: The sorption of trivalent and tetravalent Pu on kaolinite has been studied as a function of pH. The sorption studies were performed by batch experiments under aerobic and anaerobic conditions. A pH range of 0 - 12 was examined with Pu(III) and Pu(IV) concentrations of 10^{-7} - 10^{-9} M and a solid phase concentration of 4 g/L kaolinite. Plutonium carbonate complexes are the dominant species in aqueous solution in the presence of CO_2 at higher pH for both tri- and tetravalent Pu. A similar sorption behaviour can also be reported for the trivalent americium and the tetravalent thorium. The desorption of Pu(IV) from kaolinite is only 1 - 10% for the studied pH range.

The obtained results will be briefly discussed.

References
[1] B. Kuczewski, et al., Analytical Chemistry **75**, 6769-6774 (2003).
[2] C. Grüning, et al., International Journal of Mass Spectrometry **235**, 171-178 (2004).
[3] S. Bürger, et al., Radiochimica Acta, submitted (2005).
[4] T. Jianxin, et al., Radiochimica Acta **61**, 73-75 (1993).

Speciation of actinides in contaminated groundwaters from Russian nuclear waste repository sites

A. Novikov[*], S. Kalmykov[†], B. Myasoedov[*], W. Halsey[‡]

*Vernadsky Institute of Geochemistry and Analytical Chemistry, Moscow, Russia,
†Lomonosov Moscow State University, Moscow, Russia,
‡Lawrence Livermore National Laboratory, USA.

The study on environmental behavior of the actinides (U, Np, Pu and Am) at contaminated sites of Russia has been the major task of this work. It includes the study on speciation, transport properties and processes in both sites of deep underground disposals and near surface aquatic ecosystems.

Several sites exist in Russia to study actinide behavior in the environment including:

- Deep borehole injection of liquid radioactive wastes near Tomsk (SCC) and Krasnoyarsk.
- Near surface groundwater, soil, lake and river sediments contamination at the territory of PA "Mayak".

The field studies include sampling of groundwater from the contaminated area and outside it with aquifer and outside this with *in-situ* measurement of groundwater hydrogeochemical characteristics. The multi-channel hydrogeochemical probe was used for this purpose. The sampling was performed by the pumping of the aqueous samples with electrical pump. The pumping rate was 2-2,5 m^3/hour. The glass bottles were used for sampling previously purified by blowing of nitrogen with 1% carbon dioxide. The samples were placed to the bottles in nitrogen atmosphere avoiding contact with air. The same method was used for collecting the sub-samples after the micro- and ultrafiltration in the laboratory.

It was established that at Mayak site U and Np are presented as U(VI) and Np(V). Plutonium behaves as if it is a mixture of Pu(IV) and Pu(V). Despite highly oxic conditions near Karachay Lake Pu in hexavalent form was not found. The presence of Pu(V) in groundwater samples should be considered as one of the main mechanisms of migration however the share of pentavalent Pu is not high since mostly this element is bound to solid phases including Fe-, Mn-oxides and clays. For surface waters of some industrial reservoirs the share of Pu(V) is 50-80% from the total concentration of true soluble species, however 99,9% of this element is bound to bottom sediments and is presented in tetravalent form[1].

For SCC contaminated groundwaters the main fraction of actinide including uranium are presented in low oxidation states. However despite the anoxic conditions in uncontaminated waters (well A-15) the natural U is presented as U(VI). Therefore it is possible that either U is present in tetravalent form in waste effluents that were injected or it is reduced upon interaction with surrounding geologic media. The following facts should be taken into consideration:

- The concentration of complexing substances is significant in waste solutions that possibly can shift the equilibrium between different redox forms.
- Nitrite ions are formed due to radiolysis in the injection well[2].
- The high sorption affinity of actinides in low oxidation states towards colloids can alter the initial redox equilibrium.

Therefore the reduction of actinides in water proof horizon is possible. This is also supported by the fact that the share of U(IV) and Np(IV) in groundwater samples from SCC is proportional to the total U concentration.

For groundwater samples from Mayak site actinides are bound to relatively small colloid particles (5-10 nm) and filtrate fraction. The mass fraction of actinides bound to colloids decrease in the following sequence: $Pu > Zr \geq Am \geq Eu >> Np > U$. The share of U and Pu bound to colloidal matter increase upon dilution of waste effluents with preferential association of U with small particles (filtered by 3-10 kDa ultrafilter) and Pu with larger particles of 10 kDa and more. It is probably that U forms true hydroxo-colloids upon shifting of equilibrium between carbonate complexes and hydrolyzed complexes. In case of Pu it is sorbed on the clay particles with formation of pseudo-colloids.

In case of SCC U and other actinides are found to be bound to relatively large colloid particles. In the first case U is in hexavalent form and is not bound to colloids. In contrast to Mayak site the groundwater samples from SCC the following sequence of inclusion of radionuclides to colloid particles is observed: $U > Np > Pu \geq Am \geq Zr \geq Zn \geq Eu$.

The manner of actinide inclusion to colloid particles for Mayak site is reasonable taking into account the results of redox speciation. For SCC groundwater samples one would expect another manner of actinide distribution. However since they are represented in low oxidation states (IV or III for TPU), this sequence is governed by their total concentration that changes in the following sequence: $U >> Np >> Pu > Am$.

The elemental distribution on the surface of colloid particles were studied using secondary ion mass spectrometry with nanometer scale resolution (nanoSIMS-50, Cameca, France).

<u>Sample from Mayak.</u> According to the high-resolution TEM measurements performed as well with the same sample the mineral composition of colloids is formed by amorphous Fe oxide or hydroxide, MnO_2, TiO_2, $CaCO_3$, $BaSO_4$, clays and zeolites. The aim of this study was to determine the main colloidal phase responsible for sorption of [238]U. For this purpose the following U, Fe, Mn, Al, Si, Ca and Ti distribution was studied. It was observed from the experimental data that [238]U distribution follows the distribution of Fe while Al, Mn or Si containing particles were not enriched with U. The main chemical form of [238]U is uranyl sorbed onto Fe oxide colloids.

<u>Sample from SCC.</u> According to the measurements of actinide redox speciation uranium is present in tetravalent state (U, Np and Pu are present in tetravalent form). Therefore the possibility of formation of U(IV) true colloids is possible. The elemental distribution of U, Fe, Mn, Ti, Ca, Si, Al was studied. In contrast to sample collected at the Mayak site the distribution of U is anti-correlated with major elements that is due to the formation of U true colloids.

---

[1] B.F. Myasoedov, A.P. Novikov. Radiochemical procedures for speciation of actinides in the environment. Methodology and data obtained in contaminated by radionuclides regions of Russia. Proceedings of Speciation Work Shop, October 25-28, 1999, Tokai-Mura, Japan, P.3-21.

[2] Rybaltchenko A.I., Pimenov M.K, Kostin P.P. et al. The deep injection of LNW, Moscow IzdAT, 1994, p. 256 (in Russian).

Neptunium Sorption onto Hematite and Goethite in Presence of Different Humic Acids

A.B. Khasanova*, St.N. Kalmykov*, I.V. Perminova*, S.B. Clark[†]

* Lomonosov Moscow State University, Chemistry Department, Moscow, 119992, Russia
[†] Washington State University, Chemistry Department, Pullman, WA 99164-4630, USA

INTRODUCTION

Organic and mineral colloids may enhance the mobility of pollutants in subsurface environment, including actinides. The effect of humic substances in actinide-mineral interaction is essential for modeling of actinide behavior in the far-field conditions of nuclear wastes repository sites. The goal of this work is to study the effect of humic acids (HA) with different content of hydroquinone groups on Np(V) sorption by goethite (α-FeOOH) and hematite (α-Fe$_2$O$_3$) colloids in the broad pH range.

EXPERIMENTAL

Samples of hematite and goethite were synthesized according to Penners and Koopal[1] and Atkinson et al.[2] accordingly. Their physical characteristics were obtained using XRD, SEM, potentiometric titration and BET surface analysis.

The hydroquinone-enriched derivative of HA was synthesized according to Perminova et al.[3] using the reaction of formaldehyde copolycondensation between parent humic material (leonardite humic acid, CHP) and hydroquinone. The derivative was obtained for monomer : CHP ratio of 100 mg per 1 g and marked as HQ-100.

The batch sorption and kinetic experiments were studied in 50-ml polypropylene tubes in NaClO$_4$ solution in a glove-box in N$_2$-atmosphrere and in the absence of UV-light.

Micro- and ultrafiltrations were used for solid/liquid separation. The redox speciation of Np(V) and Pu(V), formation of actinide-humate complexes and determination of HA concentration in the solution were studied by solvent extraction[4], Vis-NIR spectrophotometry and X-ray photoelectron spectroscopy.

RESULTS AND CONCUSIONS

The batch kinetic experiments indicated that the steady state equilibrium of Np(V) sorption in binary goethite / Np and hematite / Np systems was achieved for 3 days while in case if HA are present it took more than one
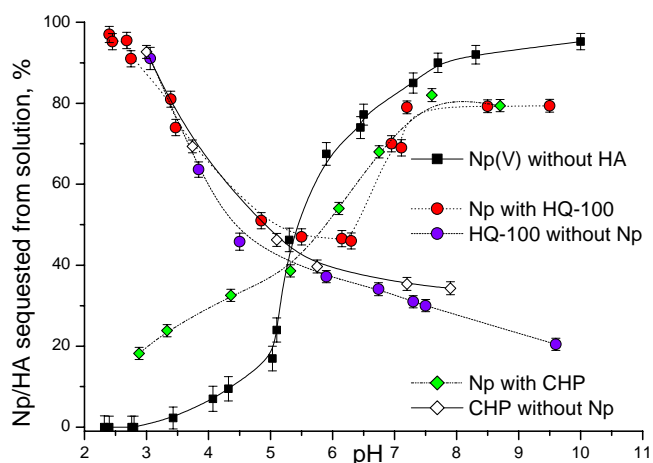
Fig 1: The pH dependences of Np(V) sorption by α-FeOOH (c=0.22 g/l) in the presence of HQ-100 (44 ppm) or CHP (43 ppm); c(Np)=5.8·10^{-7} M.

month to reach steady state equilibrium.

The sorption of Np(V) onto goethite in binary and ternary systems is presented in Fig. 1 for CHP and HQ-100. The presence of hydroquinone-enriched HQ-100 sample enhanced Np(V) sorption at the pH < 6 with slight effect in case of CHP sample (Fig. 1). The explanation of these effects is due to the reduction of Np(V) by Np(IV) by HQ-100 at low pH values that is not the case for CHP sample. The distribution of Np fits the distribution of HQ-100 at low pH values in case of goethite that is demonstrated in Fig. 2. It was established that the sequestration of Np at low pH values upon interaction with quinone enriched HA was observed only in case of goethite colloids and not in case of hematite colloids.
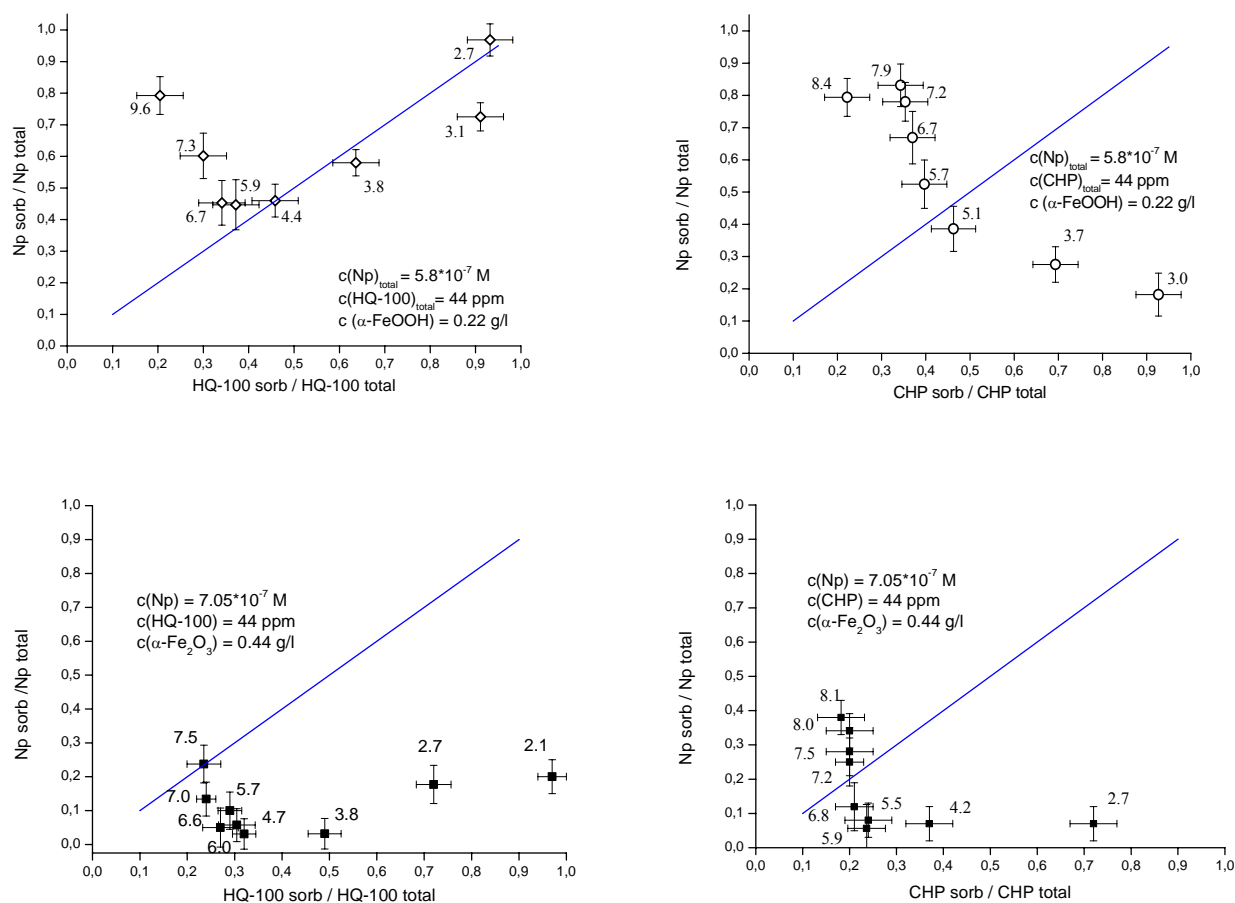
Fig 2: The correlation of Np sorbed / Np total concentrations to HA sorbed / HA total concentrations for studied ternary systems at different pH values.

1   N.H.G. Penners, L. K. Koopal, J.Coll.Surf. **19,** (1986).
2   R.J. Atkinson, A.M. Posner, J.P. Quirk, J. Phys. Chem. **71(3),** (1967).
3   I.V. Perminova, A.N. Kovalenko, *et al.*, Environ. Sci. Technol. **39(21)**, (2005).

Pu(V) and Np(V) Reduction by Hydroquinone Enriched Humic Derivatives

N.S. Shcherbina[*], St.N. Kalmykov[†], I.V. Perminova[†], A.N. Kovalenko[†]

[*]Vernadsky Institute of Geochemistry and Analytical Chemistry, Laboratory of Radiochemistry, Moscow 119991 Russia
[†]Department of Chemistry, Lomonosov Moscow State University, Moscow 119992, Russia

INTRODUCTION

The concept of deep underground repositories in geological formations is accepted in many countries as a final step of nuclear fuel cycle. The multi-barrier systems are designed at the repository sites and are aimed to prevent radionuclide release into the environment. Materials commonly used as engineered barriers should have high sorption properties towards radionuclides, maintain low Eh values of groundwaters and have low hydrolytic conductivity. Among proposed materials are bentonite clays, cements, etc. This study deals with the possible application of humic substances (HS) derivatives as nano-sized material for sequestration of actinides from aqueous solutions.

Natural HS are known to reduce Pu(V) and Pu(VI) to less mobile Pu(IV) and even to Pu(III). Marquardt et al.[1] established stepwise reduction of Pu(VI) to Pu(IV) and Pu(III) by humic materials from Gorleben groundwater. Similar results were obtained by Andre and Choppin[2]. However, the ambiguous results were reported for Np(V). According to Choppin[3], Np(V) is not reduced by natural HS, while Artinger at al.[4] showed slow reduction of Np(V) by HS from Gorleben groundwater. The capability of HS to reduce Pu, Np, and other actinides offers their use as reducing agents for in situ remediation technologies. It was hypothesized that reducing performance of natural humics can be enhanced by incorporating additional hydroquinone moieties. The aim of this research was to evaluate reducing performance of leonardite humic acids and of their hydroquinone-enriched derivatives with respect to Pu(V) and Np(V).

EXPERIMENTAL PART

The quinonoid-enriched humic derivatives were obtained as described in Perminova et al.[5] using the reaction of formaldehyde copolycondensation between parent humic material (leonardite humic acid, CHP) and hydroquinone at hydroquinone (HQ): CHP ratio of 100 mg per 1g of CHP. The obtained derivative was designated as HQ100.

The reduction of Pu(V) by humic derivatives at tracer level concentrations of plutonium ($2.3 \cdot 10^{-8}$ M) and HS concentrations of 10 mg/l was studied by solvent extraction technique[2]. The visible-near-IR spectrophotometry[4] was used to study reduction of Np(V) at macro-concentrations ($3.5 \cdot 10^{-5}$ M) and HS concentrations of 250 mg/l. Reduction of Pu(V) was studied using solvent extraction described by Andre and Choppin which allows tracing trivalent form[2]. Np(V) reduction was studied by tracing of NpO_2^+ and Np(V)-humate absorbance at 980.9 and 987.5 nm respectively.

Pu(V) and Np(V)reduction was studied in plastic 20 mL vials foiled to prevent HS photolysis. In case of Np(V), all manipulations were carried out in the glove box under N_2 atmosphere. Pu(V) reduction was studied on the air. All experiments were carried out at pH of 4.5±0.2 without a

background electrolyte. The oxidation states were tracked by sampling 1.5 ml aliquots for solvent extraction in case of Pu(V), and for NIR-spectrophotometry - in case of Np(V).

RESULTS AND DISCUSSION

Reduction of Pu(V) and Np(V) by HQ100 sample is presented in Figure 1. As it can be seen, only slight reduction was observed for Np(V). At the same time complete reduction of Pu(V) was observed in the presence of HQ 100 within 180 h despite the presence of air oxygen. No Pu(III) was found in the reaction mixture over total exposure time (180 h) that indicates a predominance of Pu(IV). Hence, under environmental conditions reduction of Pu(V) to Pu(III) is hardly possible and Pu immobilization could be achieved. It appears that hydroquinone groups play a major role in Pu(V) and Np(V) reduction by HS.

Fig. 1 Pu(V) and Np(V) reduction by CHP and HQ100; C(Pu)=2.3·10^{-8} M, C(Np)=3.5·10^{-5} M, pH 4.5±0.2, I=0 M

The obtained results demonstrate a viability of the undertaken approach to producing humic materials of the enhanced redox properties. This opens a way for broad application of the humic materials in the practice of remediation technologies.

1   *C.M. Marquardt, A. Seibert, R. Artinger, M.A. Denecke, B. Kuczewski, D. Schild, Th. Fanghanel, Radiochim. Acta **92**, 617-623 (**2004**).*

2   *C. Andre, G.R. Choppin, Radiochim. Acta **88**, 613-616 (**2000**)*

3   *G.R. Choppin, Proceedings of NEA Workshop, Bad Zurzach, Switzerland, 14-16 Sept. 1994, p.75-79, NEA OECD, (**1994**)*

4   *R. Artinger, C.M. Marquardt, J.I. Kim, Radiochim. Acta 88, 609-612 (**2000**)*

5   *I.V. Perminova, A.N. Kovalenko, P. Schmitt-Kopplin, K. Hatfield, N. Hertkorn, E.Y. Belyaeva, V.S. Petrosyan,. Environ. Sci. Technol. 39(21), 8518-8524 (**2005**).*

U – Pu Coprecipitation Experiments in granitic-bentonitic groundwater under oxidizing and anoxic conditions.

J. Quiñones[*], E. Iglesias[*], S. Perez de Andres[*], A. Martínez Esparza[†]

[*]CIEMAT. Avda Complutense, 22. 28040 – Madrid. SPAIN
[†]ENRESA. C/ Emilio Vargas 7, 28043 – Madrid. SPAIN

ABSTRACT

The definition and the evolution of the source term of the High Level Waste repository are some of the key issues related to the performance assessment studies. In this way, it is essential to determine which is the most conservative and realistic concentration for each radionuclide under repository conditions. The stability of spent fuel and its ability to retain radionuclides is not an inherent materials property but it rather depends on the waste package and the properties of containment and corrosion behaviour by groundwaters. Important processes controlling radionuclide release in case of water access are: dissolution of gap and grain boundary inventories of segregated radionuclides, radiolytic production of oxidants, oxidative dissolution of the fuel matrix, sorption of radionuclides on solid phases surface in the near field and formation of secondary solid alteration products by precipitation or coprecipitation providing new host phases for retention of radionuclides[1,2].

This empirical approach is particularly important as thermodynamic databases but is not complete enough to predict unambiguously solubilities in multicomponent systems such as aqueous media in contact with spent fuel. Furthermore, the ongoing work will help realistic geochemical modelling of spent fuel/groundwater interactions by identifying radionuclides, elements thermodynamic properties are needed in order to be described in terms of solid solution, which solubility is better described by pure phases.

As the title remarks this is one of a group of papers related to coprecipitation phenomena with initially dissolved spent fuel in different media[2-4]. This paper is focussed on the results obtained on studying precipitation and coprecipitation from a supersaturated solution on U–Pu under granitic-bentonitic groundwater. In addition to assess the influence of the α radiation field (Pu in solution) on the U secondary phases formed and the final concentration value obtained for U and Pu.

EXPERIMENTAL PROCEDURE & RESULTS

The experimental procedure followed is exactly the same that those described in previous papers [2-4]. These experiments were carried out (in glove box) under different pH and redox conditions, i.e., oxidizing conditions and anoxic conditions (air and Ar – CO_2 atmosphere, respectively; see Figure 1). Aliquots of filtered (membrane pore diameter 220 nm) and ultrafiltered (membrane pore diameter 8 nm) solutions were analysed by α-spectroscopy and ICP-MS (represented in plots as solid and open symbols, respectively).
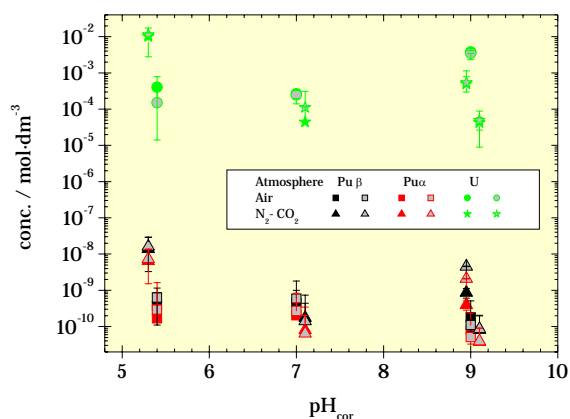

Fig 1: Reactor vessel used.

Fig 2: Evolution of the U & Pu conc. vs pH and the initial redox conditions.
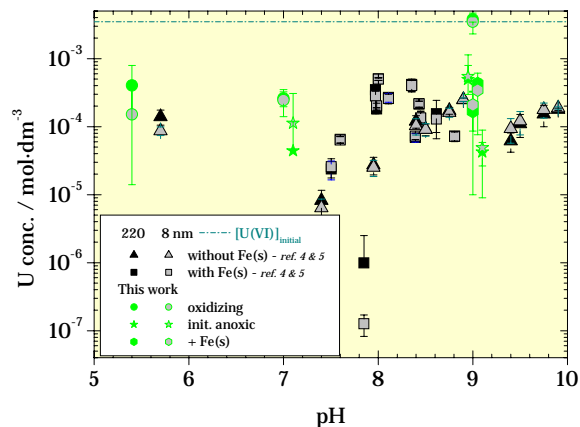
Fig 3: Influence of redox, pH and presence of Pu on the U concentration in solution.

Figure 2 shows the mean U & Pu concentration data obtained for each one selected value (both filtered and ultrafiltered data). The behaviour observed points out that with independence of the initial redox conditions the differences between the U concentration values achieved is small. However, in the case of Pu concentration values this difference it is not observed. When these results are compared with other performed in similar conditions but in absence of α-radiation field[4] (see Figure 3) for pH > 8, similar U concentration behaviour is observed. This U behaviour observed could be explained as a consequence of the water α-radiolysis. Radiolysis generates oxidant species that produce an increase of the final U concentration in solution measured. In the case of Pu the final concentration in solution measured is very similar to those measured both in spent fuel[5] and/or Pu-dopped pellet leaching[6] experiments. This experimental evidence demonstrates that a coprecipitation process between U-Pu is not observed in the studied system, under the environmental conditions simulated. Furthermore, the physicochemical characterization of the solid precipitated (by ICP-MS and XRD) shows the following evidences: i) the Pu/U ratio in the solid is the same than in the initial solution; ii) unlike with those previous experiences performed in absence of Pu[4], amorphous structure (XRD-pattern) of all solid phases were found.

REFERENCES

[1]   B. Grambow, SKB Technical Report **TR-89-13** (1989).

[2]   J. Quiñones, B. Grambow, A. Loida, and H. Geckeis, J. Nucl. Mater. **238,** 38 (1996).

[3]   J. Quiñones, J. A. Serrano, and P. P. Díaz Arocas, J. Nucl. Mater. **298** (2001).

[4]   J. Quiñones, A. González de la Huebra, and A. Martínez Esparza, in *Scientific Basis for Nuclear Waste Management XXVIII*; *Vol. 824*, edited by S. Stroes-Gascoyne, J. Hanchar, and L. Browning (Material Research Society, San Francisco. USA, 2004), p. 425-430.

[5]   J. A. Serrano, V. V. Rondinella, J. P. Glatz, E. H. Toscano, J. Quiñones, and P. P. Diaz, Radiochimica Acta **82,** 33-37 (1998).

[6]   J. Quiñones, J. Cobos, P. P. Díaz Arocas, and V. V. Rondinella, in *Scientific Basis for Nuclear Waste Management XXVII*; *Vol. 807*, edited by V. M. Oversby and L. O. Werme (Materials Research Society, 2004), p. 409-414.

MEASUREMENT OF ENVIRONMENTAL LEVELS OF PLUTONIUM IN SOIL

Thompson P., Thomas M.A., and Thomas N.

AWE, Aldermaston, Berkshire RG7 4PR, United Kingdom.

INTRODUCTION

Many organisations, including AWE, are required to measure environmental levels of plutonium in soil. Measurements are made using isotope dilution analysis, radiochemical separation of plutonium from the matrix and preparation of sources for measurement by alpha spectrometry.

At AWE, the recovery of plutonium from environmental samples for the past ten years has used two separate methods. The two methods were designed for different sample sizes, 1 and 10 grams. The aim was to develop a single generic method to be used for both sample sizes. It was desired that analysis time be shorter, resources used to be minimised and if possible the purity and recovery of the plutonium to be improved.

RESULTS AND DISCUSSION

Samples requiring measurement of environmental levels of plutonium in soil are first treated by ashing and addition of ^{242}Pu tracer. The plutonium is removed from the soil matrix by acid leaching and then separated and purified by ion exchange chromatography. Sources are prepared by electrodeposition for alpha spectroscopy. Further measurements of the isotopes present can be made using mass spectrometry.

The original method for analysis of 10g soil samples utilised a cation exchange resin for initial separation of the plutonium. This step required large amounts of acid for conditioning and elution and took several days to complete. The Pu eluate was purified by anion exchange chromatography using BioRad AG1 x 4 resin.
For gram size samples, boric acid was used following the acid leaching process to neutralise the fluoride ions present. Successive ammonia precipitations were then performed to remove insoluble hydroxides prior to anion exchange purification using BioRad AG1 x 8 resin.

Using these original methods, a generic method for samples up to 10g of soil has been developed. Following acid leaching and complexing of the fluoride ions as boron trifluoride, the leachate is reduced to low bulk and converted to a nitrate form. The hydroxide is precipitated using ammonia which once dissolved in 8M nitric acid is passed through an anion exchange column using BioRad AG1 x 8 resin. Hydriodic acid is used as a reducing agent for this and the eluate is passed through a second anion exchange column to further reduce the level of impurities.

Alpha spectrum of Standard Reference Material.

NIST-4350b Columbia river sediment

Certified values of Plutonium

^{239}Pu + ^{240}Pu - 5.08E-04 Bq/g

^{238}Pu -1.3E-05 Bq/g

Pu 242 tracer @ 4900 KeV

Pu 239/40 @ 5150/5160 KeV

Pu 238 @ 5490 KeV

Counts

Channel
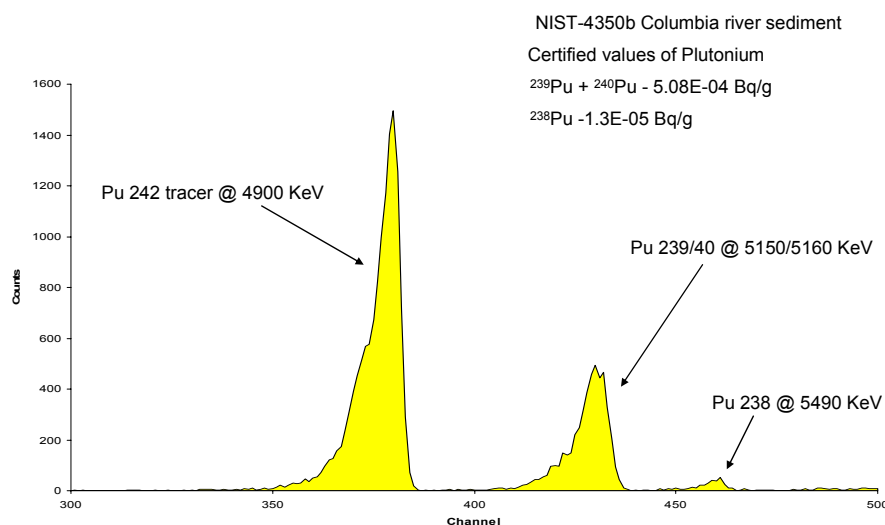
The benefits of the method development are that there is now a generic method for use with the range of soil samples. It has led to faster analysis time, reduction in the amount of chemical waste and a reduction in the costs of materials and manpower required. The additional purification step has also reduced the impurities present in the plutonium fraction. Future development work will focus on achieving total dissolution of the soil matrix and investigating new resins available which may further improve separations.

Synthesis and Use of Humic Derivatives Covalently Bound to Silica Gel for Np(V) Sequestration

I.V. Perminova[†], L.A. Karpiouk[†], N.S. Shcherbina[*], S.A. Ponomarenko[§], St.N. Kalmykov[†], and K. Hatfield[‡]

[†]Department of Chemistry, Lomonosov Moscow State University, Moscow 119992, Russia
[*]Vernadsky Institute of Geochemistry and Analytical Chemistry, Russian Academy of Sciences, Moscow 119991, Russia
[§]Institute of Synthetic Polymer Materials, Russian Academy of Sciences, Moscow 117393, Russia
[‡]Department of Civil and Coastal Engineering, University of Florida, Gainesville, FL-32611, USA

INTRODUCTION

The most commonly applied technology for treatment of groundwater contaminated with metals and/or radionuclides is "pump and treat", followed by disposal or re-injection of treated water. This process can be costly and inefficient due to difficulties arising from the ineffective capture of contaminated groundwaters and the sorption of contaminants on mineral surfaces[1]. A permeable reactive barrier (PRB) is an alternative technology to "pump & treat" systems. A PRB is a subsurface wall of reactive permeable medium emplaced across the flow path of a contaminant plume[2]. The most commonly used reactive materials are zero valent iron (ZVI), activated carbon, zeolites, and cellulose solids. Most PRBs use ZVI to treat chlorinated hydrocarbons, while a limited number remove nitrate, hexavalent chromium, and radionuclides[3]. A typical PRB is costly to install but economical to maintain. Much of the installation cost is related to excavation of aquifer material that is then replaced with reactive porous medium[2].

The goal of this study was a proof of the concept that the reactive agents of a new technology can be designed that can be used for creating broad spectrum sorptive PRBs without excavation. As those agents, the proposed innovative technology uses soluble Humic Substances (HS) that have been specifically modified to adhere to the surfaces of the mineral support and to mediate redox-transformations of actinides. These customized humic materials are immobilized onto silica gel to imitate reactive media of in situ created PRB and to assess their sequestering performance with respect to highly mobile actinide species – NpO_2^+.

EXPERIMENTAL PART

A sample of leonardite humic material of enhanced redox activity with incorporated hydroquinone moieties (HQ100) was synthesized as described by Perminova et al.[4] and kindly provided by A.N. Kovalenko. Parent and modified leonardite materials (CHP and HQ100, respectively) were used for preparing alkoxysilyl-derivatives as described in our PCT-application[5]. 3-amino-propyltrimethoxy-silane (APTS) was used to incorporate alkoxysilyl-groups into both humic materials. To prepare solid-phase humic scavengers, aqueous solutions of either HA-APTS or HQ-APTS at concentrations of 5 g/L (10 mL) were added with 0.1 g of silica gel and mixed for 24 hours. The silica gel with immobilized APTS-derivatives was centrifuged

and washed with distilled water. The carbon content in HA-APTS, immobilized on silica gel, was 9.2% mass, and in HQ-APTS, immobilized on silica gel, – 3.3% mass.

The experiments on Np(V) sequestration were conducted under anoxic conditions in the dark in the glovebox. Solutions of Np(V) at concentration of $3.5 \cdot 10^{-5}$ M (20 mL) were added with 40 or 70 mg of solid HA-APTS-SiO$_2$ or HQ-APTS-SiO$_2$, respectively, and adjusted to pH 4.5. The prepared solutions were sampled over 9 days exposure. The content of Np(V) in the solution was determined using extraction with HDEHP followed by liquid scintillation counting[5].

RESULTS AND DISCUSSION

Figure 1 shows the sequestration kinetics of Np(V) in the presence of pure SiO$_2$, HA-APTS-SiO$_2$ containing not enriched leonardite HA and of HQ-APTS-SiO$_2$ containing hydroquinone enriched leonardite HA at pH 4.5. As it can be seen from the shown kinetic curves, both humic containing scavengers efficiently sequester Np(V) from solution with efficiency of hydroquinone-enriched scavenger being higher, as compared to that of the non-enriched scavenger.

The obtained results demonstrate a viability of the undertaken approach to producing reactive humic materials applicable for in situ installation of sorptive PRBs in actinide-contaminated aquifers. This opens a way for broad application of the humic materials in the practice of remediation technologies.
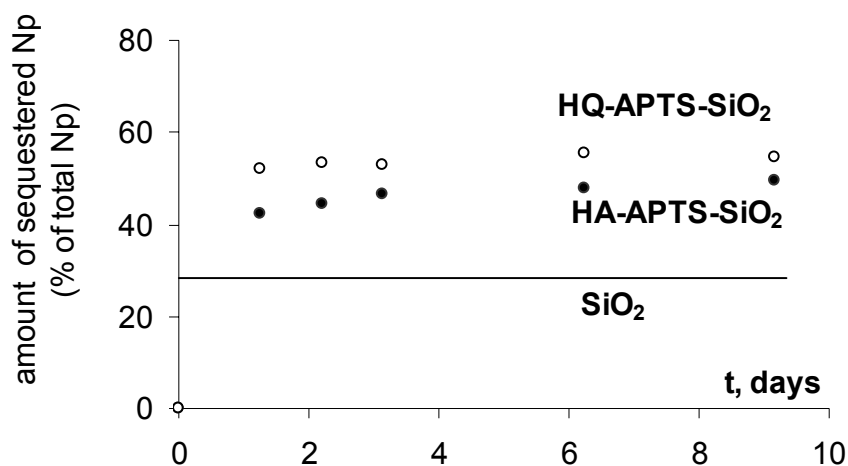
Fig. 1. Sequestration kinetics of Np(V) in the presence of pure SiO$_2$ and of SiO$_2$ with covalently bound leonardite HA (HA-APTS-SiO2) and of their hydroquinone enriched derivative (HQ-APTS-SiO$_2$) at pH 4.5.

1   R. Renner, Environ. Sci. Technol./News **31**: 30A-31A (1997).
2   M. Scherer, S. Richter, R. Valentine, P. Alvarez, Crit. Rev. Environ. Sci. Technol. **30**, 363-411 (2000)
4   I.V. Perminova, A.N. Kovalenko, P. Schmitt-Kopplin, et al. Environ. Sci. Technol. **39**, 8518-8524 (2005).
5   I.V. Perminova, et al. Humic derivatives, methods of preparation and use. Patent pending. (PCT application)
6   A. Morgenstern, G.R. Choppin, Radiochim. Acta 90, 69-74 (**2002**)

Combined Procedure for the Determination of Actinides in Environmental and Radioactive Waste Samples

 M. H. Lee, K. K. Park, J. Y. Kim, Y. J. Park, W. H. Kim

Nuclear Chemistry Research Division, Korea Atomic Energy Research Institute, 150 Deokjin-dong, Yuseong, Daejeon, Korea

Recently, several studies have been reported on the combined procedure for the determination of the radionuclides in environmental samples with extraction chromatographic materials such as TRU Spec, TEVA Spec resins and Diphonix [1,2]. However, the combined methods for the nuclides in soil or sediment samples are limited because it is somewhat difficult to purify the radionuclides due to major salt ions in the soil. Also, these combined methods were focused on only Pu and Am isotopes, not including the Np and U isotopes. In this study, an extraction chromatography method using anion exchange resin and TRU Spec resin was developed for rapidly and reliably determining the low levels of Pu, Np, Am and U isotopes in environmental samples and radioactive waste samples. The developed analytical method for Pu, Np, Am and U isotopes was validated by an application to IAEA-Reference samples.

A total of 20 g of soil was weighed into a porcelain dish and ashed in a muffle furnace with a gradual heating program up to 600 ^{o}C to eliminate the organic matter. To compensate for the chemical recovery, ^{242}Pu, ^{243}Am and ^{232}U, as yield tracers, were added into the soil sample. The calcined samples were dissolved with each 10 mL of concentrated HNO_3 and HF and evaporated to a dryness. The residue was dissolved with 30 mL of 9 M HCl or 8 M HNO_3. The oxidation states of Pu and Np were adjusted to tetravalent plutonium and hexavalent neptunium with 0.2 M $NaNO_2$. The fractions of Pu and Np were purified by an anion exchange resin, and those of Am and U were purified by a TRU Spec resin and anion exchange resin [3]. The purified Pu, Np, U and Am isotopes were electroplated onto stainless steel planchets and measured by alpha spectrometry [4].

The measured concentrations of ^{239,240}Pu in the IAEA-375 and IAEA-326 were consistent with the reference values reported by the IAEA. There was no significant difference in the chemical recoveries for Pu between the 9 M HCl / 0.1 M HNO_3 media and the 8 M HNO_3 media. However, with the anion exchange method in the 8 M HNO_3 medium, the tracer level of U was often detected in the final Pu fraction during the routine analysis. There was not ^{237}Np detected in the IAEA reference soil. The concentrations of ^{241}Am and ^{238}U in the IAEA-375 and IAEA-326 were within the confidence interval. Also, the chemical recoveries for Am and U isotopes with TRU resin in the 8.0 M HNO_3 media were lower than those in the 9.0 M HCl media. This result means that a lot of irons which leached from the soil hinder adsorption of Am and U isotopes onto the TRU resin, even if ascorbic acid is added to the sample solution to reduce the Fe (III). Therefore, in the nitric acid media, it is necessary to remove Fe by means of an oxalic coprecipitation before loading the solution containing Am and U isotopes onto the TRU resin. On the other hand, in the 9 M HCl media, lots of irons are strongly adsorbed onto the anion exchange resin and thus only a

small portion of Fe was eluted in the passing and washing solution. Hence, it is not necessary to remove Fe before loading the solution onto the TRU resin.

Sequential separation method of the Pu, Np, Am and U Isotopes in the soil samples investigated in this study is rapid and reliable. The activity concentrations of the ^{239,240}Pu, ^{241}Am and ^{238}U in the IAEA-375 and IAEA-326 reference samples were close to the reference values reported by the IAEA. In the separation of Pu and Am using an anion exchange resin and TRU resin, a hydrochloric acid medium is favoured over a nitric acid medium. The sequential method of the Pu, Np, Am and U Isotopes will be applied for the low level radioactive waste samples.

1. E. P. Horwttz, M. L. Dietz, D. M. Nelson, J. J. La Rosa, W. D. Fairman, Anal. Chim. Acta **238**, 263 (1990).
2. E. P. Horwttz, R. Chiarizia, M. L. Dietz, H. Diamond, Anal. Chim. Acta **281**, 361 (1993).
3. J. Moreno, N. Vajda, P. R. Danesi, J. J. Larosa, E. Zeiller, M. Sinojmeri, J. Radioanal. Nucl. Chem. **226**, 279 (1997).
4. M. H. Lee, C. W. Lee, Nucl. Instr. and Meth. A **447**, 593 (2000).

Kinetics of redox reactions of Pu(V) in solutions containing different fractions of humic substances

<u>O.A. Blinova</u>*, A.P. Novikov[†], I.V. Perminova[+], R.G. Haire[‡]

*A.N.Frumkin Institute of Physical Chemistry and Electrochemistry, Moscow, Russia,
[†]Vernadsky Institute of Geochemistry and Analytical Chemistry, Moscow, Russia,
[+]Lomonosov Moscow State Univercity, Moscow, Russia,
[‡]Oak Ridge National Laboratory

Humic substances (HS) play an important role in speciation of actinides in the environment due to complexing, redox and sorptive interactions. Actual work is devoted to plutonium speciation studying on hematite (α-Fe_2O_3) -natural water interface with presence of humic substances.

Sorption of Pu(V) onto low-temperature hematite was studied in presence of natural occurring and synthetic humic acid (HA) under different concentration of HA. Sorption was carried out at pH $6.0 - 6.1$ in 0.01M NH_4ClO_4 (as a background electrolyte) and at range of HA concentration from 57.0 to 0.57 ppm. It was shown by solvent extraction method that all Pu adsorbed onto hematite surface in presence of HA posed as Pu(IV).

To study the reduction of Pu(V) by natural occurring HS was humic and fulvic acids (FA) were eluted from sod-podzol and chernozem soils sampled near PA "Mayak" (Russia) using conventional method and separated to fractions depending on their nature (FA or HA), solubility and affinity to mineral part of soil. Obtained fractions of humic substances then were separated by molecular size for more detail studying of their reducing ability. Kinetic curves were obtained for each fraction and compared with results obtained for synthetic HS.

On the base of curve slope, reducing ability is increased in order: HA < FA < low molecular size fraction.

Obtained data show that different HS can play different parts in Pu(V) migration ability due to different reducing and complexing properties that allow to estimate influence of different HS to actinides behavior in actual geological system (prevention or promotion their sorption on minerals and clays).

Partitioning of Pu between organic matter fractions in the contaminated soils and bottom sediments

O.A. Blinova*, T.A. Goryachenkova[†], A.P. Novikov[†], S. Clark[‡]

*A.N.Frumkin Institute of Physical Chemistry and Electrochemistry, Moscow, Russia,
[†]Vernadsky Institute of Geochemistry and Analytical Chemistry, Moscow, Russia,
[‡]Washington State University

The aim of the study is to develop the optimized scheme for sequential extraction of radionuclides from soil or bottom sediment samples. Several procedures were used as described in:

- Smith, G.E. Fractionation of Actinides Elements in Sediments Via Optimized Protocol for Sequential Chemical Extraction, Masters Thesis, Florida State University, (1998),
- Miller W.P., Martens D.C., Zelasni L.W. J. Soil Sci. Soc. Am, V.50, P.598-601 (1986),
- Tessier A., Campbell P.G.C., Bisson M. Anal. Chem., V.51, P.844-851 (1979),
- Pavlotskaya F.I. Problems of Radiochemistry and Cosmochemistry, Moscow, Nauka, P.148-179 (1992).

The bottom sediment sample with high plutonium content from the reservoir 10 located at "Mayak" Production Association Plant has been chosen for carrying out of comparative researches . The reservoir was constructed for storage of low activity waste solutions and self-cleaning of water by sorption on bottom sediments. The sample used in this study was light loam of dark gray color with high peat content. Chemical and mineralogical content of the sample was thoroughly studied. The major part of plutonium (92 - 93%) is bound to amorphous compounds. This is in good agreement with earlier obtained data for various soils and sediments. The major part of plutonium in organic fraction (86-91%) was associated with low soluble humic compounds and their compounds with $R_2O_3 \cdot nH_2O$ (where R=Fe, Al). The pentavalent plutonium compounds are the most soluble among other oxidation states that was demonstrated by speciation experiments. Only about 1% of total plutonium is extracted by water but 80% of it is found in Pu(V) form. The share of Pu(V) in exchangeable fraction (extracted by acetate) reach 55%.

Pu(VI) Speciation In Environmentally Relevant Solutions

S. D. Reilly, W. Runde, M. P. Neu

Los Alamos National Laboratory, Los Alamos NM 87545 USA

INTRODUCTION

Plutonium exists in the environment as a result of nuclear energy and weapons production. Plutonium has rich redox chemistry and can exist in the environment in the four oxidation states III through VI. Each oxidation state has unique solubility and complexation chemistry that contributes to the overall speciation and mobility of Pu. Cations of all the oxidation states form molecular complexes with anions that are common in environmental media. The higher valent species Pu(V) and Pu(VI) tend to adsorb to minerals and other matrices to a lesser extent than lower valent species, and are therefore particularly important to characterize. Carbonate and hydroxide compounds are of interest because they form strong and sparingly soluble complexes. Chloride complexes are comparatively weak, being significant primarily in areas containing brine. The extent to which these anions stabilize plutonium(VI) and influence the behavior of Pu in the near field of radioactive waste repositories and other nuclear sites is being determined.

Fig 1: Numerous plutonium(VI) species can exist in aqueous solution. Complexation, solubility, sorption, and redox equilibria exist.

RESULTS

We have investigated the environmentally-relevant equilibria shown in Figure 1 using a variety of experimental techniques. We studied the chloride complexation of Pu(VI) in NaCl media using visible-near infrared (vis-NIR) spectrophotometry and determined the stability constants of the PuO_2Cl^+ and $PuO_2Cl_2^0$(aq) complexes.[1] The initial hydrolysis of Pu(VI) was studied using complementary potentiometric and vis-NIR techniques.[2] We found evidence for both monomeric and dimeric initial hydrolysis species, depending upon the Pu(VI) concentration, but not trimeric species that are important in U(VI) hydrolysis.

We determined the solubility product of PuO_2CO_3(s) in NaCl and $NaClO_4$ media as a function of electrolyte concentration using vis-NIR spectrophotometry and potentiometry. Vis-NIR spectra of Pu(VI) in solutions containing excess carbonate relative to Pu (Fig 2) show absorbances characteristic of both carbonate and hydroxide species. We are analyzing spectrophotometric and potentiometric data to determine the stoichiometries and stabilities of the species formed under these conditions.

We have also studied the redox and speciation of Pu in synthetic brine solutions that were stored in contact with actual TRU waste for several years. For example, spectra of Pu(VI) in these brine solutions show absorbances attributable to Pu(VI) hydroxides and carbonates (Fig 3).
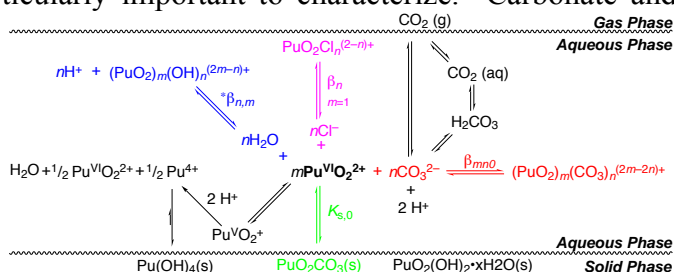
Interestingly, spectra of Pu in brine that had been in contact with pyrochemical TRU waste for weeks to months showed the presence of Pu(VI) hydroxide (Fig 3).
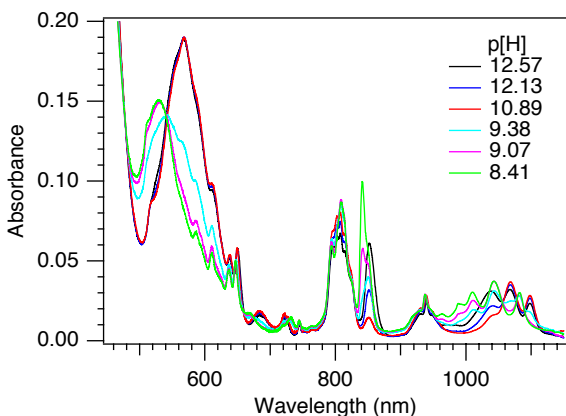
Fig 2: Spectrophotometric titration of 4 mM Pu(VI) in the presence of excess CO_3^{2-}.
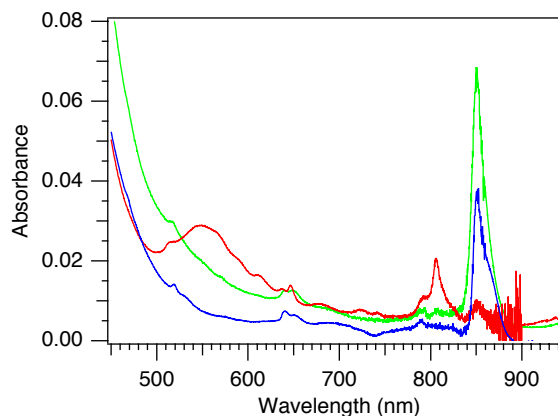
Fig 3: Spectrum of synthetic WIPP brine contacted with TRU waste (blue). Reference spectra of 0.5 mM Pu(VI) in Castile brine (green) and Brine A (red).

DISCUSSION

Plutonium solution thermodynamics and speciation studies are often complicated by multiple complexation, redox, and solubility equilibria. Based on analyses of environmental samples from Pu contaminated sites and from seawater, Pu(VI) species account for a relatively small fraction of the total Pu present. However, common soluble carbonate and hydroxide complexes are highly stable and likely contribute to the overall environmental mobility of Pu. Additional ligands, such as chloride in brines, further increase the stability and solubility of Pu(VI) under oxic conditions.

We and others have found that plutonium(VI) exhibits concentration-dependent initial hydrolysis behavior. Monomeric Pu(VI) hydrolysis species persist at sub-millimolar concentrations. The solubility of $PuO_2CO_3(s)$ is greater in solutions containing high chloride concentrations due to the formation of Pu(VI)-chloro complexes, and the mono-carbonato solution species, $PuO_2CO_3(aq)$, has a relatively large stability field. The unexpected observation of Pu(VI) hydroxide in brine contacted with test TRU waste confirms that Pu(VI) complexes should not be neglected from plutonium speciation models.

1   W. Runde, S. D. Reilly, and M. P. Neu, Geochim. Cosmochim. Acta **63**, 3443 (1999).
2   S. D. Reilly and M. P. Neu, Inorg. Chem. **45**, 1839 (2006).

Neptunium Dioxide Precipitation Kinetics in Aqueous Solutions

A.M. Johnsen[*†], K.E. Roberts[†], S.G. Prussin[*†]

[*]Department of Nuclear Engineering, University of California, Berkeley CA 94720 USA
[†]Lawrence Livermore National Laboratory, Livermore CA 94552 USA

The proposed Yucca Mountain nuclear waste repository poses many questions about the behavior of nuclear materials stored underground for tens of thousands of years. The chemical and transport behavior of ^{237}Np in such a repository is of particular interest, as it has a 2.14 million year half-life.

Previous studies of Np solubility in Yucca Mountain groundwaters supersaturated with Np(V) and performed at temperatures below 100°C for up to a year reported different solid phases, although all were Np(V) solid phases[1-3]. However, thermodynamic modeling of Np indicated that Np(V) under those conditions should have resulted in the precipitation of the slightly more thermodynamically stable NpO_2(cr); it was hypothesized that the Np(IV) solid phase was not seen in earlier experiments because of kinetic limitations[4]. Roberts, *et al.* performed solubility experiments with aqueous Np(V) in very dilute NaCl solutions at near neutral pH at 200°C, resulting in the precipitation of crystalline NpO_2 and suggesting that the Np(IV) solid phase was indeed kinetically limited[5].

We are continuing studies of aqueous Np(V) solutions at elevated temperatures. Experiments at varying temperatures near 200°C are being performed to determine the activation energy for the reduction/precipitation reaction. This will allow for the estimation of relevant time scales for the reaction at lower temperatures, such as those found in Yucca Mountain. Studies are also being conducted to evaluate the effect of ionic strength on precipitation kinetics. This is also an important issue, as the ionic strength of Yucca Mountain groundwaters varies by a factor of approximately 10. Finally, we are investigating the effects of O_2 and CO_2 on the equilibrium concentration of various species.

1   H. Nitsche, *et al*. Los Alamos National Laboratory Report No. LA-12562-MS, 1993.
2   H. Nitsche, *et al*. Los Alamos National Laboratory Report No. LA-12563-MS, 1994.
3   D.W. Efurd, et al. Environ. Sci. Technol. **32** (1998).
4   T.J. Wolery, *et al*. "The Neptunium Solubility Problem in Repository Performance Assessment: A White Paper," Lawrence Livermore National Laboratory, 1995 (unpublished).
5   K.E. Roberts, *et al*., Radiochim. Acta. **91**, (2003).

Interactions of Heavy Elements with Microorganisms

T. Ohnuki[*], T. Yoshida[*,†] , T. Ozaki[*], F. Sakamoto[*], N. Kozai[*], T. Nankawa[*], Y. Suzuki[‡], A. J. Francis[§]

[*]Japan Atomic Energy Agency, Tokai, Ibaraki, 319-1195 Japan
[†] National Institute of Advanced Industrial Science and Technology, Tsukuba, Ibaraki, 305-8567 Japan
[‡] Graduate School of Engineering, Nagoya University,Furo-cho, Chikusa, Nagoya 464-8603, Japan
[§]Brookhaven National Laboratory, Upton, NW, 11973, USA

INTRODUCTION

The presence of actinides in nuclear reactors and radioactive wastes is a major environmental concern due to their long radioactive half-lives, their high-energy radiation emissions, and their chemical toxicity. In order to determine the mobility of actinides in the environment, studies have been designed to examine its interactions with soils and subsoils composed of abiotic and biotic components, principally minerals, organic matter and bacteria[1,2]. Among the biotic components, microorganisms have been shown to sorb actinides on cell surfaces[2,3]. The high capacity of microbial surfaces to bind actinides may affect the migration of actinides in the environment. However, we have only limited knowledge of the role of microorganisms in the migration of actinides in the environment.

The interaction of actinides with microorganisms involves (i) adsorption, (ii) oxidation/reduction, (iii) degradation of actinide-organic component complexes and (iv) mineralization. The interaction of actinides with microorganisms results in changes in the chemical state of actinides (biotransformation). We have been conducting basic scientific research on microbial interactions with actinides in order to elucidate the environmental behavior of actinides under relevant microbial process conditions.

ADSORPTION OF ACTINIDES-DFO COMPLEXES WITH BACTERIA

Adsorption of Pu(IV)-, Th(IV)- and Eu(III)- desferrioxamine B (DFO) on bacteria was studied[4]. A Gram-negative bacterium *Pseudomonas fluorescens* or a Gram-positive bacterium *Bacillus subtilis* was exposed to Pu(IV), Th(IV) or Eu(III) solution in the presence of DFO. At 3 hours after contact of the 1:1 Th(IV)- and Eu(III)-DFO complexes with the cells, the sorption of Pu(IV) and Th(IV) on the cells increased with a decrease in pH from 7 to 4. On the contrary, without DFO most of Pu(IV), Th(IV) and Eu(III) were precipitated in the solution of pH between 7 and 4. Adsorption of DFO on the cells was negligible in the solution with and without metals. Adsorption of Pu(IV), Th(IV) and Eu(III) on *P. fluorescens* cells decreased in the order Eu(III) > Th(IV) > Pu(IV), which corresponds to the increasing the stability constant of the DFO complexes. These results indicate that Th(IV), Pu(IV) and Eu(III) dissociate by contact with cells, after which the metals are adsorbed, and that pH dependence of adsorption density of metal ions on cells is dominated by the stability of the metal-DFO complexes.

REDUCTION OF Pu(IV) BY SULPHATE REDUCING BACTERIUM

Reduction of Pu(IV) by *Desulfovibrio desulfuricans* was studied in the presence of citric acid at pH 7.0[5]. Plutonium(III) in spent medium was determined by the extraction with

thenoyltrifluoroacetone (TTA) solution after oxidizing with $Cr_2O_7^{2-}$ solution. Effect of 2,6-anthraquinone disulfonate (AQDS) was also examined. After the exposure of Pu(IV) to *D. desulfuricans* approximately 10% of Pu was present as Pu(III). No Pu(III) was detected in the solution without bacterium. These findings suggested that Pu(IV) is reduced to Pu(III) by the activity of sulphate reducing bacteria. Fraction of Pu(III) in the spent medium containing AQDS was nearly the same as that without AQDS, suggesting that AQDS does not enhance the reduction of Pu(IV) to Pu(III).

BIOMINERALIZATION OF H-AUTUNITE BY YEAST

Mechanism of uranium mineralization by the yeast *Saccharomyces cerevisiae* was examined by batch experiment at pH 3.2[3]. FESEM-EDS analyses revealed the formation of a U(VI)-bearing precipitate on the yeast cells. Analysis of the U(VI)-bearing precipitates by FESEM-EDS, TEM, and visible diffuse reflectance spectrometry demonstrated the presence of H-autunite, $HUO_2PO_4 \cdot 4H_2O$. Thermodynamic calculations suggest that the chemical compositions of the solutions were undersaturated with respect to H-autunite, but were supersaturated with ten-times more U(VI) and P than were actually observed. Apparently, the sorbed U(VI) on the cell surfaces reacts with P released from the yeast to form H-autunite by local saturation. These findings indicate that the yeast's cell surfaces, rather than the bulk solution, offer the specific conditions for this geochemical process.

EFFECT OF Eu(III) ON DEGRADATION OF MALIC ACID BY A SOIL BACTERIUM

We studied the effect of Eu(III) on the degradation of malic acid by the bacterium *Pseudomonas fluorescens*[6]. Its breakdown depended upon the ratio of Eu(III)- to malic acid-concentrations; the higher the ratio, the less malic acid was degraded. The resulting chemical species of Eu(III), determined by calculations using thermodynamic data, indicated that predominant species were $Eu(Mal)_2^-$ and $EuMal^+$; free Eu(III) was less than 1% of the total Eu(III). The degradation of malic acid was independent of $Eu(Mal)_2^-$, and was hindered by the presence of $EuMal^+$, as well as by free Eu(III). These results suggest that Eu(III) retards the degradation of malic acid, and the effect can be masked through its complexation with malic acid. The degradation of malic acid was followed by the production of unidentified metabolites which were associated with Eu(III). One of the metabolites was analysed to be pyruvic acid.

Our findings indicate that biotransformation of actinides caused by adsorption, reduction, mineralization and degradation should be taken into account for predicting environmental behaviors of actinides.

_____

1   T. D. Waite, et al., *Geochim. Cosmochim. Acta* **58,** 5465(1994).
2   A. J. Francis, et al., Radiochim. Acta **92,** 481(2004).
3   T. Ohnuki, et al., Chem. Geol. **220,** 237(2005).
4   T. Yoshida, et al., J. Nucl. Radiochem. Sci., **6**, 77(2005).
5   T. Yoshida, et al.,To be submitted (2006).
6   T. Nankawa et al., J. Nucl. Radiochem. Sci., **6**, 95(2005).

Selective extraction of Pu by a calix[6]arene bearing hydroxamic groups. Application to bioassays

B. Boulet*, C. Bouvier-Capely*, G. Cote[†], L. Poriel*, C. Cossonnet*[1]

*IRSN/DRPH/SDI/LRC, BP 17, 92262 Fontenay aux Roses - FRANCE
[1]Present address: IRSN/DEI/STEME/LMRE, Bat 501, Bois des Rames, 91400 Orsay - FRANCE
[†]ENSCP/LECA - UMR 7575 - 11, rue Pierre et Marie Curie, 75231 Paris Cedex 05 - FRANCE

INTRODUCTION

Individual monitoring of workers exposed to a risk of internal contamination with actinides is achieved through *in vivo* measurements (anthroporadiametry) and *in vitro* measurements (urine and feces). The procedures currently used for actinides analysis in urine are well established and validated but are time-consuming, which limits the frequency and the flexibility of individual monitoring. The aim of this work is to propose an alternative radiochemical procedure for plutonium and possibly in the presence of uranium. Indeed when Pu and U are both analyzed, it is necessary to separate them prior to alpha spectrometry measurement.

In our previous work, a calixarene-based uranophilic extractant, the $1,3,5$-OCH_3-$2,4,6$-$OCH_2CONHOH$-p-*tert*butylcalix[6]arene (LH$_3$) (see Figure 1), has been selected and has already shown a very good affinity towards uranyl ion[1]. Furthermore, the hydroxamic chelating functions (CONHOH) of LH$_3$ are supposed to present a very high affinity towards Pu(IV)[2].

The aim of this work is to study the affinity of LH$_3$ towards plutonium by solvent extraction and to define experimental conditions allowing to separate plutonium from uranium.

Fig 1: Structure of
$1,3,5$-OCH_3-$2,4,6$-OR-
p-*tert*butylcalix[6]arene

R = CONHOH (LH$_3$)
R = COOH (L'H$_3$)

RESULTS

To be representative of the concentrations currently measured in routine monitoring, Pu and U concentrations were in the order of 10^{-9}M.

Preliminary experiments have been realized to study the affinity of LH$_3$ towards plutonium at the three most stable oxidation states in aqueous phase (III, IV, and VI) using typical oxidizing or reducing agents ($ClNH_3NOH$, $NaNO_2$, and $KMnO_4$). The results have confirmed that LH$_3$ presents the best affinity for Pu(IV). Thus, a protocol has been chosen to control the Pu oxidation state to have only the Pu(IV) species in solution prior to the extraction by LH$_3$.

Then, the affinity of LH$_3$ towards Pu(IV) has been studied as a function of pH. The results have shown that LH$_3$ extracts quantitatively Pu from pH 2. At this pH, the $1,3,5$-OCH_3-

2,4,6-OCH$_2$COOH-p-$tert$butylcalix[6]arene (L'H$_3$) (see Figure 1) does not extract Pu(IV). This result confirms the very good affinity of hydroxamic functions for Pu(IV).

Lastly, in order to determine experimental conditions to isolate Pu from U, we have compared the extraction of Pu(IV) and of U(VI) by LH$_3$ as a function of pH (see Figure 2). The extraction curves show that both elements can be selectively extracted in function of the pH value of the aqueous phase. Indeed, a first step allows to extract quantitatively plutonium at pH 2. Then, the increase of the pH of the aqueous phase at pH 5 allows to extract quantitatively uranium.
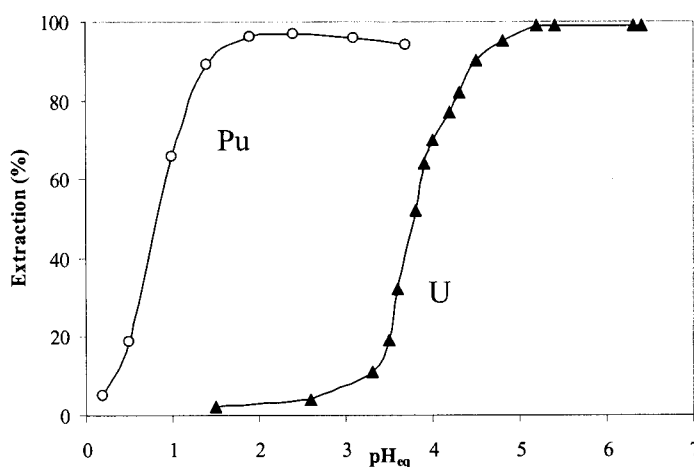
Fig 2: Extraction (%) of Pu and U by LH$_3$ versus pH

CONCLUSION

In this work we have studied the affinity of a calix[6]arene bearing hydroxamic groups towards plutonium and uranium. The results have shown the very good affinity of this molecule for Pu(IV) and the possibility to separate Pu from U at the extraction step by choosing the adequate pH value.

1   B. Boulet, C. Bouvier-Capely, C. Cossonnet, G. Cote, *to be published to*: Solvent extraction and Ion exchange.
2   R.J. Taylor, I. May, A.L. Wallwork, I.S. Denniss, N.J. Hill, B.Ya. Galkin, B.Ya. Zilberman, Yu.S. Fedorov, J. Alloys and Compds, **271**, 534 (1998).

Plutonium Interactions with Aerobic Microorganisms and Microbial Chelators.

Hakim Boukhalfa, Sean, D. Reilly, and Mary. P. Neu*

Chemistry Division, Los Alamos National Laboratory Los Alamos, New Mexico 87545

Microorganisms and their metabolites affect the chemistry of metals present in their environment through solubility and speciation changes, chelation, biosorption, bioaccumulation and other transformations. Bio-molecules can solubilize, oxidize, reduce or precipitate major metal contaminants in soils and ground water and affect their distribution, mobility and bio-availability. We are studying the fundamental interactions between actinides and natural microorganisms to gain an understanding of how they could affect environmental contaminant behavior. The specific interactions we have focused on are bacterial cell surface and bi-products such as siderophores and extracellular polymeric substances (EPS) interaction with Pu species. We examined Pu(IV) binding by classes of natural siderophores, including pyoverdin, desferrioxamine B, desferrioxamine E and rhodotorulic acid; characterized the redox properties of the complexes formed; examined Pu accumulation by biofilms and EPS substances; and quantified Pu uptake through multi-protein siderophore mediated uptake systems in aerobic bacteria.

We found that siderophores have strong binding affinity for Pu(IV) and that all Pu species (III, IV, V, and VI) rapidly and irreversibly form Pu(IV)-siderophore complexes. We will show that Pu(IV)-siderophore complexes are as stable as their Fe(III)-siderophore complexes analogues with the same composition, and that additional complexes can form due to the exceptionally large Pu coordination sphere. We have also found that Pu-siderophore complexes can be recognized by protein membrane transporters and transported across the cell membrane and thereby accumulated intracellularly. Selected data from this broad range of experiments, including biosorption of plutonium, spectroscopic characterization of plutonium-siderophore complexes, the thermodynamic values of the stability constants of the complexes formed and their electrochemical behavior will be presented.

The Surface Properties of UO$_2$ Related to Disposal of SNF and Possible Application of Depleted Uranium

St. N. Kalmykov[*], O.N. Batuk[*], V.P. Petrov[*], E.V. Zakharova[†], Yu.A. Teterin[††], B.F. Myasoedov[†††], V.I. Shapovalov[††††], T.V. Kazakovskaya[††††]

[*]Radiochemistry Division, Chemistry Department, Lomonosov Moscow State University, Moscow 119992, Russia
[†]Frumkin Institute of Physical and Electrochemistry RAS, Moscow, Russia
[††]Science centre "Kurchatovskiy institute", Moscow, Russia
[†††]Vernadsky Institute of Geochemistry and Analytical Chemistry RAS, Moscow, Russia
[††††]Russian Federal Nuclear Centre – VNIIEF, Sarov, Russia

INTRODUCTION

The behavior of UO$_2$ under different conditions and its interaction with fission products and actinides is a key parameter in modeling radionuclide release from irradiated nuclear fuel. Such information is essential in case of direct disposal of spent nuclear fuel (SNF). On the other hand huge quantities of depleted uranium (DU; primarily as UF$_6$) is accumulated worldwide. Despite DU being considered a low-level waste, its conversion to stable oxide forms and subsequent emplacement in a near-surface disposal facility is not an appropriate means of disposal. Use of DU in deep repositories for high level nuclear waste (HLW) may be beneficial. DU can be used in the form of UO$_2$ for heavy concrete casks as shielding over-pack, as a floor material component (drift "invert"), or as fill and backfill material [1]. The goal of this study is to develop a molecular-level understanding of the interaction of Np(IV) and Np(V) with UO$_{2+X}$.

METHODS

Industry produced sample of DU dioxide was studied. The sample was prepared from UF$_6$ and then annealed at 625°C in H$_2$/Ar gas mixture. The average particle size was about 1.5 μm with low free surface area about 1.5 m^2/g as determined by dynamic light scattering technique, scanning and by N$_2$-sortion and fitting by BET equation.

Partial oxidation of U(IV) to U(VI) takes place for sample as a result of oxygen diffusion to its crystal structure. This leads to the decrease of lattice constant value. The bulk ratio of U/O of the sample was studied by powder X-ray diffraction and surface ratio of U/O was studied by X-ray photoelectron spectroscopy. According to the measurements the bulk composition was close to UO$_2$ while the surface composition was close to UO$_{2.25}$.

The solubility and the sorption of the sample were studied in aqueous solutions at constant pH x Eh values in Ar atmosphere. Redox speciation of uranium in solutions was determined by solvent extraction technique. Sorption of Np(IV) and Np(V) by UO$_{2+x}$ was studied in batch mode at total Np concentration of 1·10^{-10} M (using ^{237}Np and ^{239}Np mixture). The radioactivity of solution aliquots was measured by liquid scintillation counting after filtration. For the comparison the sorption of Th(IV) was studied under exactly the same conditions using ^{232}Th and ^{234}Th mixture.

RESULTS AND DISCUSSION

The sorption of Np(IV), Np(V) and Th(IV) by the studied sample is presented in Fig. 1. It was established that at steady state equilibrium the sorption of Np(IV) and Np(V) was almost similar. The decrease of sorption at neutral pH values is established that is not typical for cation sorption. The explanation of this phenomenon is due to the redox reactions that take place at different pH values. At pH < 3.5 - 4.0 due to high solubility of U(VI) (Fig. 2) the sample surface is "washed" and its composition is close to UO_2. The reduction of Np(V) takes place at these pH values upon contact with UO_2 that favors its high sorption. This is supported by Th(IV) sorption that is close to 100% at pH>2. Due to low free surface area it is not possible to use any spectroscopic methods for Np redox speciation on the surface.

At pH>3.5 the surface composition changes from UO_2 to UO_{2+x} that prohibit the reduction of Np(V). This is the reason of that sorption decrease at pH= 3.5 − 8. At higher pH values Np(V) is stabilized and is sorbed by the surface complexation mechanism.

The effect of surface mediated redox reactions at different pH values and their influence should be considered in case of direct SNF disposal and use of DU dioxide in HLW repositories.
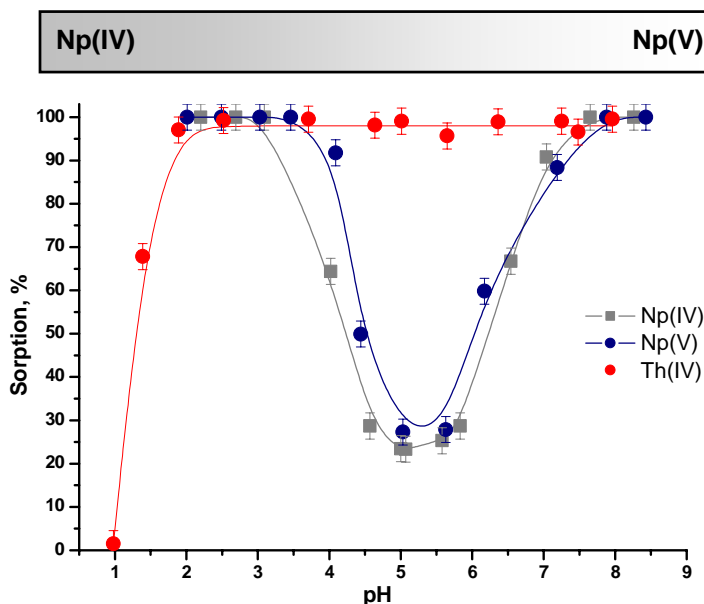

Fig 1: Sorption of Np(IV), Np(V) and Th(IV) by DU dioxide sample.
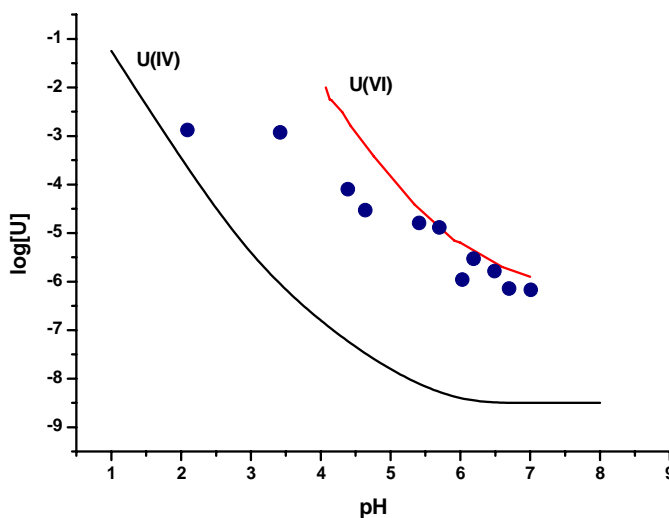
Fig 2: Solubility of DU dioxide sample as a function of pH.

1   M. Betti, J. Environ. Radioactivity, 64, 113–119 (2003).

Actinide Analysis and Leaching of Samples Collected from the Glovebox Excavator Method Project

W. F. Bauer, G. S. Groenewold, R. V. Fox, B. J. Mincher, A. K. Gianotto

Department of Chemical Sciences, Idaho National Laboratory, Idaho Falls ID, USA

INTRODUCTION

The transport of radionuclides in the subsurface is a topic of concern, which is motivated by the disposal of contaminated material in unlined waste pits. At the Idaho National Laboratory (INL), these practices were used from the 1950s to the early 1970s to dispose of radioactive wastes from a wide range of activities, most notably plutonium milling operations conducted at the Rocky Flats, CO plant. Estimation of transport involves modelling hydrologic flow occurring in the geologic subsurface that is coupled to the geochemistry of the radionuclides of interest. The modelling requires knowledge of the contents of the source term, and of the solubilisation properties of the radionuclides. Source term contents are normally inferred from disposal records, and substantiated by subsurface gamma probes. Solubilization behavior generally is derived from solid-solution partitioning studies conducted on model systems in the laboratory. However, there are few studies where samples from radioactive waste disposal pits were measured for radionuclide content and solubilisation properties. This is because sampling would require disinterring the burial zones, which is onerous on account of exposure and environmental concerns.

In late 2003 – early 2004 waste and soil samples were collected during a waste retrieval demonstration (Glovebox Excavator Method Project) in Pit 9, which is part of the Subsurface Disposal Area. The Subsurface Disposal Area (SDA) is a radioactive waste landfill located in the Radioactive Waste Management Complex at the INL in southeastern Idaho. The samples presented a unique opportunity to measure actinide contamination, leaching, and speciation in material that has been buried more than 30 years.[1]

EXPERIMENTAL METHODS

The Glovebox Excavator Method consisted of a backhoe housed in an enclosure that was constructed over the Pit 9 dig area, and was designed to eliminate release of airborne particulate contamination during operations (Figure 1). The excavation was not designed for sample collection, however grab samples of both soil and waste were intentionally collected from the waste zone to ensure acquisition of actinide contaminated material.

The samples were dissolved using a sodium peroxide fusion procedure, and then analyzed using inductively coupled plasma-mass spectrometry, with mass acquisition focused on actinide contaminants. Leaching studies were conducted by contacting the solid samples with a leachate

Fig 1: Backhoe bucket grabbing a barrel.

solution, and analyzing the actinide concentrations that were partitioned into the solution. Sequential aqueous extractions were conducted using a modified Tessier-type procedure.

RESULTS

Nearly all of the soil and waste samples were contaminated with plutonium, and most had elevated levels of uranium, americium, or neptunium. This observation was consistent with the grab sampling procedure that targeted collection of contaminated material. Samples that were not visually contaminated contained [239]Pu at concentrations ranging from 80 ppb to not detected, and had uranium concentrations consistent with the natural background. On the other hand, highly contaminated soil samples were collected (a) from soil caked to graphite mold fragments, and (b) after rupture of a jar containing graphite mold scarfings that contaminated the excavation area: [[239]Pu] ranged from 30 to 80 ppm in these samples. The [239]Pu/[240]Pu and [239]Pu/[241]Am isotope ratios indicated that much of the actinide contamination was derived from weapons-grade plutonium originating from Rocky Flats Plant.

Leaching of plutonium at ambient pH generated operational soil/aqueous distribution coefficients (K_d) of about 10^3 mL/g for organic waste, 10^4 to 10^5 mL/g for low-contamination soil, and about 10^6 mL/g for highly contaminated soil (Figure 2). The excavation logs indicate that the highly contaminated soil was probably exposed to Pu-bearing graphite dust. The K_d values are consistent with sequential aqueous extraction results that showed large percentages of plutonium in the nonextractable fraction. High K_d values were also measured for americium. Leaching studies of uranium and neptunium showed enhanced aqueous partitioning at pH values of $<\sim$4. Complete leaching as a function of pH and ionic strength and studies of sequential aqueous extraction were reported for uranium, neptunium, plutonium, and americium.
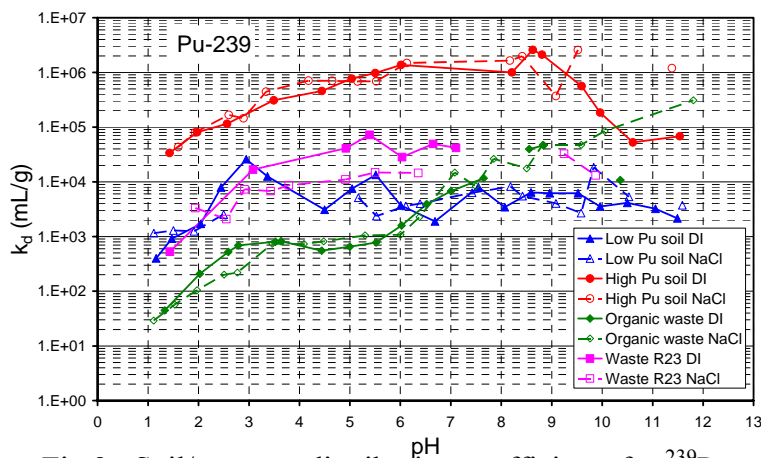

Fig 2: Soil/aqueous distribution coefficients for [239]Pu plotted versus pH. Note that the soils containing high levels of Pu were probably contaminated with graphite dust, and displayed very little leaching.

[1] G. S. Groenewold, et al., "Actinide Analysis and Leaching of Samples Collected from the Glovebox Excavator Project for OU 7-13/14", DOE Report ICP/EXT-04-00439, April, 2005.

Uranium (VI) Solubility from Over-saturation in Carbonate-free Brines

Jean-Francois Lucchini, Marian Borkowski, Michael K. Richmann, Donald T. Reed
Los Alamos National Laboratory, EES-12 Carlsbad Operations, Actinide Chemistry and Repository Science Program, Carlsbad, NM, USA

Introduction

The environmental chemistry and the subsurface mobility of actinides are of primary importance for a transuranic waste repository such as the Waste Isolation Pilot Plant (WIPP). In WIPP Performance Assessment (PA), the uranium (VI) solubility was estimated to be $(8.8\pm0.1)\times10^{-6}$ M in the absence of carbonate, but this value has not being experimentally confirmed under the WIPP specific conditions (highly concentrated brines at pH $\leq$12)[1]. At high pH, carbonate complexation is expected to compete with hydrolysis, leading to lower uranyl U(VI) solubility in the absence of an amphoteric effect[2]. Determination of the relative importance of these two processes is the objective of our experimental program.

This study was conducted with carbonate-free simulated WIPP brines to establish a baseline for the effect of carbonate on the solubility of the +VI oxidation state of actinides (including Pu) in the WIPP. Herein we present the results of uranium (VI) solubility experiments, performed using the over-saturation approach in two simulated WIPP brines, for 250 days, at pH=6-12 and in the absence of carbonate.

Results

The over-saturation approach of these solubility experiments consisted of sequentially adding dissolved uranyl until precipitation was observed, and a steady-state concentration was achieved.

The two simulated WIPP brines used were ERDA-6 brine (multi-component sodium chloride-based brine at ionic strength = 5.0 M) and GW brine (multi-component magnesium chloride-based brine at ionic strength = 6.8 M). Significant effort was made to establish carbonate-free conditions. The removal of carbonate from the brines was a two-step process: acidification of the brines to convert carbonate into carbon dioxide, and a smooth removal of the dissolved gases using a slow pump-down process. The solutions were continuously kept in a nitrogen-controlled atmosphere glove box (oxygen level $\leq$ 10 ppm).

Because of the high ionic strength and strong buffer capacity of the brines, the negative logarithm of the hydrogen ion concentration, called pC_{H+}, was determined by adding an experimentally measured constant (0.94 for ERDA-6 brine, 1.23 for GW brine) to the measured pH.

The experiments were initiated by first adding uranyl-spiked brine (1.7×10^{-5} M) into pC_{H+}-adjusted brines. The solutions were periodically sampled, ultra centrifuged, filtered (30,000 Daltons cut off) and analyzed for uranium content by ICP-MS. A second addition of uranyl-spiked brine (8.6×10^{-5} M) was performed into pC_{H+}-adjusted brines at day 215. The pC_{H+} values of the solutions were experimentally checked and did not change during the 250 days of the experiment.

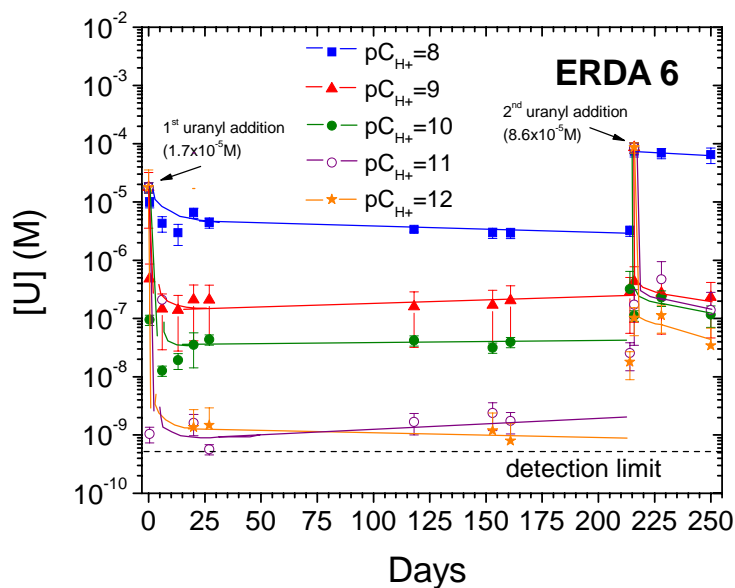Fig.1: Concentration of uranium, in ERDA 6 brine and a nitrogen atmosphere, with time. Data are shown consecutively for pC_{H+}=8 (top) to 12 (bottom). The effective detection limit of uranium in brine with our sampling protocols, is 5×10^{-10} M.
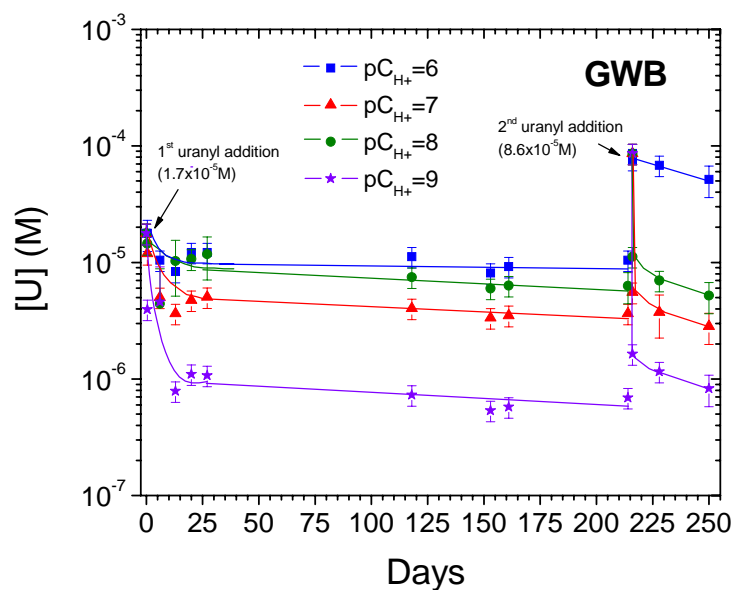

Fig. 2: Concentration of uranium, in GW brine and a nitrogen atmosphere, with time. Uranium concentration profiles correspond to pC_{H+}=6, 7, 8 and 9.

Discussion

The uranium concentration profiles (in Figure 1 for carbonate-free ERDA-6 brine and in Figure 2 for carbonate-free GW brine) suggest that before the second uranyl addition, the uranium solubility was close to equilibrium in all solutions when the initial uranium concentration introduced in solution was above the uranium solubility. The decrease of the uranium concentration to the apparent equilibria obtained before the second uranyl addition seemed faster in GW brine than in ERDA-6 brine. Based on these results, we estimate that the uranium (VI) solubility in carbonate-free brines at high pC_{H+} is about 10^{-6}-10^{-5} M in GW brine and below 10^{-6} M in ERDA-6 at pcH $\geq$ 9, which are lower than the PA theoretical predictions. Further work will be performed to establish the role of the ionic strength in the uranium (VI) solubility difference between the two brines.

A strong pC_{H+} dependence was observed in carbonate-free ERDA-6 brine. Uranium (VI) concentrations were lower when pC_{H+} increased (Fig.1). They were slightly less than the second uranyl addition concentration at pC_{H+}=8, but about 3 orders of magnitude lower at $pC_{H+} \geq$ 9. This pH dependence was mostly a hydrolysis effect. We observed a yellow precipitate, presumably a uranyl hydroxide phase, in ERDA-6 in nitrogen-controlled atmosphere at pC_{H+}=12. We will characterize the precipitate at the end of the experiments.

The uranium concentration trends observed over time at pC_{H+} values up to 12 in carbonate-free ERDA-6 brine indicate that uranium (VI) does not exhibit amphoteric behavior under the conditions investigated.

We compared our data with the most similar published work, performed by Diaz Arocas and Grambow[3]. They performed uranium (VI) solubility experiments in 5 M NaCl at 25°C and different basic pH values, under an argon atmosphere using an over-saturation approach[3]. The uranium solubility data measured in our ERDA-6 experiments at pC_{H+}=9 are lower by two orders of magnitude than Diaz and Grambow's data. Some identical experiments were performed with less stringent CO_2 controls in sealed vessels kept in room air, leading to CO_2 uptake during sampling. The uranium concentrations obtained were two orders of magnitude higher than in our nitrogen-controlled atmosphere and comparable with Diaz and Grambow's data.

These data on solubility of uranium (VI) in WIPP brines are the first at high pC_{H+} under what we believe to be a truly carbonate-free system. They establish a uranium solubility, in the absence of carbonate, that is 10-100 times lower than published results. These estimated values define a "baseline" carbonate-free uranium solubility that will be used to evaluate the effect of carbonate on uranium (VI) solubility in future studies.

References
1) Hobart, D.E., Moore, R.C.: Analysis of Uranium (VI) Solubility Data for WIPP Performance Assessment. Unpublished report, May 28, 1996. Albuquerque, NM: Sandia National Laboratories. WPO 39856.
2) Clark, D.L., Hobart, D.E., Neu, M.P.: Actinide carbonate complexes and their importance in actinide environmental chemistry, Chemical Reviews 95, 25 (1995).
3) Diaz Arocas, P., Grambow, B.: Solid-liquid Phase Equilibria of U(VI) in NaCl Solutions, Geochimica et Cosmochimica Acta 62/2, 245 (1998).

Aerosol Monitoring During Works inside the Object "Shelter": Analysis of Dispersity and Concentration for Different Work Types

P. Aryasov, S. Nechaev, N. Tsygankov

Radiation Protection Institute, 04050, Kiev, Ukraine

INTRODUCTION

Results of aerosol monitoring inside the Object Shelter (OS) are presented in the given work. Taking into account the fact, that dispersity of aerosol is one of the main dose-forming factors of internal exposure dose, principal task of the investigation was determination of radioactive aerosol distribution an aerodynamic diameter (AD). At that, special attention was paid on content in the aerosol of transuranium elements as the main dose-forming radionuclides for the OS conditions. At present, works on stabilization of unstable constructions of the OS are in their active stage. Most of the works inside the OS lead to increased generation of radioactive aerosols. At that these works are carried out in highly contaminated premises of the OS, where radioactive situation is unstable and has been formed during the accident.

DESCRIPTION OF EXPERIMENTS

Results on two major directions of the experiments are presented in the work: the first – dispersity and radionuclide composition determination directly in breathing zone of the personnel during works, and, the second - experiments on aerosol distribution determination in different radiationally dangerous rooms with stationary impactor equipment usage. Six- and eight-cascade Marple personal impactors 290 Series and air pumps GilAir-5 and Gilian 3500 were used for the first task, and two set of Hi-Q Environment company impactors SA-235 model was used for the second task. Special program of monitoring was developed. This program included four major directions: preparation and organization; quality assurance program; air

Fig 1: Personal air sampling by individual impactor during work area preparation, room G 635/3, mark +33

sampling procedure; radiometric measurements. According to the analysis results, works were divided into 5 major types. In fact all radiationally-dangerous works with the increased probability of radioactive aerosols generation were covered, namely: preparation of the workplace (see Fig. 1), elements mounting and cleaning, welding, drilling, cutting of metal.

RESULTS

According to the developed program, for the period from September 2005 till February 2006 more than 100 impactor measurements were carried out. Data on aerosol distribution, radionuclide composition and concentrations of the radioactive aerosols during the works inside the OS is analysed. All air samples obtained during the monitoring underwent measuring of total activity of alpha- and beta-emitters, and selected - for further radiometric analysis of Cs-137 content and radiochemical separation of Pu-239, Am-241. Generalized results on dispersity, radionuclide composition and concentrations of the radioactive aerosols dependences on the type of work are presented in the paper. Analysis of experimental data allows to determine the most radiationally-dangerous types of works. Results of the investigations are used for planning and optimization of radiation protection.

XANES IDENTIFICATION OF PLUTONIUM SPECIATION IN RFETS SAMPLES

V. LoPresti, S. D. Conradson, D. L. Clark

Los Alamos National Laboratory, Los Alamos, NM 87545 USA

Using primarily X-ray Absorption Near Edge Spectroscopy (XANES) with standards run in tandem with samples, probable plutonium speciation was determined for 13 samples from contaminated soil, acid-splash or fire-deposition building interior surfaces, or asphalt pads from the Rocky Flats Environmental Technology Site (RFETS). Save for a single extreme oxidizing situation, all other samples were found to be of Pu (IV) speciation, supporting the supposition that such contamination is less likely to show mobility off site. EXAFS analysis conducted on two of the 13 samples supported the validity of the XANES features employed as determinants of the Pu valence.

References:
1. J. M. Haschke et al., Science **287**, 285 (2000).
2. W. Runde, et al., Applied Geochem. **17**, 837 (2002).
3. S. D. Conradson et al., J. Am. Chem. Soc. **126**, 13443 (2004).

REDOX REACTIONS OF PLUTONIUM WITH HYDROQUINONE AND HUMIC SUBSTANCES

C.M. Marquardt[*], A. Seibert[*†], Th. Fanghänel[*]

[*] Institut für Nukleare Entsorgung (INE, Forschungszentrum Karlsruhe, P.O. Box 3640, 76021 Karlsruhe, Germany

INTRODUCTION

The interaction of humic substances, a ubiquitous compound in natural aquifers, with radionuclides in aqueous solutions are manifold, e.g. complexation of metal ions, sorption of metal colloids and redox reactions. For the migration behaviour of plutonium in aquifers nearby nuclear waste repositories in deep geological formations, the redox stability of plutonium species is one of the key questions. Therefore we wanted to know, what are the dominant species in presence of humic substances and under anaerobic conditions and can this redox behaviour be described with a thermodynamic approach? For that studies have been performed on the interaction of plutonium with GoHy-573 fulvic and humic acid. Unfortunately, the exact composition of reducing entities of humic substances are not known and this makes the interpretation of experiments difficult. Therefore it is convenient to use simultaneously more simple reducing compounds as model substances in the experiments. As one model substance hydroquinone has been chosen, because it is generally accepted that hydroquinone-like entities can act as redox centres in humic substances.

RESULTS AND DISCUSSION

To hydroquinone (H_2Q) solution hexavalent plutonium (PuO_2^{2+}) was added at various pH values between pH 1 and 7 and 0.1 M $NaClO_4$ as background electrolyte. The final Pu and H_2Q concentrations were typically $1-2 \cdot 10^{-4}$ M and $2-3 \cdot 10^{-3}$ eq/L, respectively. The process of the reduction has been followed by absorption spectroscopy and solvent extraction with BMBP[1] as chelating agent. In a first step, the reduction of PuO_2^{2+} to pentavalent Pu (PuO_2^+) was studied. We have observed that the reduction is fast and complete within less than one minute. To get the stoichiometry of the reaction, $1-2 \cdot 10^{-4}$ M Pu(VI) was titrated with $1 \cdot 10^{-3}$ M H_2Q until all Pu(VI) is reduced. At pH 3 for each mol of hydroquinone 2 mol of Pu(VI) are reduced that confirms the following redox reaction, where H_2Q stands for $C_6H_4(OH)_2$ (Hydroquinone), and Q stands for $C_6H_4O_2$ (Benzoquinone):

$$2\,PuO_2^{2+} + H_2Q \rightleftharpoons 2\,PuO_2^+ + Q + 2\,H^+$$
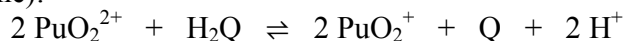
This result coincides with observations from Newton[2], who has performed the experiment in 1 M $HClO_4$.

The next step in the reaction sequence is the reduction of Pu(V) to lower oxidation states Pu(III) and (IV). Here, we have focused first on the rates and on the Pu oxidation state distribution. For that excess of H2Q was added to the solutions from the titration experiment and the evolution of the lower oxidation states were observed with time. The rate of this step is much

slower and reduction is completed after about two months. Depending on the pH value Pu(III) or Pu(IV) is the prevailing Pu oxidation state. At pH below 3 mainly Pu(III) is formed, but Pu(IV) is dominating at pH values above 3. The results are illustrated in Fig. 1. On the left the characteristic absorption bands of the Pu(III) are observed in the absorption spectrum at pH 1 and 3. At pH 3 a tilted background spectrum evolves coming from colloidal Pu(IV) and superposes the Pu(III) spectra. At higher pH values, that is shown on the right, only the background spectra of colloidal Pu(IV) is observed. At the present conditions, the main part of Pu(IV) precipitates as a brownish solid, indicating that the colourless hydroquinone was converted to a brown reduction product, that was sorbed on the Pu(OH)$_4$(am). Similar experiments have been done with Pu and purified GoHy-532 fulvic acid. From the results so far the prevailing Pu species are Pu(III) or Pu(IV) depending on the pH range. Pu(III) is dominating in the acidic pH range below pH 3, whereas Pu(IV) is the most stable oxidation state in the near neutral pH range.
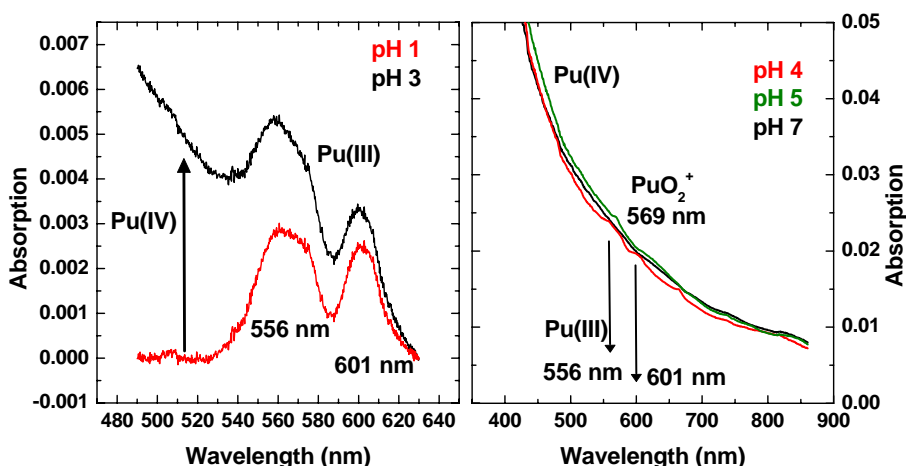

Fig 1: Absorption spectra of Pu, added as Pu(V), in hydroquinone solutions after a reaction time of 2 months at pH 1 and 3 (left hand) and pH 4, 5, 7 (right hand).

CONCLUSIONS

From our results we can conclude that Pu(V) and Pu(VI) are not stable in solutions containing hydroquinone and hydroquinone-like organic compounds like humic substances, and under oxygen free conditions. The tetravalent Pu will be the main species in solution at pH values relevant for aquifers in deep geological formations (pH 5-9), provided that similar redox conditions prevail like in our experiments. It cannot be excluded, that the Pu(III) might be more stable in aquifers containing stronger reducing organic compounds than the GoHy-573-FA batch we used. This batch was separated and purified under air conditions from a Gorleben groundwater and has presumably changed its redox state.

REFERENCES

1   Nitsche, H., Roberts, K., Xi, R., Prussin, T., Becraft, K., Mahamid, I.A., Silber, H.B., Carpenter, S.A., Gatti, R.C., Radiochim. Acta, **66,** 3 (1994)
2   Newton, T.W., J. Inorg. Nucl. Chem., **36**, 639-643 (1974).

Neodymium Analog Study of An(III) Solubility in WIPP Brine

M. Borkowski, J-F. Lucchini, M. Richmann and D. Reed

Los Alamos National Laboratory, Carlsbad Operations, NM 88220 USA

The solubility of An(III) and An(IV) in brine is important to the Waste Isolation Pilot Plant, WIPP, primarily from the point of view of release of transuranium elements to the near-field environment. The solubility of Am(III) and Nd(III), which is an established analog for Am(III), was measured in low ionic strength solutions[1-6], as well as in 3-4 M NaCl and $NaClO_4$ solutions[7,8]. These data were used by WIPP PA for modeling An(III) solubility in brines[9]. The goal of the present work, conducted using an Nd(III) analog, was to measure the effect of pC_{H+}, carbonate concentration, and brine composition on Nd(III) solubility to verify model calculations. Long term experiments (>150 days) were performed in three kinds of brine: ERDA-6, GWB and in 5 M NaCl in the basic pC_{H+} range, in the presence and absence of carbonate ions at a temperature of ~25 ^{o}C. Both over-saturation and under-saturation approaches were used.

CARBONATE FREE EXPERIMENTS

These experiments were designed to provide baseline data for the effect of carbonate. Carbonate was carefully removed from the brine. The brine solution was acidified and bubbled with high-purity nitrogen. The brine was then placed in a nitrogen glove box and the atmosphere was controlled for the duration of experiment. The desired pC_{H+} was adjusted in each bottle and a stock neodymium solution at pH~4 (HCl) was used as a spike in the over-saturation approach. For the under-saturation experiments, commercialyy-available neodymium hydroxide was used as the solid phase. The results of these experiments are presented in Figure 1.
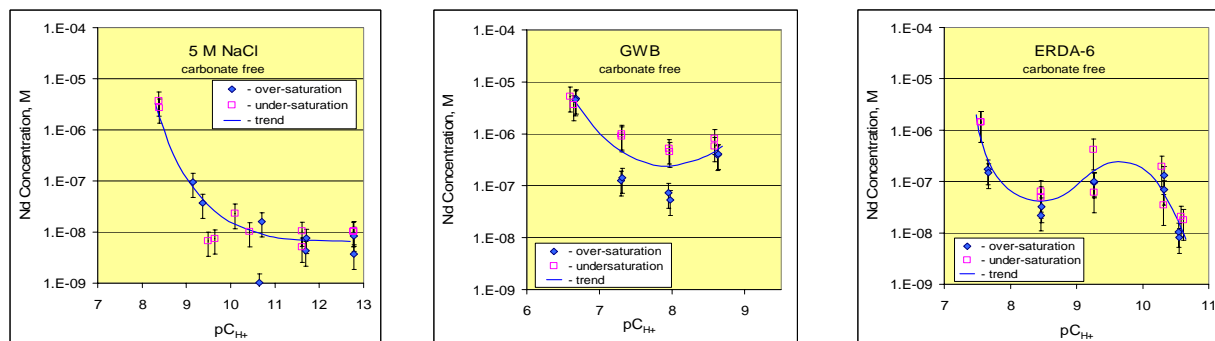

Fig 1. Solubility of Nd(III) measured after 150 days of equilibration without carbonate ion as a function of hydrogen ion concentration. Neodymium concentrations measured for over-saturation and under-saturation were very close to each other.

The pC_{H+} neodymium concentration trend for 5 M NaCl is analogus to the Am(III) solubilities reported for low ionic strength solutions[1-4] but is shifted up by about two orders of magnitude. At pC_{H+} ~8.5, the likely value expected in the WIPP, the lowest Nd(III) solubility was found in ERDA-6 (the low magnesium brine) and was almost one order of magnitude lower than in GWB (high magnesium brine). The shoulder observed for ERDA-6 brine with a

maximum at $pC_{H+} = 9.6$, can be assigned to neodymium complex formation with brine components. This shoulder probably exists in GWB brine but could not be measured due to the precipitation of this brine at $pC_{H+} \geq 8.9$.

EFFECT OF CARBONATE, pC_H AND BRINE COMPOSITION

The carbonate effect was measured in similar systems. Four concentrations of total carbonate were used: 10^{-2}, 10^{-3}, 10^{-4} and 10^{-5} M. In each sample, pC_{H+} was adjusted to the desired value and stock neodymium solution at pH~4 (HCl) was used as a spike in the over-saturation approach. The initial neodymium concentration was equal to 5×10^{-5} M. For under-saturation experiments, $NdCO_3OH$, prepared in our laboratory, was used as a solid phase. The results of these experiments are presented in Fig. 2.

The solubility of neodymium measured as a function of pC_{H+} in GWB and ERDA-6 brines for all carbonate concentrations used, reproduces to a good approximation the dependencies found in the carbonate free experiments. In 5 M NaCl solution with $pC_{H+} > 9$, a shoulder similar to the ERDA-6 case in the carbonate free system was found. This change in neodymium solubility observed in the 5 M NaCl solution with carbonate in respect to

Fig 2.   Neodymium concentrations as a function of pC_{H+} after 220 days of equilibration. Experimental points are presented for various carbonate concentrations. The trend curve (dashed line) was transferred from the graph in Fig 1 for the carbonate free GWB system to the carbonate GWB under-saturation case for comparison.

carbonate free system, can be explained as carbonate complexation, however this effect did not increase with increased carbonate concentration. Characterization of solids controlling solubility collected in broad range of pC_{H+} values will give us more information to better explain this phenomenon.

The Nd(III) complexation with carbonate ion does not appear to play a significant role for neodymium solubility in the WIPP brine. The solubility of neodymium is mostly controlled by the hydroxyl ion concentration and decreases as pC_{H+} increases. For $8.5 < pC_{H+} < 10.5$, a shoulder in neodymium solubility was found in some cases. This shoulder was assigned to complexation of neodymium with carbonate ion or with brine component (e.g. borate) in carbonate free system. These observations are consistent with the literature data[4,6]. However, the literature data are reported for low ionic strength solutions and hydroxyl ion concentrations used were not high enough to observe the further decrease we noted at higher pC_{H+}.

The An(III) solubilities calculated in GWB and ERDA-6 brines using the Pitzer model[9] at pC_{H+}~8.5 are equal to 3×10^{-7} M and 1.7×10^{-7} M respectively and are in good agreement with the neodymium solubility data measured in the present work.

References

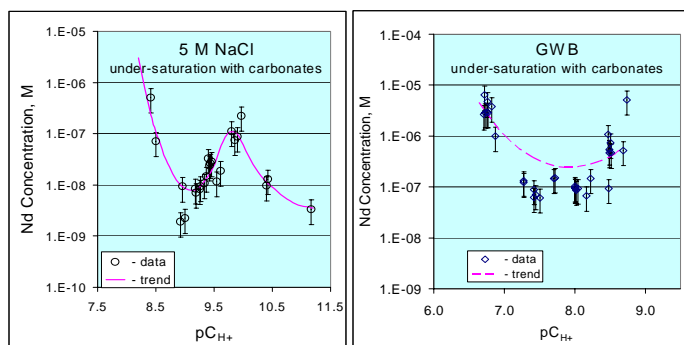1   Rai D., Strickert R.G., Moore D.A., Ryan J.L., Radiochim. Acta, **33** (1983) 201-206.

2   Stadler S., Kim J.I., Radiochim. Acta, **44-45** (1988) 39-44.

3   Silva R.J., Report LBL-15055, Lawrence Berkeley Laboratory, Berkeley, California, 1982, 57 pp.

4   Kim J.I., Bernkopf M., Lierse Ch., Koppold F., ACS Symp. Ser., No. **246**, Washington, D.C.: American Chemical Society, (1984) 115-134.

5   Meinrath G., Kim J.I., Radiochim. Acta, **52/53** (1991) 29-34.

6   Felmy A.R., Rai D., Fulton R.W., Radiochim. Acta, **50** (1990) 193-204.

7   Robouch P.B., Report CEA-R-5473.Commissariat à l'Energie Atomique, Gif-sur-Yvette, France, 1989, 216 pp.

8   Giffaut E., Vitorge P., Mat. Res. Soc. Symp. Proc., **294** (1993) 747–751.

9   Title 40 CFR Part 1991 Subparts B and C Compliance Recertification Application 2004, Appendix PA, Attachment SOTERM, November 10, 2003, DOE CBFO.

The effect of extracellular polymeric substances (EPS) on adsorption of Pu(IV) and (V) on silica particles.

<u>K.A. Roberts</u> [*], P.H. Santschi[*], K.A. Schwehr[*], C.C. Hung[†]

[*]Laboratory for Oceanographic and Environmental Research, Texas A&M University at Galveston, 5007 Ave. U Galveston, TX 77551
[†] Institute of Marine Environmental Chemistry and Ecology, National Taiwan Ocean Univ., Keelung, Taiwan

ABSTRACT

Phytoplankton and bacteria exude extracellular polymeric substances (EPS) that are acid polysaccharide-rich and expected to affect the mobility and adsorption of actinides in surface and ground water. EPS are predicted to enhance adsorption onto particles, especially if they are amphiphatic and contain hydrophobic moieties, such as proteins. Because plutonium can occur in several oxidations states under normal environmental conditions, the focus of the work presented here will be on comparing the adsorption of Pu(IV) and Pu(V) onto silica particles in the presence or absence of EPS harvested from laboratory cultures. The hypothesis that will be tested is that EPS also contains reducing moieties capable of reducing Pu (V) to Pu (IV), thereby favoring Pu immobilization by rendering Pu more particle active. Preliminary data on particle-water partition coefficients (Kd) for Pu(IV) and Pu(V) to EPS from *Pseudomonas fluorescens* Biovar II with and without proteins, in 0.1M $NaClO_4$ and Tris buffer at pH of 8.4±0.1, after 2 days exposure of Pu tracer to EPS, and subsequent separation by ultrafiltration through 1 kDa ultrafilters, will be presented. Log Kd of Pu(IV) to EPS without protein was significantly lower (7.51 vs. 7.93), when EPS was dissolved in EPS for less than one day before a short-term sorption experiment. However, the more mobile Pu(V), prepared according to Saito et al.[1], equilibrated for 4 days with EPS that was pre-equilibrated for 4 days in distilled water, showed much lower log Kd than the more particle-reactive Pu(IV), regardless of protein content (6 vs 7.3). The experimental results will also be compared to chemical composition data of the EPS used such as carbohydrate and protein content, and the relative hydrophobicity of EPS as characterized by the hydrophobic contact area.

1   A. Saito *et al*., Anal. Chem. **57**, (1985).

The Effects of Extracellular Polymeric Substances (EPS) on Plutonium Sorption Behavior

R. M. Tinnacher[*], B. D. Honeyman[*], J. B. Gillow[*,†]

[*]Laboratory for Applied and Environmental Radiochemistry, Environmental Science and Engineering Division, Colorado School of Mines, Golden CO 80401 USA
[†]Environmental Sciences Department, Brookhaven National Laboratory, Upton NY 11973 USA

EXTRACELLULAR POLYMERIC SUBSTANCES AND PLUTONIUM MOBILITY

Until relatively recently, the potential for plutonium (Pu) transport through soils and sediments as a constituent of the mobile aqueous phase was considered to be limited. The aqueous solubility of Pu ranges from atamolar to femtomolar, and its solubility may be further reduced through sorption onto mineral surfaces[1]. The implication of mineral colloids[2] in facilitating Pu transport through groundwater systems has been demonstrated to be a reasonable mechanism for enhanced Pu transport. Biocolloids (biologically-generated organic macromolecules and bacteria) may also serve to enhance Pu mobility in some circumstances.

RESEARCH GOALS

In this study, we investigate the effects of microbial extracellular polymeric substances (EPS) on plutonium sorption behavior in bench-scale laboratory systems. EPS is defined as "extracellular polymeric substances of biological origin that participate in the formation of microbial aggregates"[3]. These microbially produced ligands represent an organic matter fraction at the very beginning of the microbial food-chain. In the early stages of biofilm research, polysaccharides had been considered the most abundant components of EPS; however, proteins, nucleic acids as well as amphiphilic compounds are now also known to contribute substantially to biofilm formation. Previous research indicates that EPS has the ability to strongly complex plutonium in solution[4], and preliminary data also suggest that plutonium sorption is affected by the presence of EPS in solution.

This investigation focuses on two aspects of the role of EPS on Pu mobility: (1) the potential decrease of plutonium sorption to the mineral phase due to Pu-EPS complexation in solution, and (2) the potential remobilisation of sorbed plutonium as a result of the presence of mobile-phase EPS. The first question is

Fig 1: Experimental static column setup used for the investigation of the effects of EPS on plutonium sorption behavior.

essential to determine if Pu-EPS complexes found in solution can possibly be further transported in the subsurface. The latter question represents an attempt to simulate seasonal changes in the soil column during spring run-off, when moisture and nutrient conditions improve, and microorganisms tend to release EPS from cell surfaces.

EXPERIMENTAL SETUP

EPS used in experiments has been extracted from *Pseudomonas fluorescens* Biovar II and gone through a detailed characterization concerning its chemical composition[5]. EPS found in nature is probably more heterogeneous in composition and affected by the microbial diversity of the soil of interest than is our target EPS. The use of EPS from one particular soil bacteria culture, however, provides a controllable and reproducible organic matter composition throughout the course of the experiments. Pretreated silica sand (Q-ROK #1, U.S. Silica) was used as a soil surrogate to minimize the contribution of soil organic matter other than EPS to the organic carbon content of pore water solutions. In addition to the silica sand, which represents a complex 'geomedia' due to commonly found surface impurities, we also evaluate Pu sorption to goethite. Goethite provides a good reference material and has been used for plutonium batch sorption studies in the past[6]. Further, solution conditions, such as pH and ionic strength, are controlled during the course of experiments.

This investigation includes two types of experimental setups, the commonly used batch sorption experiments and a static-column setup[7] (see Fig. 1). Static columns represent pseudo-advective systems with a high solid-to-liquid ratio, which allow the controlled exchange of pore volumes during experiments. Therefore, static columns can be used as a good screening tool prior to the performance of advective column experiments.

1   T. R.. Garland and R.. E. Wildung. In *Biological Implications of Metals in the Environment*, Proceedings of the Fifteenth Annual Hanford Life Sciences Symposium, CONF-750929, 254, (1977).
2   A. B. Kersting, *et al*., Nature, **397**, 56 (1999).
3   G. G. Geesey, ASM News, **48**, 9 (1982).
4   C. Kantar, R. M. Harper, B. D. Honeyman (unpublished).
5   Ch.-Ch. Hung, P. H. Santschi, J. B. Gillow, Carbohydrate Polymers, **61**, 141 (2005).
6   L. Duro, *et al.*, Mat. Res. Soc. Symp. Proc., **807** (2004).
7   J. P. Loveland, *et al*., Colloids and Surfaces A: Physiochemical and Engineering Aspects, **107**, 205 (1996).

Effect of Microbial Activity on the Release of Plutonium from, and the Transport within, Contaminated Soils

A.D. Diaz[*], J.B. Gillow[*†], B.D. Honeyman[*]

[*]Laboratory for Applied and Environmental Radiochemistry, Environmental Science and Engineering Division, Colorado School of Mines, Golden, CO 80401 USA
[†]Environmental Sciences Department, Brookhaven National Laboratory, Upton, NY 11973 USA

PLUTONIUM IN THE ENVIRONMENT

The behavior of plutonium (Pu) in natural environments is generally poorly understood; it is the objective of this work to help elucidate the effect of microbial activity on the fate of Pu. Although there is a comprehensive knowledge base for the microbial transformation of uranium under various redox conditions, relatively little information is available for Pu on the major microbially-catalyzed processes that are expected to affect its transport behavior.

PLUTONIUM AND MICOORGANISMS

Over the last several years, mounting evidence has indicated that small amounts of Pu are mobile in saturated groundwater systems. For the most part, models of Pu transport via the 'colloid pathway' have focused on Pu transport by inorganic colloidal species [1]. However it is clear from our recent laboratory studies that bacterial metabolic products such as citric, alginic and galacturonic acids, and exocellular polymeric substances (EPS), are capable of complexing Pu; such complexes have the potential of fostering the transport of Pu under advective flow conditions. In addition, microbial activity can alter the local geochemical environment through such processes as the reductive solubilization of Fe(III) oxides.

^{239,240}Pu Mobilization - Incubation Experiment

Figure 1: Enhanced ^{239,240}Pu transport resulting from incubation of indigenous Rocky Flats soil microbes in static columns. Note: batch studies resulted in 4% total Pu released.

PRELIMINARY RESULTS

Batch reactors and 'static columns' [2] were used to examine the microbially-stimulated release (i.e., solubilization) and transport (i.e., mobilization) of Pu from Rocky Flats, Colorado, USA soil samples. Soils under study have ^{239,240}Pu activities ranging from 50-300 pCi/gram. Metabolic activity of indigenous soil microorganisms was stimulated by the addition of electron donors. Amendments of soil isolates with glucose under batch conditions resulted in the production of Fe(II) and potentially mobile Pu (approximately 4% of the soil Pu was found in the solution phase as compared to deionized water-amended controls). These results indicate that microbial
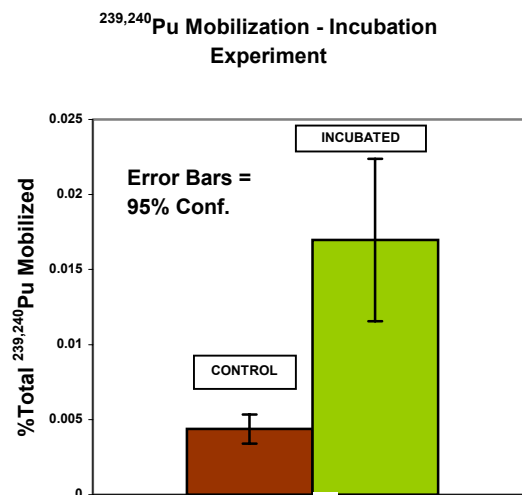
activity may mobilize Pu as Pu colloids in contaminated soil, possibly due to dissolution of iron phases and or complexation with microbial exudates.

While batch experiments allow for the investigation of Pu release, static columns permit the assessment of Pu release and transport as a result of microbial activity at solid/solution ratios more appropriate for saturated groundwater systems without the complexity of full column studies. Static column experiments conducted include incubation experiment where glucose is the electron donor provided to indigenous microbes and EPS experiments where *Pseudomonas fluorescens* EPS is introduced into the column to determine if enhanced transport occurs and to assess EPS biodegradation and the resulting fate of Pu. In both batch and static column experiments where glucose is provided as the electron donor products of metabolic activity were identified and microbial activity resulted in both the enhanced release and transport of Pu.

Batch and static columns have substantially different soil/solution ratios (e.g., 0.125 g/mL vs. 1.5 g/mL, respectively). Initial results indicate that the greater soil/solution ratio in the static columns results in a decreased microbial activity compared to batch systems and a greater amount of Pu released in the batch studies when compared to the amount of Pu released and transported in the static column experiments (Figure 1). The magnitude of acid production and the percent of total soil Pu released/mobilized also is a function of the soil/solution ratio. While iron release was detected in the batch systems, there was no detectable iron present in the effluent of the static columns after ten days of incubation; we also believe this to be a consequence of the soil/solution ratio.

Preliminary static column experiments conducted in the presence of *P. fluorescens* EPS, a microbially produced ligand, indicate that the transport of Pu is enhanced in the presence of the EPS. The potential for microorganisms to utilize EPS as their primary carbon source exists [3]. This work will investigate such a potential for *P. fluorescens* EPS and indigenous Rocky Flats soil microbes in static columns. Changes in molecular weight will be determined with 2-dimensional polyacrylamide gel electrophoresis (2D PAGE) while high performance liquid chromatography (HPLC) will detect the production of organic acid metabolites as a result of biodegradation.

This work also involves sequencing extracted DNA from "raw" Rocky Flats soil, non-amended static column soil (i.e., control), and amended static column soil (i.e., incubated with either glucose or EPS). DNA sequencing will provide information regarding the link between microbial community and changes in biogeochemistry responsible for enhanced Pu transport. Knowledge in this area is currently lacking.

1   B.D. Honeyman and J.F. Ranville. Soil Geochemical Process of Radionuclides. Chapter 7. Soil Science Society of America Special Publication. p. 131 – 163 (2002).
2   J.P. Loveland, J.N. Ryan, G.L Amy, and R.W. Harvey. Colloids and Surfaces A: Physiochemical and Engineering Aspects*, **107**, 205 (1996).
3   M. Ratto, A. Mustranta, and M. Siika-aho. Applied Microbiology and Biotechnology, **57,** 182 (2001).

Effect of HEDPA on Partitioning of Np(V) and Pu(V) to Synthetic Boehmite (γ-AlOOH)

B. A. Powell[*], L. Rao[*], K. L. Nash[†]

[*]Lawrence Berkeley National Laboratory, Berkeley, CA 94720 USA
[†]Washington State University, Pullman, WA 99164 USA

INTRODUCTION

A fundamental understanding of actinide partitioning to natural and synthetic minerals is necessary for the reliable prediction of hydrogeochemical behavior of the actinides, to evaluate the risk posed by subsurface contamination, and to design remediation strategies for contaminated sites and high-level wastes. Sorption of actinides to aluminum oxides and oxyhydroxides is proposed to be a primary control of migration[1-2]. Therefore, a detailed description of Pu(V) and Np(V) interactions with aluminum oxyhydroxides will aid in the refinement of models predicting subsurface actinide transport. Additionally, aluminum oxides are a principle component of the sludge phase within the underground storage tanks at the Hanford site. In order to develop an efficient waste treatment process, interactions between Pu/Np and this predominant sludge component must be understood. To reduce the cost of vitrification of the sludge, reduction of the sludge volume via dissolution of the aluminum oxide phase is desirable. For such a process to be effective, the partitioning of the actinides during dissolution must be examined.

Pentavalent actinides generally have a lower affinity for solid phases relative to other actinide oxidation states due to their low effective charge of approximately $+2.2^4$. At low pH values where metal oxide solid phases possess an overall positive charge, electrostatic repulsion prevents sorption of the cationic AnO_2^+ species. As the pH increases and the surface develops an overall negative surface charge, sorption generally increases. The presence of naturally-occurring or synthetic organic ligands will drastically affect the partitioning of Np/Pu through formation of Np/Pu complexes and dissolution of the solid phase. The objective of this study was to investigate the effect of 1-hydroxyethane-1,1-diphosphonic acid (HEDPA) on the sorption of Pu(V) and Np(V) to synthetic boehmite (γ-AlOOH). HEDPA is a diphosphonate complexant that forms strong complexes with actinides and aluminum in acidic to neutral and basic solutions.

RESULTS and DISCUSSION

The effect of HEDPA on sorption of Np(V) and Pu(V) over time was examined via batch sorption experiments. Np(V) and Pu(V) were equilibrated with 600 mg L^{-1} boehmite suspensions until a steady state was reached. Then HEDPA was added and the concentration of Np and Pu in the aqueous phase was measured over time. Data describing the effect of HEDPA on Np(V) and Pu(V) sorption to boehmite are shown in Figure 1. In the absence of HEDPA, sorption edges for Pu(V) and Np(V) (defined as the point at which 50% is sorbed) occurred at approximately pH 6.6 and 8.0, respectively. This is consistent with the point-of-zero-charge of 8.1 for boehmite measured via potentiometric titration.

Addition of HEDPA effects the partitioning of Np and Pu through formation of Np/HEDPA and Pu/HEDPA complexes and by dissolution of the solid phase, although these reactions occur
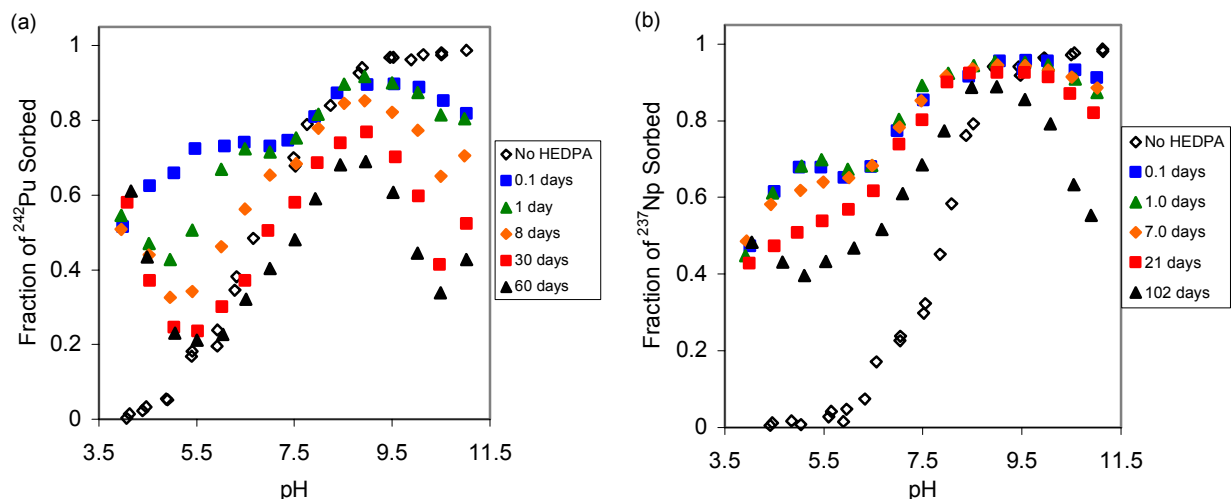
Fig 1: Effect of HEDPA on Pu(V) (a) and Np(V) (b) sorption to boehmite (γ-AlOOH). System parameters: [HEDPA] = 5.4 mM; [γ-AlOOH] = 600 mg L^{-1}; [NaCl] = 1.0 M; [^{242}Pu(V)] = 1.9 μM; [^{237}Np(V)] = 9.4 μM. Open symbols represent steady state distribution (10 day equilibrium) of Pu(V) (a) and Np(V) (b) without HEDPA present.

on different time scales. Within the first few days following HEDPA addition, formation of Np/HEDPA and Pu/HEDPA complexes modified the distribution of Np and Pu between the solid and aqueous phase. At pH values below the original sorption edge, where the surface is predominantly positively charged, addition of HEDPA caused increased sorption of Np and Pu relative to the HEDPA free system. Conversely, at pH values above the original sorption edge, HEDPA caused leaching of Np and Pu into the aqueous phase. These results indicate that Np/HEPDA and Pu/HEDPA complexes are primarily anionic.

At extended time periods, the fraction of Np and Pu in the aqueous phase slowly increased. This is likely due to dissolution of boehmite facilitated by HEDPA. The change in Np and Pu partitioning in this system was concurrent with dissolution of boehmite by HEDPA[5]. Maximum boehmite dissolution was observed at pH 4 and 11. As the pH increased from pH 4 and decreased from pH 11, the Al concentration decreased monotonically until converging at pH 7.5. Addition of HEDPA clearly effects the partitioning of Np and Pu in these systems through dissolution of the solid phase and formation of Np-HEPDA and Pu-HEDPA complexes.

1   L. Righetto, G. Bidoglio, B. Marcandalli, I. R. Bellobono, Radiochim. Acta, **44/45**, 73-75 (1988).
2   J. D. Prikryl, R. T. Pabalan, D. R. Turner, B. W. Leslie, Radiochim Acta, **66/67**, 291-296 (1994).
3   J. W. Morse and G. R. Choppin, Rev. Aqu. Sci., **4**, 1-22, (1991).
4   B. A. Powell, L. Rao, K. L. Nash, L. Martin, in Basic Science, Applications, and Technology, Eds. J. Sarrao, A. Schwartz, M. Antonio, P. Burns, R. Haire, H. Nitsche (Mat. Res. Soc. Symp. Proc.Vol. 893, Warrendale, PA, 2005), 0893-JJ07-02.

Actinides in Sediment and Submerged Plants of the Yenisei River

A. Bolsunovsky and L. Bondareva

Institute of Biophysics SB RAS, Akademgorodok, Krasnoyarsk 660036 Russia

INTRODUCTION

The Yenisei is one of the world's largest rivers, over 3000 km long, flowing into the Kara Sea. The Mining-and-Chemical Combine (MCC) at Zheleznogorsk is situated on the right bank of the Yenisei River, 60 km down of the city of Krasnoyarsk. The Combine has been producing weapons-grade plutonium in uranium-graphite reactors since 1958, when the first reactor was started up. The irradiated uranium is reprocessed at the radiochemical plant to separate uranium, plutonium, and fission products. The reactor plant houses three reactors. Two of them used the Yenisei water as coolant, i.e. the water was taken from the river to remove heat from the core, passed through the reactor fuel channels, and returned to the Yenisei. Both of these reactors were shut down in 1992, but the third reactor is still working. It has been proposed to put it out of service in 2007-2009. This reactor also uses the Yenisei water as coolant for some channels and releases radionuclides of activation origin into the river.

Scientific expeditions revealed that the Yenisei River flood plain is contaminated with artificial radionuclides, including plutonium isotopes, within 2000 km downstream of the plutonium complex[1]. However, earlier investigations ignored the radioactive contamination of components of the aquatic ecosystem. Gamma-spectrometric and radiochemical analysis of samples of aquatic plants and animals collected from the river near the MCC during the 1997-2004 expeditions revealed a broad spectrum of long-lived and short-lived radionuclides[2]. Among the short-lived radionuclides the highest activity concentration in aquatic plants and animals was recorded for ^{239}Np. The Yenisei River continuously receives a wide range of radionuclides, both long-lived and short-lived, and, thus, the aquatic ecosystem of the Yenisei River is a unique object that can be used to study the migration mechanisms of various radionuclides in the environment.

The aim of our investigation was to assess the levels of actinides in sediments and aquatic plants both near the MCC and at a considerable distance from it, down the Yenisei River.

MATERIALS AND METHODS

During the expeditions of 1997-2005, samples of sediment and aquatic plants were collected from the Yenisei River at different distances downstream of the MCC. The aquatic plants sampled were of two species: *Potamogeton lucens* (shining weed) and *Fontinalis antipyretica* (water moss). As control, we used samples of aquatic plants collected upstream of the MCC. Samples of sediments and aquatic plants were prepared for investigations following standard procedures. In some cases, parts of the aquatic plant *Potamogeton lucens* (leaves and stem) were measured separately. For radiochemical and some γ-spectrometric investigations samples of sediments and aquatic plants were ashed. For the radiochemical analysis to determine the content of actinides in samples of aquatic plants, the ash was treated with acid in an MLS 1200 mega microwave system (Milestone) equipped with high pressure TFM vessels. Methods of radiochemical analysis of samples for actinides and ^{90}Sr were

described in detail elsewhere[1,3]. Radiochemical determination of actinides in sediment and plant samples was performed at the RPA RADON (Moscow)[1] and γ-spectrometric measurements of ^{241}Am and ^{239}Np – at the Institute of Biophysics (Krasnoyarsk). Sequential extraction technique proposed by Tessier and modified by Klemt and his colleagues[4] was used to investigate sediment samples. An abbreviated procedure was used to perform sequential extractions in aquatic plant samples and the obtained fractions were exchangeable, adsorbed fractions, organics, and mineral residue.

RESULTS AND DISCUSSION

Investigations of the Yenisei River sediment samples revealed high activity concentrations of transuranic elements (^{238}Pu, ^{239,240}Pu, and ^{241}Am), which were 10 and more times higher than those reported earlier and 100 times higher than their global levels. These local anomalous spots can be found both in the top and in the deep layers of sediments. In these spots specific activities of transuranic elements can be very high: ^{239,240}Pu up to 280 Bq/kg, ^{241}Pu up to 1429 Bq/kg, ^{241}Am up to 48 Bq/kg, ^{237}Np up to 5.6 Bq/kg. These anomalies are indicative of mobile behavior of transuranic radionuclides in the environment and of continued disposals of artificial radionuclides by the MCC[2].

Sequential extraction of samples of sediments collected near the MCC showed that the amounts of extracted ^{152}Eu and ^{241}Am were the largest (60-80% of initial activity), then followed ^{60}Co (30%), and, last, ^{137}Cs (5-15%). The largest amounts of the radionuclides are extracted from such fractions as organics, sesquioxides and hydroxides, and amorphous silicates. Exchangeable fractions contain not more than 2% of total radionuclides. In the sediment – Yenisei River water systems spiked with ^{241}Am the distribution of the actinides released at different extraction stages was not the same as in the unspiked samples.

It was found that aquatic plants of the Yenisei River collected both near the MCC discharge site and at a distance up to 200 km downstream contained a wide range of artificial radionuclides, including actinides (plutonium isotopes, americium, and neptunium). The aquatic moss *Fontinalis antipyretica* was found to have the highest radionuclide concentration factors. Leaves of *Potamogeton lucens* contained higher levels of radionuclides, including ^{239}Np, than stems. Sequential extraction of radionuclides from samples of aquatic plants showed that ^{239}Np levels in exchangeable and adsorption fractions of *Potamogeton lucens* biomass were higher than in the respective fractions of *Fontinalis antipyretica* biomass.

1   A.Ya. Bolsunovsky, *et al.*, Doklady Rossiiskoi Akademii Nauk. **387**, (2002).
2   A. Bolsunovsky, Aquatic Ecology. **38(1)**, (2004).
3   I.A. Kashirin, *et al.*, Applied Radiation and Isotopes. **53**, (2000).
4   E. Klemt, *et al.*, Environmental Radioactivity in the Arctic & Antarctic. (Ed. Per Strand, Torun Jolle and Ase Sand). Norwegian Radiation Protection Authority, Norway. (2002).

Biotransformation of Plutonium (IV) Adsorbed to Iron Oxides

J.B. Gillow[*,†], B.D. Honeyman[†], and A.J. Francis[*]

[*]Brookhaven National Laboratory, Upton, NY 11973 USA
[†]Colorado School of Mines, Golden, CO 80401 USA

INTRODUCTION

Iron oxide coatings and mineral phases are an important sorptive phase for radionuclides in the natural environment and in nuclear waste repositories [1]. Plutonium (IV), (V), and (VI) has been shown to adsorb to iron oxides including goethite and hematite. Sorption of Pu onto iron oxides may facilitate colloidal transport; adsorbed Pu(V) has also been shown to be reduced to Pu(IV) in the case of goethite [2,3]. Once adsorbed the sequestered Pu(IV) may be transformed due to biogeochemical processes. A moderately stable, crystalline iron oxide common in the natural environment and on corroding steel surfaces is goethite (α-FeOOH). Anaerobic fermentative microbial activity can profoundly affect the stability of the iron oxides due to reductive dissolution caused by direct and indirect action including lowering of the Eh and pH and electron transfer processes that alter the mineral phase [4]. We studied the fate of Pu(IV) adsorbed to goethite in the presence of an actively growing culture of *Clostridium* sp.

Figure 1. Sorption edge of Pu(IV) onto synthetic goethite.

MATERIALS AND METHODS

Goethite was synthesized according to the methods of Schwertmann and Cornell [5]. [242]Pu(IV) nitrate was obtained from New Brunswick Laboratory (Argonne, IL). The oxidation state was determined by extraction with thenoyltrifluoroacetone at pH 0 and 4. Pu was added to 10 mg of the oxide to achieve a concentration of 1.8×10^{-7}M and pH adjusted to 2-9; adsorption to the solid oxide was determined after 19 hours by centrifugation (6,000xg) and liquid scintillation counting (LSC). The goethite with adsorbed [242]Pu was then added to culture medium containing the following: glucose, 28 mM; Na^+, 2.0 mM; Ca^{2+}, 3.4 mM; Mg^{2+}, 0.8 mM; NH_4^+, 12 mM; Cl^-, 16 mM; SO_4^{2-}, 0.8 mM; PO_4^{3-}, 0.08 mM; glycerol-1-phosphate, 1.22 mM; peptone, 0.1 g/L; yeast extract, 0.1 g/L (I=0.1 M, pH = 6.8). Triplicate samples were inoculated with the actively growing anaerobic bacterial culture *Clostridium* sp. and pH, Eh, inorganic phosphate (ascorbic acid method) and iron dissolution (Fe(II) determined by o-phenanthroline) were monitored in a time course experiment. Soluble [242]Pu was determined by filtration using a 0.45 µm syringe filter followed by LSC of the filtrate. Similar experiments were performed with [230]Th (2.4×10^{-8} M). Geochemical modelling of the Pu speciation was performed using PHREEQCi with hydrolysis
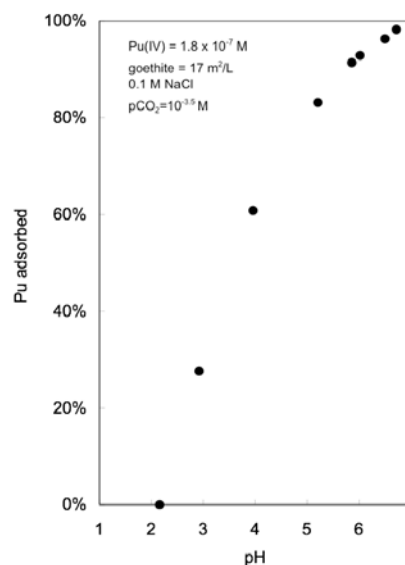
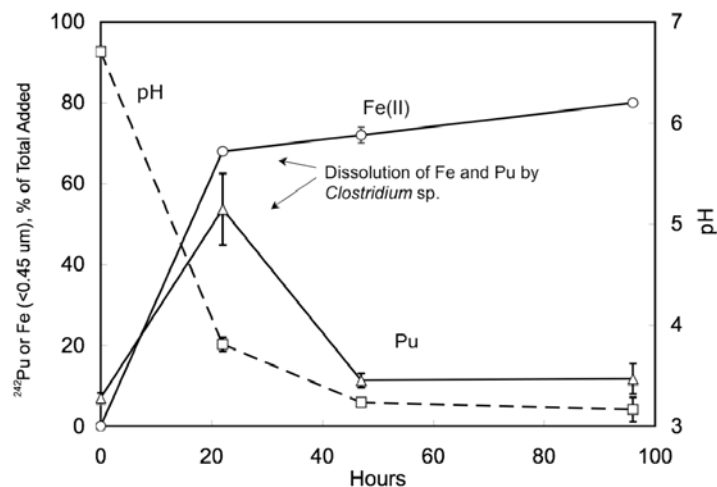constants for Pu(IV) and for formation of carbonate and phosphate species from the NEA TDB project and Lemire (6).

RESULTS AND CONCLUSIONS

The pH sorption edge for Pu(IV) onto goethite was characterized by a steep increase in adsorption between pH 3 and 6 with >95% uptake at pH 6-7 (the pH_{pzc} of goethite is ~7)(Figure 1). Biotransformation of the Pu adsorbed to the goethite resulted in dissolution of iron and a corresponding release of [242]Pu into solution (<0.45 µm)(Figure 2). At 22 hours 66 ± 3% of the iron and 54 ± 9 % of the Pu was released into solution at pH 3.5. However the Pu was removed from solution by 47 hours, with only 15 ± 1 % of the total detected in the <0.45 µm fraction.

Figure 2. Reductive dissolution of iron and release of Pu due to growth of *Clostridium* sp. BC1.

Concomitant with microbial growth is an increase in biomass and increase in the inorganic phosphate concentration in the medium (47 hrs., 0.3 mM orthophosphate). Reductive dissolution of goethite stimulated the release of phosphate (in the absence of the solid iron oxide phosphate was not detected in solution at 47 hours). Studies of [230]Th in this system showed that the Th(IV) was solubilized over the same period of time and rapidly precipitated at 48 hours. Geochemical modelling of Pu(IV) in the growth medium reveals that at pH 3 and in the presence of 0.3 mM PO_4^{3-}, actinide phosphate species dominate and could precipitate Pu as insoluble or colloidal phases. In addition, phosphate rich functional groups at the bacterial cell surface, and exudates released in the medium stimulated by solid iron oxide dissolution, can interact with the mobilized actinide. These studies demonstrate the redistribution of Pu due to anaerobic microbial activity.

1. C.J. Dodge, A.J. Francis, J.B. Gillow, G.P. Halada, C. Eng, C.R. Clayton. Environ. Sci. Technol. **36** (2002).
2. W. Keeney-Kennicutt and J.W. Morse. Geochim. Cosmochim. Acta **49**, (1985).
3. B.A. Powell, R.A. Fjeld, D.I. Kaplan, J.T. Coates, and S.M. Serkiz. Environ. Sci. Technol. **39**, (2005).
4. A.J. Francis, and C.J. Dodge. Environ. Sci. Technol. **24** (1990).
5. U. Schwertmann and R.M. Cornell, Iron Oxides in the Laboratory. New York: Wiley-VCH (2001).
6. R.J. Lemire. Chemical Thermodynamics of Neptunium and Plutonium. OECD-NEA (2001).

Plutonium in seawaters of the Pacific Ocean

K. Hirose[*], M. Aoyama[*], C.S. Kim[†]

[*]Meteorological Research Institute, Nagamine 1-1, Tsukuba, Ibaraki 305-0052, Japan
[†]Korea Institute of Nuclear Safety, Daeduk-Danji Daejeon 305-336, Korea

INTRODUCTION

Plutonium in seawater of the Pacific has been introduced in ocean surface by global fallout due to atmospheric nuclear weapons testing, from which the major fallout occurred in the early 1960's.[1,2] A significant amount of plutonium was injected into seawater by close-in fallout from the US nuclear explosions conducted at the Pacific Proving Grounds in the Marshall Islands in the 1950's[3,4] and the French nuclear explosions conducted at the French Polynesia.[5] As a result, the Pacific waters have been contaminated by plutonium. The vertical and horizontal distributions of plutonium in the Pacific as did its temporal trend and biogeochemical behaviour have been reviewed by Livingston et al. (2000)[6], Hamilton et al. (1997)[7], and Hirose and Aoyama.[8]

Until 1997, there is a little information on the spatial distribution of plutonium concentrations in seawater of the Pacific except the GEOSECS expedition[3] and the continuous monitoring of the western North Pacific.[9] Recently, some research projects have been conducted to survey artificial radioactivity contamination in the World Ocean, in which Worldwide Marine Radioactivity Studies (WOMARS: an IAEA's Co-ordinated Project)[10] and Southern Hemisphere Ocean Tracer Study (SHOTS: MRI, JAMSTEC, IAEA-MEL, KINS and others) were included.[11] These projects provide new data of plutonium concentrations and plutonium isotope ratios in seawaters of the Pacific, especially the South Pacific. As a result, we can depict the current features of plutonium contamination levels in the Pacific waters as do the transport processes of plutonium in the ocean and the interaction of plutonium with biogenc particles in seawater.

SAMPLING AND METHOD

Surface water samples were collected during cruises on board the R/V Ryofu-maru (the Japan Meteorological Agency) and the R/V Mirai (the Japan Marine Science and Technology Center), respectively, over the period from 1997 to 2004. All water samples were filtered through a fine membrane filter (Millipore HA, 0.45 μm pore size) immediately after sampling.

Plutonium isotopes dissolved in seawater were coprecipitated with Fe hydroxides from 50 to 200 L of seawater samples. Plutonium (^{239,240}Pu) concentrations were assayed using α-spectrometry and SF-ICPMS[12] following radioanalytical separation using anion exchange resin and extraction chromatographic resin (TEVA), described in detail elsewhere.[9] The chemical yield was determined by the addition of a known amount of ^{242}Pu.

PLUTONIUM IN THE PACIFIC

In the 1970s, ^{239,240}Pu concentrations in surface waters of the Pacific showed a typical latitudinal distribution of high in mid-latitudes of the North Pacific and low in the South Pacific.[8] This pattern has been considered to reflect the geographical distribution of global fallout due to the atmospheric

nuclear weapons testing. We examined the latitudinal distribution of surface ^{239,240}Pu in the period from 1997 to 2004. The present ^{239,240}Pu concentrations in surface waters of the North Pacific were in the range of 1.5 to 9.2 mBq m^{-3}, whereas the ^{239,240}Pu concentrations in surface waters of the South Pacific were in the range of 0.8 to 4.1 mBq m^{-3}. Surface ^{239,240}Pu showed no marked inter-hemisphere distribution in the North Pacific, although spatial variation of surface ^{239,240}Pu has been observed. In fact, there is the longitudinal variation of surface ^{239,240}Pu along 30°S as shown in Fig. 1. The result suggests that the current level of surface ^{239,240}Pu in the Pacific is controlled by oceanographic processes such as advection and diffusion as well as biogeochemical processes.

The vertical profiles of ^{239,240}Pu observed in mid-latitudes of the North Pacific are characterized by a typical distribution pattern with surface minimum, subsurface maximum (700 - 750 m depth) and gradual decrease with increasing depth. In the South Pacific, the vertical profiles showed the similar pattern as that in the North Pacific. However, the ^{239,240}Pu concentrations in deep waters (> 700 m depth) of the South Pacific were significantly lower than that in the North Pacific. It has been reported that the subsurface maximum of ^{239,240}Pu in mid-latitudes of the North Pacific has moved into deeper water.[6] This pattern of vertical ^{239,240}Pu profiles and their temporal change

Fig. 1 Longitudinal distribution of ^{239,240}Pu concentrations in the mid-latitude region of the South Pacific

has been demonstrated by particle-scavenging processes, the removal of ^{239,240}Pu by sinking particles following regeneration of dissolved ^{239,240}Pu due to the biological degradation of particles.
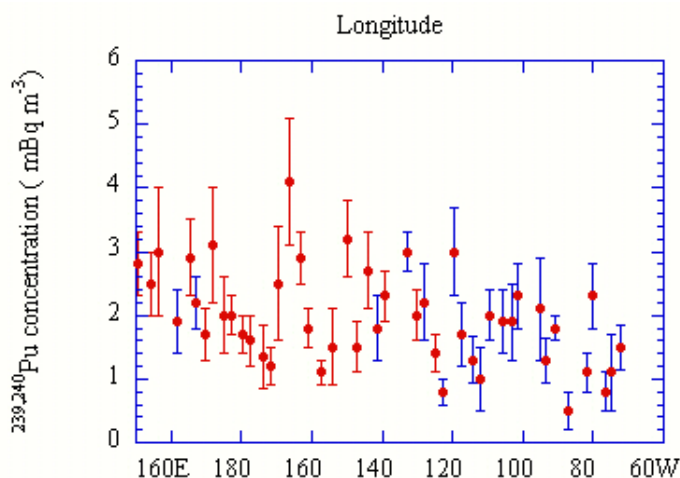
1   J.H. Harley, J. Radiat. Res., 21, 83 (1980).
2   K. Hirose, *et al*., Plutonium in the Environment, A. Kudo, Ed , Elsevier Science (2001).
3   V.T. Bowen, *et al*., Earth Planet. Sci. Let., 49, 411 (1981).
4   K.O. Buesseler, J. Environ. Radioact., 36, 69 (1997).
5   R. Chiappini, *et al*., Sci. Total Environ., 237/238, 269 (1999).
6   H.D. Livingston, *et al*., Plutonium in the Environment, A. Kudo, Ed , Elsevier Science (2001).
7   T.F. Hamilton, *et al*., Radionuclides in the Ocean Inputs and Inventory, eds., P. Guéuéiat, et. al., (1996).
8   K. Hirose and M. Aoyama, Deep-Sea Res. II, 50, 2675 (2003).
9   K. Hirose, *et al*., J Radioanal Nucl Chem 248, 771 (2001).
10   P.P Povinec *et al.*, J. Environ. Radioact., 81, 63 (2005)
11   M. Aoyama *et al.*, Intern. Conf. on Isotopes in Environmental Studies- Aquatic Forum 2004, (IAEA-CN-118)
12   C.S. Kim, C.K. Kim and K.J. Lee, Anal. Chem., 74, 3824 (2002).

On the possibility of application of ultrashort pulses of laser radiation to study the properties of metallic Pu under extreme conditions

A.Ya. Uchaev, V.T. Punin, N.I. Sel'chenkova, E.V. Kosheleva

Russian Federal Nuclear Center – VNIIEF, Russia, 607188, Nizhni Novgorod region, Sarov, Mira avenue 37, uchaev@expd.vniief.ru

At present the knowledge of matter behavior under extreme conditions is acute as, for example, ultimate capabilities of current technology and unique scientific facilities are related to the processes caused by powerful impulse action on the matter.

The knowledge of behavior of metallic *Pu* under extreme conditions is acute at present due to insufficient knowledge of properties of metallic *Pu* of different age and its behavior at high-intense pulse action.

To study the dynamic failure phenomenon[1-3], there were applied the methods of explosion and shock-wave loading (longevity is $10^{-5} < t < 10^{-8}$ s), the heat shock method (HS - longevity range t $\sim 10^{-6} \div 10^{-10}$ s); as well as to study the dynamic failure in subnanosecond range ($10^{-9} \div 10^{-11}$ s), there were applied ultrashort pulses of laser radiation (USPLR) with power density J of laser radiation up to J $\sim 10^{14}$ W/cm^2.

 The paper contemplates a possibility for applying the critical phenomena theory and theory of second-kind transitions to the description of failure process at the final stage in the dynamic longevity range (submicro-subnanosecond range).

As a result of a large scope of research[1, 2] it was shown that arising dissipative structure – failure centers cascade - puts up the resistance of the body to the external action in the dynamic longevity range. The failure centers cascade is a fractal cluster.

A model of lattice gas was applied for adequate mathematical modeling of the arising failure centers cascade which is a percolation cluster at the stage of macro-failure.

At present it is known that canonical distribution function in the Ising model is similar to the function of distribution of large canonical ensemble in the lattice gas model. This reflects the analogy between the model of Ising ferromagnet and the lattice gas model.

Application of the apparatus of critical phenomena theory and second-kind transition theory in an effort to describe the dynamic failure processes at the final stage allowed determination of universal attributes of metals behavior in the dynamic failure phenomenon conditioned by self-organization and instability in dissipative structures.

On the basis of complex approach to the work there is considered a possibility for obtaining quantitative characteristics of behavior of a number of metals including metallic Pu, under extreme conditions on the macro-level on the basis of analysis of quantitative characteristics of dissipative structures, arising on different scale levels, whose behavior is similar to behavior of systems near the second-kind transition.

The approach proposed specifies the possibility for predicting behavior of a number of metals, including metallic Pu [4] on different scale-time levels basing upon experimental studies performed in the laboratory environment on small samples.

1. R. I. Il'kaev, A.Ya. Uchaev, S. A. Novikov, N.I. Zavada, L. A. Platonova, N. I. Sel'chenkova. Universal metal properties in the dynamic failure phenomenon // DAN, 2002, vol. 384 (3), P. 328-333.

2. R. I. Il'kaev, V. T. Punin, A. Ya. Uchaev, S. A. Novikov, E.V. Kosheleva, L. A. Platonova, N. I. Sel'chenkova, N. A. Yukina. Time regularities of metals dynamic failure process conditioned by hierarchic properties of dissipative structures – failure centers cascades //DAN, 2003, vol. 393 (3), P.326-331.
3. A.Ya. Uchaev, V.T. Punin, S. A. Novikov, E.V. Kosheleva, A.P. Morovov, L. A. Platononva, N. I. Sel'chenkova, N.A. Yukina. "Substantiation of the possibility of obtaining of quantitative characteristics of metals behavior under extreme conditions on the macro-level on the basis of regularities of behavior on meso-level". Matter extremal states. Detonation. Shock waves. Proceedings of the International Scientific Conference, the VII Khariton Readings. 14-18 March 2005. Edited by the Doctor of Sciences, Engineering, A.L. Mikhailov. RFNC-VNIIEF Sarov. 2005. P. 356-361.
4. Plutonium Handbook A Guide to the Technology, volume I. Edited by O.J. Wick Pacific Northwest Laboratories Battelle Memorial Institute. 1967 by Gordon and Breach, Science Publishers, Inc. 150 Fifth Avenue, New York.

Neutron Resonance Spectroscopy Measurements of Temperature and Velocity During Shock Wave Experiments

D.C.Swift and V.W.Yuan

Los Alamos National Laboratory, Los Alamos, NM 87545, USA

INTRODUCTION

Most of the applications of high-pressure physics, and many of the experimental measurements, involve dynamic loading and shock waves. A key outstanding problem is the measurement of temperatures within condensed matter during dynamic loading. Temperature is a critical quantity in many aspects of the response of condensed matter to dynamic loading, as it governs the activation of processes including phase transitions, chemical reactions, and plastic flow. Without reliable measurements of the temperature within a sample, the value and effects of temperature can be deduced only indirectly, for instance from surface measurements.

Neutron resonance spectroscopy (NRS) is a very powerful technique, offering the possibility of direct measurements of internal temperature on short time scales, even for opaque materials such as metals. A small number of shock wave experiments have been performed to investigate the feasibility of the technique. Temperatures measured in a model system thought to be well understood were higher than expected, highlighting unresolved issues either with the experimental technique or with the theoretical model. Here we discuss contributions to the temperature from plastic flow, and newly-quantified details of the shock-loading system which may appear as a higher apparent temperature.

PREVIOUS RESULTS FOR MOLYBDENUM

NRS measurements[1] of temperature in shock-loaded systems have been performed at the LANSCE accelerator at Los Alamos National Laboratory. In each experiment, a pulse of 800 MeV protons was used to generate a pulse of neutrons from a nuclear spallation target. The neutrons were moderated to epithermal temperatures before use in the resonance spectroscopy measurement. The sample material was dilutely doped with an element possessing suitably-chosen neutron resonances: energies of a few tens of electron-volts, fairly narrow, and clearly distinct from resonances in the sample material. A region of high and (close to) constant shock pressure was induced by the impact of a projectile. The neutron pulse was synchronized to arrive while the shock state was as constant as possible over the doped region. The neutrons interacted with the resonances in the dopant nuclei according to the energy of the neutrons in the rest frame of each nucleus; thus, in the laboratory frame, the interaction varied with the material velocity and temperature of the doped material, in a calculable way. Essentially, each absorption peak was shifted according to the relative velocity of the material and broadened according to its temperature. The modified resonance spectra were measured using time-of-flight discrimination of the neutrons at the detectors. Calibration experiments were performed on samples heated in an oven. Dynamic experiments were performed on Mo as a material for which it was expected that shock heating would be predicted accurately by continuum dynamics, and on a chemical explosive.[2]

The Mo was doped with [182]W, which has a usable resonance at 21.1 eV. In two experiments, samples were shocked to ~63 GPa, a value obtained by calculation using the laser Doppler velocimetry measured free surface velocity of the shocked sample and Mo equation of state, which describe the pressure-volume-energy relation.. The experimentally-measured temperatures were 150-300 K higher than predictions using plausible equations of state (Figure 1).

THE EFFECT OF PLASTIC HEATING

Recently a new model and numerical method of solving the shock jump conditions for general forms of material response was used to predict the magnitude of plastic heating consistent with the shock jump conditions. Using the Steinberg-Guinan model of plastic flow stress in shocked Mo, the temperature was predicted to be significantly closer to the measurements (Figure 1). The flow stress may deviate from the Steinberg-Guinan predictions by tens of percent at high pressures, though the velocimetry records indicated that the difference may not be this large.
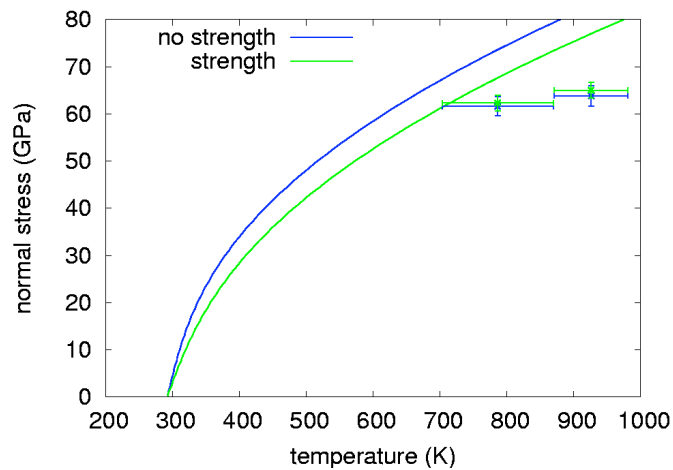

Figure 1: *Comparison of shock Hugoniots with and without strength (curves), and NRS measurements (points). Note that the stress is inferred from the particle speed using the material model, and varies slightly depending on the strength.*

POSSIBLE NON-IDEALITIES IN THE SHOCK SYSTEM

The shock-inducing projectile was launched using a high-explosive system.[3] New simulations of the system and interpretation of the velocimetry record indicate that the projectile might have been accelerating on impact, and if so the shock pressure was not constant. Simulations also suggest that the projectile may be distorted on impact. Both effects would appear as a higher apparent temperature, suggesting that the NRS technique itself is likely to be more accurate than previously thought.

1 V.W.Yuan *et al.,* Phys Rev Lett, **94**, 125504 (2005).
2 D.J.Funk *et al*., Proc. 11th Intl Detonation Symposium, 1998, U.S. Office of Naval Research.
3 C.A.Forest *et al*, *ibid.*

Future Capability for Experiments on the Dynamic Behavior of Materials at the LANSCE Scientific Firing Site

D.C.Swift, W.V.Anderson, and K.Schoenberg

Los Alamos National Laboratory, Los Alamos, NM 87545, USA

INTRODUCTION

This is an exciting time in shock physics. Recently, great advances have been made in developing new techniques for applying the load to the sample, and in probing the response of the sample. It is now possible to investigate the response at the atomic level as well as the average or bulk response, and thus to explore the contribution of different physical processes to the behavior of the material. Atomic-level measurements and simulations are also converging so that direct comparisons can be made.

Some of the new experimental capabilities require large facilities such as particle accelerators, and it is common for an experimental facility to specialize in a subset of the capabilities desirable for a thorough characterization of material response and underlying physics. We are proposing to develop a new experimental facility based around an enhancement to the LANSCE accelerator at Los Alamos National Laboratory, which would build on the exceptional diagnostics afforded by LANSCE and combine them with a selection of loading techniques other diagnostics to maximize the rigor and accuracy with which dynamic loading measurements can be made. The configuration is designed to allow great flexibility in experimental configurations and efficiency in acquiring data.

The new facility will also allow experiments on warm dense matter and the development of applications for high-energy short-pulse lasers.

DYNAMIC LOADING AND DIAGNOSTIC CAPABILITIES

The LANSCE enhancement is expected to lead to a factor of $\sim 10^2$ increase in proton current, along with changes in pulse structure. The spallation neutron source will be reconfigured to allow shock experiments to be probed without the degree of disruption currently caused to other users. A prime driver for locating the Scientific Firing Site at LANSCE is to enable experiments to use proton radiography (pRad) and neutron resonance spectrometry (NRS) more routinely and with large improvements in signal, etc. Density and damage distributions can be reconstructed from pRad measurements, with the possibility of discriminating between materials of different composition. NRS measurements can detect the temperature and velocity within materials, even if optically opaque.

Loading methods will include a gas/propellant gun, containment vessels for high-explosive drives, a ~100 kJ class capacitor bank to launch flyers or induce ramp loading, and ~5 kJ class lasers capable of inducing shock or ramp loading by surface ablation (~1 to 10 ns pulse length) or of inducing loading or launching flyer plates by tamped ablation (~0.1-2 μs pulse length). Nanosecond laser pulses will also be used to generate x-rays for radiography and diffraction. It will be possible to preheat or precool the sample.

A suite of optical techniques will be available to measure velocity, displacement, electronic band structure (e.g. from multi-band ellipsometry), vibrational modes (e.g.

from Raman spectrometry), emission spectra, and particulate holography. These will require additional, lower-power probe lasers. A pulsed-power x-ray source will be used for radiography, diffraction, and *in-situ* imaging of defects during loading. A high-power short-pulse laser (100 J class, ~100 fs-1 ps pulse length) will be included in the facility, and could be used as an x-ray source, or even to accelerate electrons or ions. The facility will be configured and managed so that the core loading and diagnostic capabilities are readily accessible and well-maintained, while making it possible to develop new capabilities. Dynamic electron microscopy is a diagnostic which we plan to develop, possibly using a short-pulse laser pulse to accelerate the electrons. An important consideration will be the synchronization of the different loading methods and diagnostics: this will be made as straightforward, reliable, and reproducible as possible for users.

The experimental area will be laid out so that several different experiments can be performed simultaneously. In particular, this means that laser – and possibly proton – beams will be designed with flexibility in the beam transport. The facility will be licensed to perform experiments on toxic and radioactive materials, including plutonium.

EXPERIMENTS ON THE BEHAVIOR OF CONDENSED MATTER

The mainstay of shock physics experiments will be the well-diagnosed single-shot measurement. There is a huge opportunity to perform experiments on the effect of the microstructure of materials on their plastic flow properties, tensile damage leading to spall and ejecta, and phase changes. For these experiments, the microstructure must be well-characterized and often constructed to investigate some particular conformation of crystals or voids, and the loading history must be controlled and understood very well. For some studies, it may be advantageous to operate at a high repetition rate, e.g. to collect statistics of the onset of a phase change in a single crystal, translating the crystal automatically between shots. It may be possible to perform some such multi-shot experiments with laser loading.

We envisage a series of experimental campaigns exploring different aspects of shock physics and material dynamics, and employing a few basic experimental configurations:

- Equation of state to a few hundred gigapascals, driven by gun, pulsed power or laser, and using velocimetry and NRS, and possibly radiography.
- Phase change dynamics from a few to a few hundred gigapascals, loaded using all of the techniques, and probed using velocimetry, ellipsometry, Raman spectrometry, and x-ray diffraction.
- Plasticity, mainly at a few to a few tens of gigapascals, loaded by all techniques and probed with velocimetry, NRS, x-ray diffraction, and x-ray imaging of defects.
- Tensile damage and ejecta, loaded mainly by gun, pulsed power and explosives, and probed with velocimetry, pRad, x-ray radiography, and holography.
- Experiments on configurations representing parts of application systems, such as inertial fusion capsules.

A huge amount of science will be accessible in this way, and we anticipate that this flexible facility will make it possible to add currently unforeseen capabilities relatively painlessly further in the future.

Actinide Sample Preparation for Materials Science, Chemistry, and Physics

M. A. Wall, J. J. Welch, A. J. Schwartz, and M. J. Fluss

Lawrence Livermore National Laboratory, Livermore CA 94550 USA

Abstract

The development of the Actinide Sample Preparation Laboratory commenced in 1998 driven by the need to perform transmission electron microscopy studies on aged plutonium alloys. Remodeling and construction of laboratory space in the Chemistry and Materials Science Directorate at LLNL was required to turn a radiological laboratory into a type III workplace. A dry-train glove box (Figure 1) with a baseline atmosphere of 1 ppm oxygen and 1 ppm water vapor was installed to facilitate sample preparation with a minimum of oxidation or corrosion. This glove box continues to be the most crucial element of the laboratory allowing essentially oxide-free sample preparation for LLNL-based characterizations such as transmission electron microscopy, electron energy loss spectroscopy, optical microscopy, electrical resistivity, ion implantation, and differential scanning calorimetry. In addition, the glove box is used to prepare samples for experiments at world-class facilities such as the Advanced Photon Source at Argonne National Laboratory, the European Synchrotron Radiation Facility in Grenoble, France, the Stanford Synchrotron Radiation Facility, the National Synchrotron Light Source at Brookhaven National Laboratory, the Advanced Light Source at Lawrence Berkeley National Laboratory, and the Triumph Accelerator in Canada.

Preparation Methodology

Nearly all of the sample preparation procedures are based upon the fundamental metallographic preparation procedures of dicing, lapping, polishing, etching, and electrochemical polishing[1]. The experimental methodology for sample preparation and design is based upon a lowest common denominator shaped sample. Simple put, a standard 3mm diameter transmission electron microscopy (TEM) sample shape is the basic geometry for virtually all of the small scale science experiments. For example, prior to thinning a 3mm diameter by 100μm thick TEM disc to electron transparency it is possible to (i) prepare one side of the sample for optical microscopy (figure 2), (ii) perform standard X-ray diffraction, (iii) measure resistivity[2] (Figure 3), (iv) further thin for EXAFS[3] (Figure 4) and/or in-elastic X-ray studies[4] (Figure 5a,b), (v) finally thin for TEM studies (Figure 6a,b).

Conclusion

The combination of small sample methodologies, adapted conventional sample preparation techniques, and custom built laboratory and glovebox designs has lead to versatile, efficient sample preparation of actinide samples for a wide variety of small-scale experimentation.
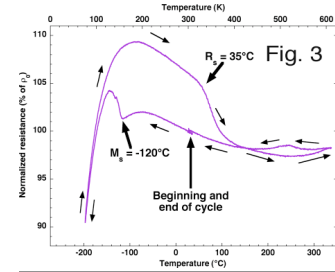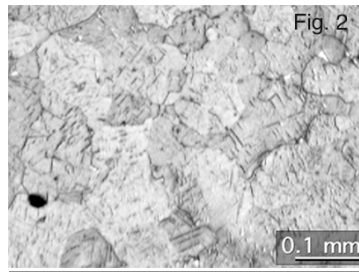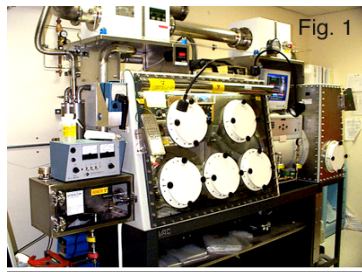
Figure 1. Glove box for small-scale sample preparation. **Figure 2**. Optical micrograph of a delta phase Pu-Ga sample after partial transformation to alpha-prime as a result of quenching to -120° C for $\approx$100 minutes. **Figure 3**.   Resistivity data from a cooling and heating cycle of a Pu-Ga "TEM" disc specimen.
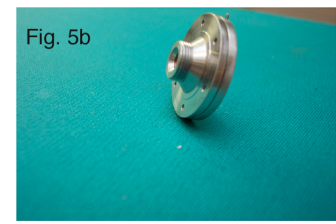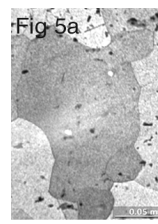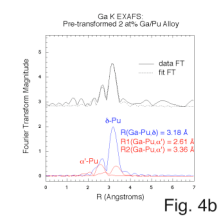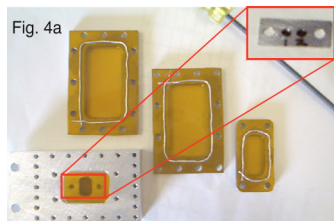

Figure 4.a) Insert shows 2 each, $\approx$10µm thin, "TEM" disc specimens that will be sealed inside a double Kapton windowed holder for EXAFS experiments. b) EXAFS data from a two-phase delta-alpha Pu-Ga sample. **Figure 5**.a) Optical micrograph of a large grain grown by stain-annealing for in-elastic X-ray experiments that produced the first measurements of

the FCC Pu phonon dispersion curves. b) Double Kapton windowed sample holder for $\approx$8 µm think "TEM" disc samples used for the phonon dispersion experiments. **Figure 6** a) Bright field TEM image of alpha-prime plates in a delta matrix. b) Electron diffraction from the alpha-prime plates and the delta matrix showing the Zocco orientation relationship.
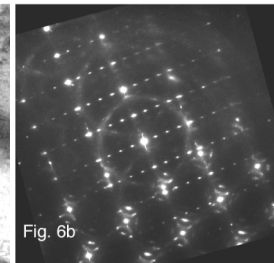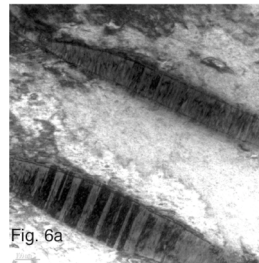
References:
1) Sample Preparation for Transmission Electron Microscopy Characterization of Pu Alloys, M. A. Wall, A. J. Schwartz and M. J. Fluss, LLNL report, # UCRL-ID-141746..
2) Phase Transformation Hysteresis in a Plutonium Alloy System, J.J. Haslam, M.A. Wall, D.L. Johnson, D.J. Mayhall, and A.J. Schwartz, MRS Proceedings, 2001, UCRL-JC-144283.
3) Local structure and vibrational properties of Alpha-Pu, Alpha-U, and the Alpha charge density wave, E. Nelson, P. Allen, K. Blobaum, M. Wall, C. Booth, Phy. Rev. B 71, 184113 (2005).
4) Phonon Dispersions of fcc -Plutonium-Gallium by Inelastic X-ray Scattering, Joe Wong , M. Krisch, D. Farber, F. Occelli, A. Schwartz, T.C. Chiang, M. Wall, C. Boro and Ruqing Xu, Science, 301, 1078 (2003).

Reinvestigating plutonium phase transitions using high purity electro-refined metal

A. Perry, M. Boyd, P. Roussel

AWE Aldermaston, Berkshire, UK, RG7 4PR

Plutonium is a unique element. In the pure state is has six temperature induced metallic phases. These phases start in the unusual monoclinic α-phase progressing through monoclinic β, orthorhombic γ to cubic (face centred) δ-allotrope. The transition from α to δ is accompanied by a 20 % density decrease. In the δ phase plutonium undergoes negative thermal expansion changing to the tetragonal δ' and finally increasing density by 4.6 % to the cubic (body centred) ϵ phase. It should be noted that there is some discrepancy within the literature on the actual transition temperatures. For example, the α to β transition has been reported in the range of 119 to 127 °C. This may arise from differences in sample purity and scan rates. Indeed, the δ' phase was only detected when metal of high purity became available.

These six temperature induced phases have been investigated in detail using a high purity electro-refined plutonium sample by dilatometry, differential scanning calorimetry and X-ray diffraction a function of heating rate.

Evaluation of the nucleation and growth of helium bubbles in aged Plutonium alloys

D.W.Wheeler, P.D. Bayer, A. Perry, S. Kitching

AWE, Aldermaston, Reading, Berkshire, RG7 4PR, UNITED KINGDOM.

The processes of radioactive decay that take place in plutonium alloys can result in significant changes to their physical, chemical and mechanical properties. In order to understand the ageing behaviour of Pu alloys it is necessary to construct a model which will enable these changes to be quantified. The present study was undertaken to determine experimentally the fundamental parameters needed for such a model. Pu alloys of different ages and compositions were analysed using dilatometry to measure bubble growth and void swelling. The specimens were subjected to isothermal heat treatments for extended durations followed by metallographic examination in order to study the microstructures. Density measurements were also performed on the alloys while the effect of ageing on the mechanical properties was studied by hardness testing.

The results have enabled the calculation of the diffusion coefficient of He in Pu from the bubble size, bubble density and inter-bubble distances. The diffusion coefficients of He in Pu at elevated temperatures appear to be close to that of Ga in Pu. Extrapolation of the swelling rates from the elevated temperatures has predicted a density decrease of 0.0004 g cm^{-3} per annum at ambient temperature. However, there are no indications of the onset of steady state void swelling in 40 year old Pu.

"PuGa and PuAl alloys density measurements using gas pycnometer: first results."

O. Ast, S. Carlet, M. Perez, Boiteux.O.

CEA Valduc, DRMN/SEMP, 21120 Is sur Tille, FRANCE.

Plutonium alloys density is an important data to determine some metallurgical and mechanical parameters like martensitic (α') phase fraction (in relation with delta phase stability study) and elastic constants versus pressure (in relation with ultra sonic waves measurements). Density also gives some information about the quality of casting through its sensitivity to impurities contents. Generally, Archimede's technique is used to measure the volume of sample[1] and the density is determined by using the following equation: M/V (where M is the mass and V the volume of the sample). This technique has however a lot of limits:

- performing this measurement is difficult due to the difficulty to put the sample in the right location;
- accuracy is limited (from 0.05 to 0.1 g/cm^3) and depends on the weight of the sample;
- as it follows, large samples are necessary which is not always possible.

The gas pycnometer technique has been developed in glove box to improve the quality of density measurements. This presentation describes the principle of this technique and the process which is used. The second part is devoted to the first results on plutonium alloys and the accuracy of measurements.

The pycnometer determines density and volume by measuring the change in pressure of helium in a calibrated volume. The principle of this process is based on Marriott's law. The process frequently used, shown on figure 1, is described below.

The expansion chamber contains a volume of helium at a precise pressure. After introducing the sample in the sample chamber, difference in pressure is precisely measured between the expansion chamber and the sample chamber which allows determining the sample's volume.
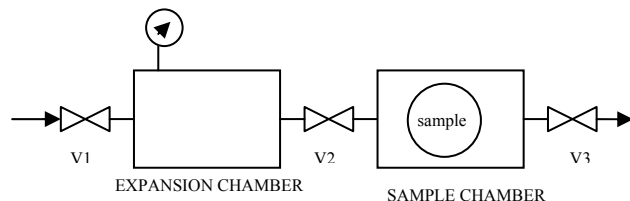

Fig 1: Schematic diagram explaining the gas pycnometer's process.

Steel and tantalum density measurements using this technique, have been performed and the accuracy has been improved (accuracy of tantalum density with pycnometry is 0.006 g/cm^3 whereas it is 0.02 g/cm^3 with Archimede's technique). Density measurements on nuclear materials are more difficult, especially for the plutonium alloys, for which we have to consider :

- the temperature instability (due to self heating and thermal expansion),
- the pressure instability due to the pressure variation in the glove box.

The second part of this work presents the study of the capability of the process (repeatability and reproducibility measurements). Some experiments have been performed on different delta stabilized plutonium alloys: PuGa 2,2 and 3,7 at% and PuAl 5 and 2 at%.

A metallurgical characterization of the alloys has been performed:

- grain size and microhardness;
- impurities (gallium, aluminum, carbon, oxygen, iron and nickel) X maps;
- alloying element contents profiles (microsegregation profiles) using EPMA.

First density measurements will be presented and compared with crystallographic density deduced from XRD measurements on the same batch of samples and from litterature [2].

The future studies aim at improving accuracy by working on the sample geometry and by using the real temperature of the sample given by modeling. Concerning aging studies, it will be interesting to study the density changes versus time. A comparison of swelling measurements by thermal expansion and density will also be done.

References

1   R.D Nelson, C. R. Becker, T. K. Bierlen, F.E. Bowman, AEC Research and Development Report, HW-80841, UC-25, Metals, Ceramics, and materials (TID-4500, 34th Ed.), (1964).
2   D.C. Miller and J.S White, Journal of Nuclear Materials 10, 4. 339-345, (1963).

Delta-phase stability in plutonium-aluminum alloys

P Bruckel[*], B. Ravat[*], L. Jolly[*], N. Baclet[*], V. Honkimaki[†], G. González Avilés[†]

[*]CEA Centre de Valduc, 21120 Is-sur-Tille FRANCE
[†]ESRF, beamline ID15, 38000 Grenoble FRANCE

INTRODUCTION

The δ-phase of plutonium is stable between 592K and 724K but can be retained at room temperature by alloying plutonium with so-called deltagen elements (gallium, aluminum, americium, cerium…). The stability of the δ-phase strongly depends on several parameters such as the deltagen-element concentration, the metallurgical state of the alloy, the temperature and the pressure [1].

In this paper, the stability of the δ-phase in Pu-Al alloys is investigated. In a first part, the degree of stability of the δ-phase at low temperatures is discussed whereas a second part deals with the mechanisms of stabilization of the δ-phase.

EXPERIMENTAL

After casting and cutting of Pu-Al alloys with various aluminum concentrations (1.8, 2.3, 3.0 and 5.8 at%Al), one half of the Pu-Al samples is homogenized during 200 hours at 723K. The second half (as-cast samples) is considered as segregated (Figure 1). A 6 hours annealing at 533K is then performed to restore the metallic structure. Before any experiments, samples are electropolished to remove surface oxides and other possible impurities.

Chemical analyses are performed by Electron Probe MicroAnalysis (EPMA). Lattice parameters are deduced from Rietveld analysis of the X-Ray Diffraction patterns (XRD). Metallurgical state is characterized by using Optical Microscopy (OM) and EPMA (elements imaging).

The degree of stability of the δ-phase in Pu-Al alloys is characterized by the martensitic transformation temperature (M_S) determined from electrical resistivity measurements performed from 300K down to 4K. Influence of both the Al-concentration and the metallurgical state is investigated.

To go further, the mechanisms of stabilization of the δ-phase are studied by X-ray Total Scattering (XTS). Experiments are performed at room temperature at ESRF on the Pu-Al samples described before. The beamline ID15 allows working with an incident beam of high energy (~90 keV) that is particularly suitable for Pair Distribution Function analysis (PDF) [2]. The PDF-method requires a good counting statistic and thus small and equiaxed grains. Therefore, samples of 300 µm thick are rolled to get a final thickness of 140
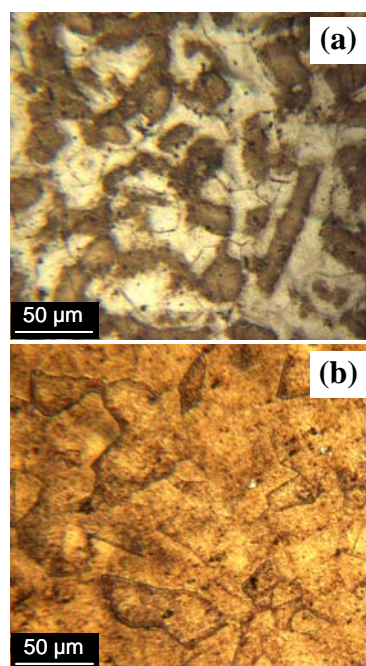

Fig 1: Micrographs of a PuAl 3at% alloy (a) in the segregated state and (b) in the homogenized state.

μm: the high mechanical strain (53%) associated to the rolling of the samples is used, in combination with an annealing treatment of 20 hours at 723K, to get small and equiaxed recristallized grains.

DEGREE OF STABILITY OF THE δ-PHASE

For δ-stabilized Pu-alloys and depending on the deltagen concentration, a decrease in temperature can lead to a martensitic transformation which product, labeled " α' " , is monoclinic with solute atoms trapped in the structure [1]. The martensitic transformation is characterized both by the temperature at which the transformation starts (M_S) and the amount of α'-phase formed. An increase in the aluminum content leads to a decrease in both the M_S temperature and the amount of α'-phase formed [1] (Figure 2), in agreement with a higher stability of the δ-Pu alloys.

Another parameter that might have an influence on the martensitic transformation is the metallurgical state of the Pu-Al alloys. In the segregated state, local micro-segregations of the Al-solute are observed (MO and EPMA): consequently, both the α- and δ-phases are present on XRD-patterns. The question lies on whether the already present α-phase makes it easier for the α'-phase to form.

Fig 2: Electrical resistivity versus temperature for the homogenized PuAl 2.3 and 3 at% Al alloys.

STABILIZATION MECHANISM OF THE δ-PHASE

The mechanisms for δ-phase stabilization in δ-Pu alloys have been widely studied, though they are still not well understood, and are known to be strongly related to the electronic structure of the plutonium atoms. Furthermore, the electronic structure of Pu-alloys is directly related to their local structure.

The aim of XTS experiments coupled to PDF-analysis is to characterize the local atomic arrangement in Pu-Al alloys, depending on their composition and metallurgical state. By now, Conradson *et al.* have shown that a new phase labeled " σ " coexists with the δ-phase in Pu-Ga alloys containing 1.70 at %Ga to 3.35 at %Ga [3]: the σ-phase is assumed to be organized in nano-domains acting as precursors for a further martensitic transformation. Since the electronic structure of aluminum and gallium are equivalent, it might be assumed that the same mechanism is responsible for the stabilization of the δ-phase in Pu-Al and Pu-Ga alloys.
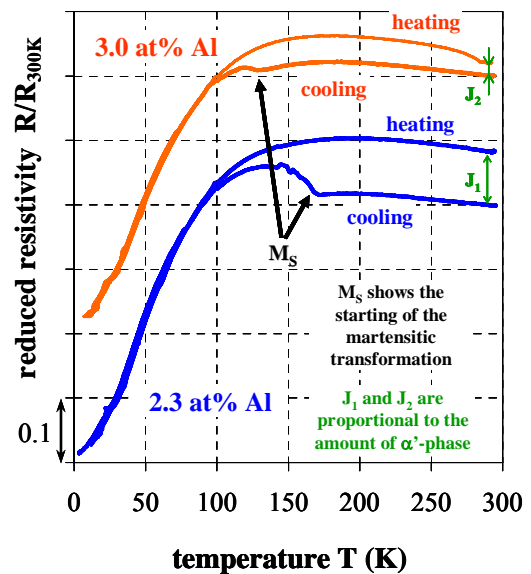
1   S.S. Hecker, Los Alamos Science, **2**, (2000).
2   T. Egami and S.J.L. Billinge, Underneath the Bragg peaks: structural analysis of complex materials, Pergamon Materials Series, **7**, (2003).
3   S.D. Conradson, Applied Spectroscopy, **52**, (1998).

THE INFLUENCE OF INTERNAL STRESSES INDUCED BY DECAY PRODUCTS ON ORIGINATION ON β - PHASE NUCLEATION DURING α→β TRANSFORMATION OF UNALLOYED PLUTONIUM UNDER ISOTHERMAL CONDITIONS.

A.V. Troshev, A.M. Lyasota, S.I. Abramenko, Yu.N. Zuev, B.V. Litvinov

Academician E.I. Zababakhin All-Russia Research Institute of Technical Physics,
456770, Snezhinsk, Chelyabinsk region, PO Box 245

INTRODUCTION

It has been found that α-decay of plutonium leads to 'self-induced' defects in the lattice and to changes of chemical composition. It is expected that these changes at atomic level should modify of plutonium physical properties with time.

Successes in research of the problem of 'plutonium self-irradiation' at cryogenic temperatures so far do not allow prediction of plutonium behavior at high temperatures. There are at least two reasons explaining difficulties of plutonium research at high temperatures. First, as well known "general observations of self-irradiation damage show no major macroscopic changes for at least 40 years – in other words, plutonium does not "crumble" [1]. That is critical changes of plutonium properties do not occur during this time. However relying on results of studies of irradiation effects on metals and alloys we can make a reasonable assumption that plutonium is so far in so called 'incubation period' of properties alteration. In this case we need research techniques quite sensitive to plutonium changes at nano- and micro-level. Second, it is clear from general notions, that thermodynamically stimulated processes transpire in metal at high temperature and these process are associated with a trend of reduction of the system intrinsic energy. Stress relaxation as a rule occurs as a result of plastic strain and diffusion processes. It is clear that this evolution of metal structure without reference to specific experimentally observed structure-dependent phenomena complicates interpretation of experimental data.

Technique of plutonium research based on measurements of kinetic dependencies in phase transformations will meet the points above as we know that kinetics of plutonium phase transformations is highly sensitive to kinetics of structure defects alteration [2].

In the present paper we report the results of the first experimental studies of kinetics of α→β-transformation in plutonium after long self-irradiation and the issues of measurement of quantities of excess energy accumulated as a result of α-decay and experimental studies of these energy relaxation kinetics.

EXPERIMENTAL RESULTS

Results of studies of isothermal phase transformation kinetics directly in plutonium performed with samples containing different levels of impurities and with nearly equal low rate of self-irradiation one more time confirm in our view the appropriate sensitivity of this technique to the level of structural defects (Fig.1).

Curves recorded from the sample with high rate of self-irradiation have demonstrated noticeable change of transformation parameters compared with initial state (Fig.2). Thus the change of chemical composition as a result of accumulation of α,β-decays products had a value by several orders of magnitude lower than initial level of impurities content. This indicates to significant (for transformation kinetics) change of metal structure specifically as a result of self-irradiation. Kinetic curve describing phase transformation in a sample with even higher rate of self-irradiation is illustrated in Fig.3. Here kinetic curve demonstrates not only noticeable alteration of transformation parameters, but also it has specific features: smooth trend of the curve is changed by stops at transformation that occur many times and are clearly observed.
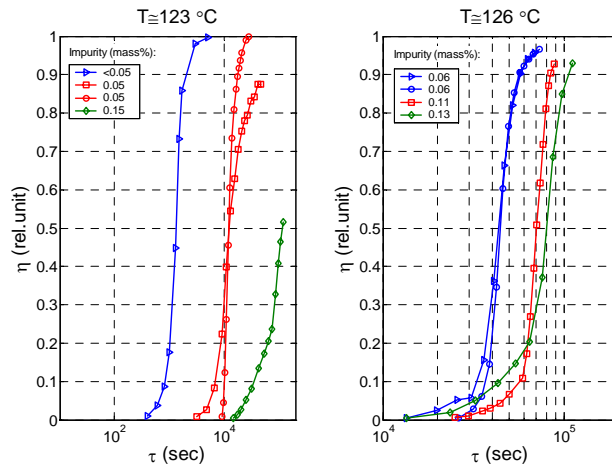
Fig.1 Kinetic curves of transformation for
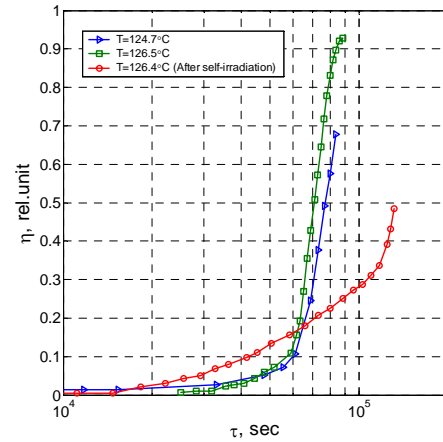the samples with different content of impurities.

Fig.2 Changes of transformation kinetics
as a result of self-irradiation

We have applied a classical approach to the issue of new phase origination at polymorphous transformation in single-component solid body for interpretation of these data [2]. According to this theory nucleation of new phase in a solid body occurs when the group of atoms overcomes the potentials barrier due to fluctuations and the energy of this barrier is proportional to the energy on the interface between the old and the new phase. It is assumed generally that the surface energy is an insurmountable barrier to transformation. Therefore the rate of phase transformation is essentially determined by the depth of elastic stress relaxation in subsurface zone of two phases interface. Accepted that the most efficient relaxation of elastic stress occurs as a result of plastic strain. Then two phases interface should be surrounded by a mesh of dislocations. Noteworthy that such dislocations mesh should have certain mobility sufficient for coalescence and growth of a new phase nuclei. We now from hardening theory that mobility of dislocations is finally determined by the dislocation elastic stress fields and the barriers to this mobility glide.

Fig.3 Variation of transformation kinetics
at increase of self-irradiation rate.

Hence we come to a hypothesis that centers of elastic deceleration occur in a metal as a result of self irradiation and these centers decelerate dislocations (reduce dislocation mobility). Therefore extent of hardening will be determined by location and dimensions of these centers. Stops at the curve (Fig.3) correspond to kinetic processes leading to softening. According to this curve the softening process has several stages that testifies to the range of structure defects having different energies.

Thus the energy of structural defects may be apparently determined from the ratio of transformation driving force proportional to exposure temperature and the sum of elastic stresses involved in nucleus origination.
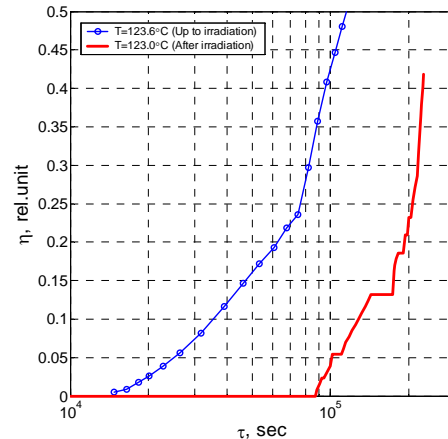
References:
1. Sigfried S. Hecker, Joseph K. Marts. Ageing of plutonium and its alloys. Los Alamos Science. Number 26, (2000).
2. J. W. Christian. The theory of transformations in metals and alloys. Part 1: Equilibrium and general kinetic theory. Pergamon press. 1975.

Semiempirical Models for Describing Thermodynamic Properties of f-metals

V. M. Elkin, E.N. Mikhaylov, E.A. Kozlov

Institute of Technical Physics (RFNC-VNIITF), Snezhinsk, Russia 456770

ABSTRACT

The unusual thermodynamic properties (the abnormal behavior of elastic and thermophysical characteristics and the complicated and contradictory phase diagram) of some metal with unfilled f-shells (4f and 5f) are attributed to the close energies of electronic configurations. According to the present views, the electronic states differ either in the degree of spin screening of localized f-electrons (Kondo volume collapse model), or in localization and delocalization of f-electrons (Mott transition). At finite temperatures, thermodynamically stable states of a compound of atoms of different electronic structures may exist. From the literature we know about two, very similar semiempirical models which describe the states of a compound of different atoms. These are Strässler-Kittel two-level model and Aptekar-Ponyatovsky model for pseudo-binary solid solutions.

This paper studies capabilities of these models to describe the thermodynamic behavior of unalloyed cerium (4f metal), and unalloyed δ-plutonium and δ-plutonium-based alloys (5f-metals). It shows that with a small number of fitting parameters, both models adequately describe the abnormal behavior of these metals under varying temperature and pressure. However, Aptekar-Ponyatovsky model is preferable for practical purposes because it relates electronic structures to polymorphic modifications thus providing a basis for the construction of a multi-phase equation of state.

Experiments and model of dynamic deformation of U-238 and its alloy with Mo

B.Glushak, V.Pushkov, O.Ignatova

Russian Scientific-Research Institute of Experimental Physics, 607190, Sarov, Russia

INTRODUCTION

The results presented in this communication were gained by an analysis of the dynamic diagrams of uniaxial compression and tension of U-238 and its alloy with Mo (~1 wt %). The yield strengths presented in this study were assessed from the diagrams at different strain rates of $\acute{\varepsilon}$≤1800 1/s and initial temperatures T≤600°C. The data obtained served as a basis for a semi-empirical model at the heart of which was an equation of state of U-238 and its alloy with Mo[1,2]. Measurements were taken by the split Hopkinson pressure bar (SHPB) method[3].

EXPERIMENTAL RESULTS

Compression. Yield strengths $\sigma_{-0,2}$ calculated from the σ-ε diagrams at different T and $\acute{\varepsilon}$ values for uranium and its alloy with Mo are summarized in Table 1. The yield strength $\sigma_{-0,2}$ of the uranium alloy with molybdenum increased in proportion to the strain rate $\acute{\varepsilon}$ and decreased almost linearly with increasing temperature[2,3].

Tension. The yield strength and tensile strength of uranium measured at T~0°C and $\acute{\varepsilon}$ =1000 1/s were $\sigma_{+0,2}$ = (470 ± 78) MPa and σ_{+B} = (650 ± 83) MPa, respectively. The samples failed at a percent elongation from 4,0 to 4,2%. The yield strength and tensile strength of the uranium alloy with Mo were $\sigma_{+0,2}$= (900 ± 56) MPa and σ_{+B} = (1080 ± 62) MPa, respectively, at $T \sim$ 0°C and $\acute{\varepsilon}$ =1200 1/s. The samples were destroyed at a percent elongation of 15%[1,2,3].

Table 1. Yield strengths data

T, °C	U-238		U-238+Mo	
	$\acute{\varepsilon}$, 1/s	$\sigma_{-0,2}$, MPa	$\acute{\varepsilon}$, 1/s	$\sigma_{-0,2}$, MPa
20	100-420	565±42	280-360	760
	1300-1600	660±80	600-880	868±54
			1000-1400	990±70
100	520-1040	446±48		
200	160-1440	440±30	350-510	580±30
			800-1100	665±18
			1300-1800	720±67
400	540-890	300±13	200-520	370±40
			800-1000	426±52
			1200-1700	500±35
600			200-500	275±35
			850-1000	330
			1200-1400	360±26

MODEL FOR DYNAMIC DEFORMATION OF U-238 AND ITS ALLOY WITH MO

Consider U-238 and its alloy with Mo as an elastoplastic medium such that its stress strength σ_i can be represented as a function of four variables defining its strained state; in the simplest case, σ_i is a product of four simple functions f_i, each dependent on only one variable[2,4]:

$$\sigma_i = \sigma_i(\varepsilon_i, \dot{\varepsilon}_i, P, T) = A f_1(\varepsilon_i) f_2(\dot{\varepsilon}_i) f_3(P) f_4(T) \qquad (1)$$

Function $f_1(\varepsilon_i)$ in Eq.(1) allows for strain strengthening, $f_2(\dot{\varepsilon}_i)$ and $f_3(P)$, for the effects of the rate of plastic strain and pressure, respectively, and $f_4(T)$, for thermal softening. Function $f_3(P)$ looks as[2,5] $f_3(P) = 1 + \alpha_0 P$, where $\alpha_0 = $ const.

Dependence (1) was approximated by the following analytical function

$$\sigma_i = A \cdot [1 + a(\varepsilon_i)^m] \cdot \left[1 + b\left(\frac{T}{T_{ml}}\right)^n + d\left(\frac{T}{T_{ml}}\right)^k\right] \cdot \left[1 + c\left(\ln\frac{\dot{\varepsilon}_i}{\dot{\varepsilon}_{i0}}\right)^l\right] \cdot f_3(P); \qquad (2)$$

here, A, a, b, c, d, n, m, l, and k are constants, $\dot{\varepsilon}_{i0} = 1$ s^{-1}, and T_{ml} is the melting point.

Poisson's ratio μ is supposed to be a linear function of temperature, $\mu = 0{,}205 + 8{,}7\cdot10^{-5}T$, where T is an absolute temperature. By way of illustration, the experimental values of the conditional yield strength $\sigma_{-0,2}$ measured under dynamic compression are compared to their theoretical counterparts[2] calculated from Eq.(2) in Figure1.

The range of validity of the proposed model for dynamic deformation of U-238 and its alloy with Mo is[2]: P≤ 5 GΠa, $\varepsilon_i \le 0{,}12$, $\dot{\varepsilon}_i \le 2\cdot10^3$ 1/s, 293≤ T ≤873 K.
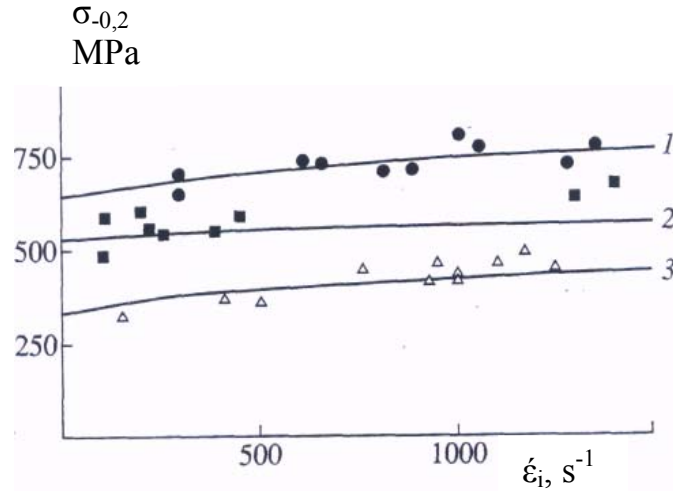

Fig 1: Conditional yield strength in the case of dynamic compression: (1)-T=293K, U-238+Mo; (2)-T=293 K, U-238; (3)-T=673K, U-238+Mo; (■, △, ●) experimental data; solid curves were calculated.

1. B.L. Glushak, *et al.*, Proceedings of abstracts of papers for the XIV International Conference "Effect of intensive flows of energy on substance", Terskol, Russia, 96, (1999).
2. S.A. Novikov, V.A. Pushkov, *et al.*, J. Chemical Physics (Rus), **18**, №10, 22-25, (1999).
3. S.A.Novikov, V.A.Pushkov, *et al.*, Mechanical Properties of Uranium under Quasi-static and Shock-Wave Loading, Preprint No.54-97, Russia, RF Nuclear Center: Scientific-Research Institute of Experimental Physics, (1997).
4. D.Steinberg, S.Cochran, and M.Guinan, J. Appl. Phys., **51**, No.3, 1498, (1980).
5. B.L. Glushak O.N.Ignatova, J. VANT (Rus). Matematicheskoe Modelirovanie Fizicheskikh Protsessov, **2**, (1998).

Melting and Crystallization Front Induced Processes in a d-phase Pu Alloy Exposed to Laser Pulses[*]

A.V. Laushkin, V.K. Orlov, P.P. Poluectov, M.Yu. Bakursky, S.A. Kiselev, I.A. Larkin

A.A.Bochvar Research Institute of Inorganic Materials (VNIINM), Moscow, Russia

Behavior of gas pores in a liquid gas-saturated plutonium over a temperature range from the melting point to ~2000 ^{o}C is phenomenologically described. A d-phase plutonium alloy was tested. The elapsed time from the Pu alloy production was 13 years. In this period the sample accumulated about 500 ppm of helium.

Pore formation and growth processes (metallography, calculation of pore size changes) are described. Photos are presented showing the pore coagulation instant. A process initiated by motion of a crystallization front is discussed that is most likely responsible for the pore structure (Figure 1).

Fig 1: Photomicrograph of a cross-sectional microsection.

The kinetic viscosity of the alloy at about 1900 ^{o}C was estimated from eddy flows generated in a bath of the molten alloy.

[*] The sanction to an information exchange: dd-2071.

RFNC-VNIIEF Capabilities to Production High Enriched ^{242}Pu and ^{244}Pu

S.Vesnovskiy

Russia Federal Nuclear Center - VNIIEF, Sarov, Nizhni Novgorod Region, 607188, Russia

The report considers the possibilities of producing highly enriched isotopes ^{242}Pu and ^{244}Pu using a method of electromagnetic separation of **plutonium** isotope mixtures with different content of ^{242}Pu and ^{244}Pu. Different isotope compositions that can be produced in Russia through neutron irradiation of ^{242}Pu in a nuclear reactor with high density of neutron flux at various start materials and different irradiation duration are studied as original material. There are proposed optimal versions of ^{244}Pu production at the rates enough to realize investigations of fundamental plutonium properties and processes of its ageing. Preliminary estimations of the cost of these isotopes production are given.

Isothermal martensitic phase transformations

in plutonium gallium alloys

B. Oudot, K.J.M. Blobaum, M.A. Wall, A.J. Schwartz

Lawrence Livermore National Laboratory, Livermore CA 94552 USA

INTRODUCTION

Under ambient conditions, the thermodynamically stable phase of pure plutonium is the brittle monoclinic alpha phase. However, the high-temperature delta phase (δ) can be retained at room temperature by alloying plutonium with a few atomic percent of gallium [1]. For Pu-Ga systems at ambient conditions, the retained δ phase is metastable and undergoes an extremely slow eutectoid decomposition to alpha (α) + Pu_3Ga. When the metastable δ phase is cooled to sub-ambient temperatures, a partial transformation to the alpha-prime (α') martensitic phase occurs. This α' phase is similar to the α phase, but it has Ga trapped in the lattice. Previously, the δ to α' phase transformation (at about -100 ºC) and its reversion (at about 30ºC) have been studied using cooling and heating cycles in a differential scanning calorimeter (DSC) [2]. Here, we investigate the kinetics of the δ to α' transformation in a Pu-2.0 at% Ga alloy under *isothermal* conditions. This δ to α' transformation is reported by Orme, *et al*. [3] to have unusual double-C curve kinetics in a time-temperature-transformation (TTT) diagram. Our work extends this TTT diagram from 200 minutes to 18 hours.

RESULTS AND DISCUSSION

The amount of α' formed during long isothermal holds at specific sub-ambient temperatures between -90ºC and -160ºC was investigated using DSC. For each experimental run, the sample was cooled from 25ºC to the isothermal hold temperature at 20ºC/min. Then it was held at a subambient temperature for 18 hours, heated to 350ºC and cooled back to 25ºC at 20ºC/min. Prior to each experimental run, the sample was annealed at 375ºC for 8 hours and then conditioned at 25ºC for 12 hours [4, 5]. The amount of α' formed during each isothermal hold was quantified using the area of the α' to δ peak observed during the heating portion of the scan.

Orme, *et al*.'s work does not explicitly define time zero, but the TTT diagram indicates that transformation does not occur above -120°C. Therefore, for the present experiments, we define time zero as the time when the sample temperature reaches -100°C. This time is indicated on the cooling portions of the DSC scans shown in figure 1. The data shown in figure 1 was collected as the samples were cooled to the isothermal hold temperature. In this figure, it is clear that some δ to α' transformation did occur prior to each isothermal hold, except before the hold at -90°C.

The transformation prior to the isothermal hold is observed as several overlapping exothermic peaks beginning at about -102°C. These peaks are very reproducible and are believed to be the result of different kinds of δ to α' martensitic transformation. This may be due to the presence of different nucleation sites and/or different morphologies.

The results of the 18 hour isothermal holds give a cross-section of the TTT diagram at 18 hours, as shown in figure 2. Instead of plotting a contour line of constant amount of transformation, as is traditionally done in TTT diagrams, the contour in figure 2 is for constant time. This data suggests a confirmation of the double-C behavior because there are two temperatures at which local maxima in the amount of transformation occur (-130°C and -155°C). Between these two temperatures, there is a valley at -145°C where isothermal holds result in smaller amounts of transformation. Thus, the results presented here suggest that the isothermal δ to α' transformation has double-C curve kinetics, even when the transformation is allowed to proceed for times significantly longer than those included in the TTT diagrams published by Orme, *et al.*
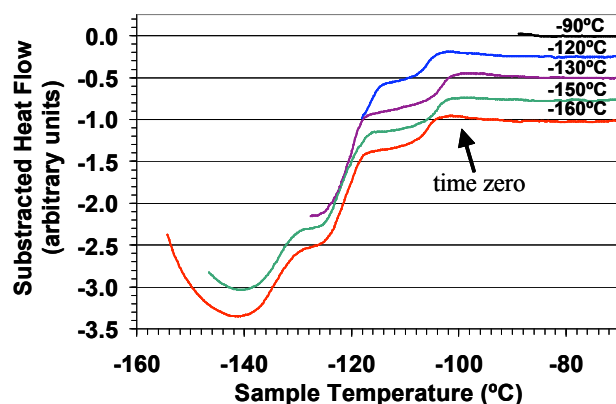
Figure 1. DSC thermograms corresponding to the δ to α' transformation during continuous cooling at 20°C/min before each 18 hour anneal. Transformation begins at about -102°C. The transformation results in and is evidenced by 3 overlapping exothermic peaks. The data have been offset along the y-axis for clarity.
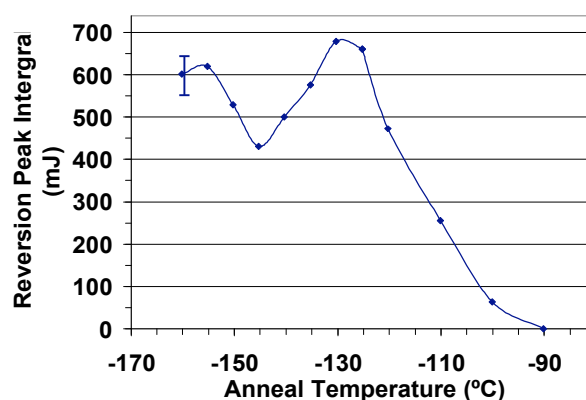
Figure 2. Integrated peak areas of the α' to δ reversion peaks following 18 hour isothermal holds versus anneal temperature. The amount of α' formed is related to the integrated area of the α' to δ reversion peak. Several runs with holds at -160°C give an approximation of the error, which is less than ±50 mJ.

REFERENCES

*[1]. F.H. Ellinger, C.C. Land and V.O. Struebing, J. Nucl. Mater., **12**, 226,(1964).*

[2] K.J.M. Blobaum, C.R. Krenn, J.N. Mitchell, J.J. Haslam, M.A. Wall, T.B. Massalski, and A.J. Schwartz, accepted by Metallurgical and Materials Transactions, 2005.

[3] J.T. Orme, M.E. Faiers and B.J. Ward, Plutonium 1975 and Other Actinides, (edited by H. Blank and R. Lindner, North-Holland Publishing Company, Amsterdam, 1975), pp. 761.

[4]. K.J.M. Blobaum, C.R. Krenn, M.A. Wall, T.B. Massalaki and A.J. Schwartz : to be submitted to Acta Mat., 2006

[5] See a separate paper entitled "Evidence for formation of alpha embryos in a Pu-Ga alloy at ambient temperature" by K.J.M. Blobaum, C.R. Krenn, M.A. Wall, T.B. Massalski, and A.J. Schwartz in this volume.

Mechanical Property Measurements using Micro Test Bar for Pu Alloy Aging Study

B. Choi[*], B. Ebbinghaus[†], G. Gallegos[†]

[*] Lawrence Livermore National Laboratory, Livermore CA 94552 USA
[†] Lawrence Livermore National Laboratory, Livermore CA 94552 USA

ABSTRACT

Modeling of the mechanical strength as a function of helium bubble in growth predicts that there can be a significant increase in the yield strength of plutonium if the helium bubbles are pressurized. For example if there is a He to vacancy ratio of 2, the increase in yield strength is about 30% in 100 years. Such a change is potentially important in assessing the lifetime of plutonium phase stabilities and in order to confirm the predictions of the model and the limited experimental data systematic tensile testing and possibly some hardness testing have been conducted on new and aged alloys.

This paper summarizes how strain rate (quasi-static), fabrication process history and prior thermal history affect the tensile property change observed from both naturally and accelerated aged plutonium alloys. For this study, the "micro tensile" test bar (about 0.060 inch diameter) and corresponding tensile test fixture has been developed and verified for use in measurement of tensile properties for the plutonium alloys under general tensile loading conditions. Initial testing has been conducted using 1100-H18 as a surrogate.
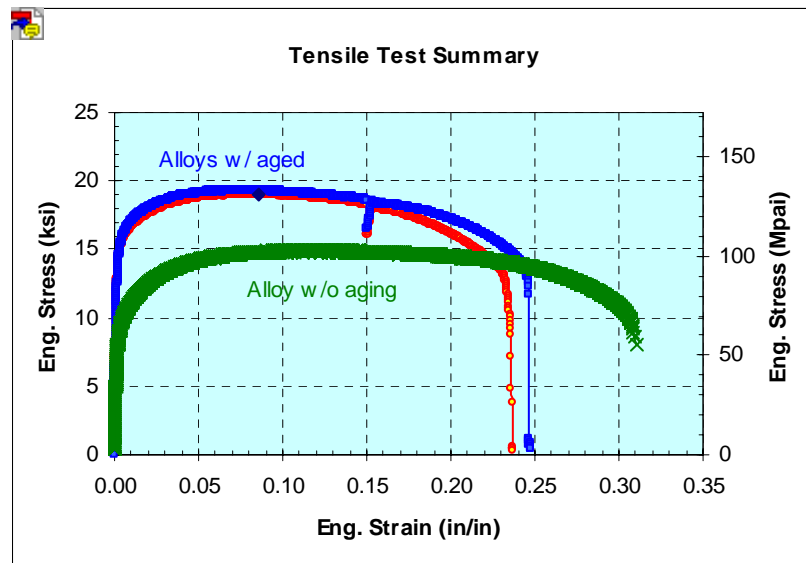
Fig 1: Engineering stress and strain
curve from tensile test results for the
delta-stabilized plutonium alloys

X-Ray Diffraction of Aged U-Nb Alloys

H.M. Volz, R.E. Hackenberg, A.M. Kelly, W.L. Hults, A.C. Lawson, R.D. Field, D.F. Teter, and D.J. Thoma

Los Alamos National Laboratory, Los Alamos, NM, 87545 USA

ABSTRACT

Uranium alloys exhibit many different stable and metastable phases, including martensite. An improved understanding of phase stability of actinides would be advantageous. In particular, we are interested in the aging of U-Nb alloys. To this end, compositionally homogeneous U-5.5 Nb and U-7.5 Nb (wt%) experimental specimens have been artificially aged by heating to temperatures of 373K, 473K, 523K, and 573K for times ranging from 10 to 100,000 minutes. It is desirable to understand any long-term changes in the structure of these materials in order to improve predictions of materials properties over time, but changes may be subtle and elude standard metallographic techniques. Therefore, we collected powder diffraction patterns on these aged polycrystalline U-Nb samples using a laboratory X-ray diffractometer (CuKα source) along with a CeO_2 standard (Figure 1, below) and analyzed using full pattern Rietveld analysis with GSAS (Figure 2, next page). Surface preparation was achieved by mechanical and
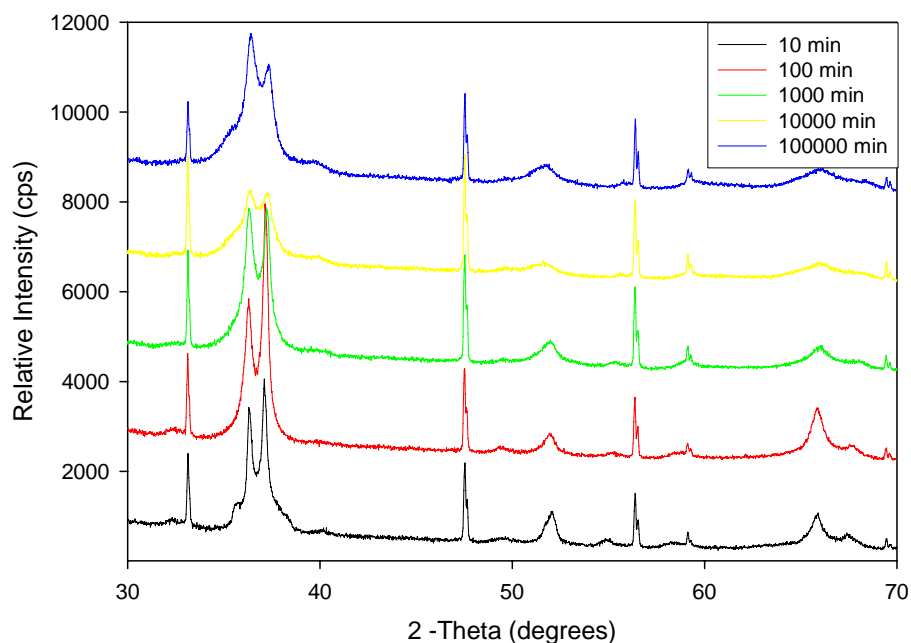
Fig 1: X-ray diffraction data of a U-7.5Nb alloy artificially aged at 573K
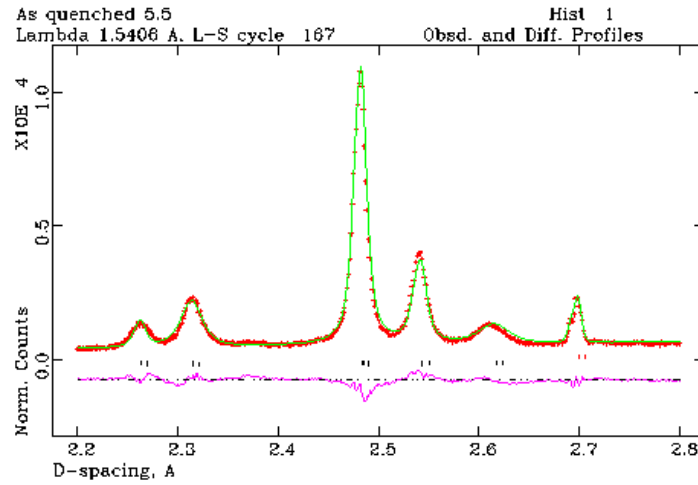for the times shown. Sharp peaks at 33°, 47°, 56° are from a ceria
standard.

Fig 2: X-ray diffraction data of an as-quenched U-5.5Nb alloy showing the monoclinic α" phase. Red are data points, green is refined Rietveld fit, black tick marks show positions of α" phase, and purple is the difference curve between the data and fit.

electrochemical polishing. Multiple metastable and equilibrium phases are possible in the range of 0 to 10 wt% niobium, making interpretation challenging. At the time of this writing, trends in crystallographic parameters that would indicate mechanisms involved are ambiguous. We will present and interpret observations of aging-induced changes (or lack thereof) in lattice parameters, unit cell volume, atomic positions in the crystal structure, and composition of phases.

The γ ↔ δ Transformation in Pure Pu: Thermal and Volumetric Characteristics and the Effect of Thermal Cycling

D. S. Schwartz[*], J. N. Mitchell[*], R. A. Pereyra[*]

[*]Los Alamos National Laboratory, Los Alamos NM 87545 USA

BACKGROUND

Plutonium is an excellent material for studying solid-state phase transformations because it goes through 6 allotropic phase transformations between room temperature and its 640°C melting point. We are using Differential Scanning Calorimetry (DSC), dilatometry, optical microscopy, and scanning electron microscopy to study solid-state transformations in pure Pu in detail. The γ ↔ δ (orthorhombic ↔ fcc) transformation is particularly interesting, and will be the focus of this paper. The γ ↔ δ transformation displays extreme asymmetry with respect to heating and cooling (Figure 1). On heating, the γ → δ transformation is a conventional solid-state transformation, characterized by a single well-defined heat absorption event initiating at ~323°C, spread over roughly
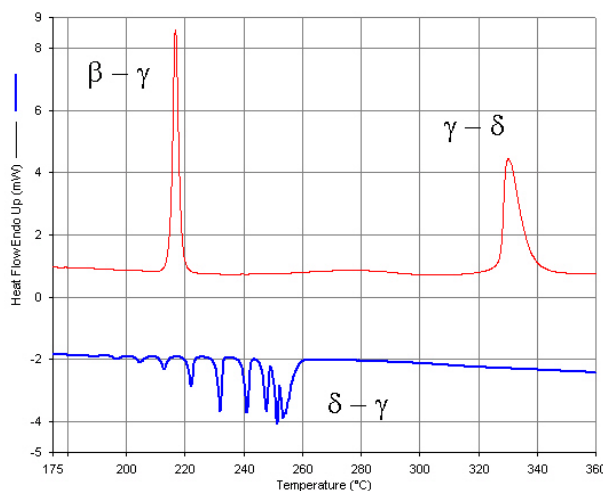

Figure. 1. DSC thermal scans comparing enthalpic absorptions on heating (red curve) to enthalpic releases on cooling (blue curve) for the γ ↔ δ transformation.

10°C at 10°C/min scanning rate. The δ → γ reversion on cooling has a completely different character. First, it initiates at 260°C, which is an unusually large supercooling of > 60°C below the onset temperature of the heating transformation. Secondly, the cooling transformation is characterized by a diminishing series of narrow heat release spikes, spread over an 80°C temperature range. This unusual transformation upon cooling was first reported several decades ago by Pascard[1], who suggested that the transformation was martensitic.

RESULTS

The effect of cooling rate was explored over the range 1°C/min to 50°C/min. The structure of the reversion was significantly dependent upon cooling rate in this range. The spacing and amplitude of the heat release spikes at the slower cooling rate was much more stochastic in character, while at the high rate the heat bursts were almost completely suppressed.

Dilatometry shows similar burst behavior to DSC. A significant difference is that the δ → γ reversion shows a clear onset at ~300°C in the form of a slope change in the ΔL/L vs.

temperature curve. This indicates that the δ-phase begins to transform, or at least contract discontinuously, without releasing heat, as no heat release is seen by DSC before reaching ~260°C. This pre-transformational phenomenon was explored by varying cooling rate and through the use of isothermal holds at different temperatures above the reversion onset.

If the heat release during cooling through the entire 260°C to 180°C temperature range is summed, it totals ~2.14 J/g, about 10% less than the heat absorbed during the γ → δ heating transformation. This suggests that some δ-phase may be retained below 180°C. To explore this further, a series of heat-cool cycles was performed through the γ ↔ δ transformation where the Pu was cooled to different temperatures, all above the β-phase field stability region. These controlled cycles will be described in detail, and their effect on phase retention and the character of the γ ↔ δ transformation will be discussed.

The heating-cooling asymmetry of γ ↔ δ transformation has some features in common with another martensitic transformation that occurs in Pu stabilized into the δ-phase with small amounts of Ga[2]. In this case, heat release bursts are seen when the martensitic phase (α′) formed by cooling to < -100°C reverts to the δ-phase upon heating. The δ → γ and α′ → δ transformations both involve significant volume changes for a phase nucleating within a δ-phase matrix. However, significant differences exist and a detailed comparison will be drawn between the two transformations.

1   R. Pascard, Plutonium 1960, eds. E. Grison, W. B. H. Lord, R. D. Fowler, Cleaver-Hume Press, London, pp. 16-25 (1960)
2   K.J.M. Blobaum, C.R. Krenn, J.N. Mitchell, J.J. Haslam, M.A. Wall, T.B. Massalski, A.J. Schwartz, Metall Mater Trans A [in press].

High-load anionic chromatography of An(IV) for recovery and purification of neptunium

T. Yamamura, T. Miyakoshi, Y. Shiokawa

Institute for Materials Research, Tohoku University, Sendai, Miyagi 980-8577, Japan

Actinide metals with very high purity are essential for the reliable studies of the physical nature of actinide compounds, especially of the physical properties such as the Kondo effect where the infinitesimal quantity of magnetic elements plays an important role. For the neptunium compounds the purity of the prepared compounds is governed by the purity of the metal because the metal is required to be produced from the supplied neptunium oxide whose purity is as low as 99.9%. Moreover, the reuse and the recovery of the neptunium element from the used compounds are strongly desired because the neptunium is the precious man-maid element. The purification system for preparing the gram-amount neptunium with high-purity should be simple and easy to be handled in laboratories. Recently new method of preparing the gram-amount actinide metals has been developed by our research group [1, 2]. This method, which only requires an aqueous acidic solution of metal ion as the starting material, is especially suitable to prepare the highly radioactive neptunium metal at the high purity. The most suitable method for the extensive purification prior to this metal preparation is the anion exchange chromatography because the formation of the stable anionic complex with nitrate ion $An(NO_3)_6^{2-}$ is characteristic to the actinide (An) chemistry.

Though purification condition for actinide(IV) at its tracer scale is already established, that at gram-amount scale generally becomes difficult due to decrease in distribution coefficient. In purification systems, both of load amount and purity should be satisfied by quantitative investigation of column condition. Anion exchange chromatography of thorium(IV) nitrate anion was examined quantitatively with a small column formerly [3]. When the amount of thorium loaded to the column is increased, the elution curve changed from Gaussian function type curve to tailing. Simultaneously, peak position moved forward and distribution coefficient decreased substantially. Optimization of these column condition based on an experiment, however, is prohibitedly difficult due to large amount (150-200 times of column volume) of radioactive effluent, as well as its long period and large costs. Therefore,
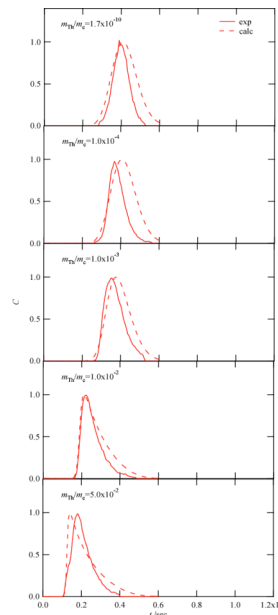

Fig 1: Comparison of elusion curve of thorium(IV) in 6M HNO3 at variety of load amount obtained in experiments (solid curves) and calculation (dashed curves).

estimation of elution curve of anion exchange chromatography should be desirable in an aid of using numerical calculation.

Though the estimation of elution curve by numerical calculation had been used in purification of gram quantity of organic compounds such as medicinal compounds [4], there is little use in purification of an inorganic compounds. Guiochon reported investigation of elution curve in highly-loaded state by numerical calculation based on adsorption isotherm [5, 6].

In this research, elution curves of actinide(IV) obtained in experiments were compared with those calculated. Excellent agreement was attained in the case of thorium(IV) (Fig. 1) and uranium(IV) with an inclusion of rate equation of Langmuir type as non-linear kinetics equation, which is contrary to model by Guiochon. Based on the above-mentioned result, elution curve for neptunium(IV) was obtained on basis of $k=10^3$ according to literatures. That estimation of the purification condition which says purity/recovery because calculation of elution curve in such a high load became possible is enabled can be expected.
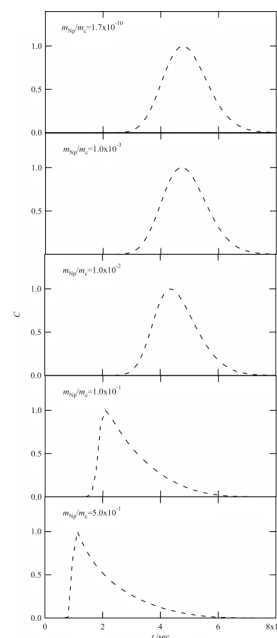

Fig 2: Calculated elusion curves for neptunium(IV) in 6M HNO_3 at variety of load amount.

[1]   Y. Shiokawa, K. Hasegawa, K. Konashi, M. Takahashi, K. Suzuki, J. Alloys Compd., 255 (1997) 98.
[2]   Y. Shiokawa, K. Hasegawa, Isotope News, 525 (1998) 6.
[3]   T. Yamamura, Y. Shiokawa, T. Mitsugashira, Research Report of Laboratory of Nuclear Science, Tohoku Univ., 32 (1999) 31.
[4]   Y.-L. Li, N.G. Pinto, J. Chromatogr. A, 702 (1995) 113.
[5]   G. Guiochon, S. Golshan-Shirazi, A. Jaulmes, Anal. Chem., 60 (1988) 1856.
[6]   L.R. Snyder, J.W. Dolan, G.B. Cox, J. Chromatogr., 483 (1989) 63.

THE SELF-CONSISTENT ONE ASSOCIATION MODEL FOR STRATIFYING MELTS OF THE BINARY SYSTEMS WITH STRONG CHEMICAL INTERACTION BETWEEN ATOMS OF COMPONENTS

A.L.Udovsky

Baikov Institute of Metallurgy and Material Science of Russian academy of sciences, Moscow, Russian Federation

The row of the binary systems, for example, the U-O, Pu-O, Fe-O, Cr-O, Fe-S, Cr-S and others systems have a phase diagrams, containing both chemicals compounds, and miscibility gap of melts. On the one hand presence of the chemical compounds in these systems are indicative of presence in these systems strong attracting inter-atomic interactions, bring about formation of these compounds. On the other hand presence of the miscibility gap is indicative of that that free energy mixing of melts as function of composition within some temperature range have local concavity, which is be situated between family of points of inflexion (or spinodal curve). At first thought simultaneous presence these fragment (chemical compound and miscibility gap) on phase diagram brings about contradiction.

In purpose of the permission this logical contradiction in persisting work is designed the self-consistent one association model (SCAM) for description of thermodynamic, as well as structured properties (distribution of atoms different kinds between single, as well as associated states) properties of melts in binary system with strong chemical interaction [1].

In work is received and analyzed the equation of the state for calculation of local stable mole fractions of associates for melts depending on composition and temperature. In work is shown that often used the law acting masses, being quotient event of the equation of state, does not allow to describe the thermodynamic characteristic stratifying melts for systems, containing chemical compounds as well as miscibility gap. While the SCAM allows modeling miscibility gap of melts for binary systems with strong inter- atomic interactions. Within the framework of the SCAM is built the algorithm of the calculation of miscibility gap for melts, here under appears the possibility of the description within the framework of one model thermodynamic, as well as structural properties of melts for system with strong chemical interaction between atoms of components.

The SCAM has applied to modeling the thermodynamic properties and miscibility gap of melts for the U-O system [2]. The optimized values of model's parameters were obtained by solution of the inverse problem. As input data have been used experimental data [3],which have obtained for two ends of tie-line at 3090 K. The two critical points of miscibility gap were calculated. Between these critical points the miscibility gap is located. The top critical point agreement with experimental phase diagram of the U-O system. The lower critical point is situated in meta-stable part under thermodynamic stable (the uranium-base liquid + solid state UO_{1-x}) – tie-lines of phase diagram of the U-O system.

Good agreement have been obtained between calculated two-phase tie-lines and experimental data for stratifying melts of the U-O system under 2700 and 3100 K measured by different researchers is received.

This approach allows to consider the interaction between of various kinds of atoms, which can form by dynamic reaction of the associations (or the reaction of dissociation) localized group of atoms (associate) either different chemical components, or atoms of one component differing some internal parameter (the varied valences or others properties).

1   A.L.Udovsky, Doklady of RAS, in press (2006)
2   A.L.Udovsky, M.V.Kupavtsev, H.A.J.Oonk The application of self-consistent on one association model for calculation miscibility gap of melts for uranium-oxygen system. Abstracts and Program. CALPHAD XXXIV Conference, May ,2005, Maahstriht, The Netherlands.
3   C. Gueneau, V.Dauvouis, P.Perodeaud, C.Gonella, O.Dugne. J. Nucl. Mater. 254 (1998) 158-174.

Phase-field Modeling of Coring Structure Evolution and Ga Homogenization Kinetics in Pu-Ga Alloys

S. Y. Hu* , M. Baskes and M. Stan
MST-8, Los Alamos National Laboratory, Los Alamos, NM 78545

During the casting of Pu-Ga alloys, the huge difference of Ga diffusivity in ε and δ phases results in the formation of coring structures which consistent of Ga-rich cores with Ga poor edges. On the other hand, the elastic interaction among different oriented δ grains and diffusive Ga might lead to an inhomogeneous diffusion and δ grain growth. In this work, phase-field approach has been used for modeling the coring structure evolution and Ga homogenization kinetics in three dimensions. We assume that the transition from ε (bcc) to δ (fcc) follows the Bain distortion. The chemical free energy is constructed according to the phase diagram. The effect of diffusivity inhomogeneity, internal stresses, anisotropy of interfacial energy and cooling rate on the coring structure evolution is systematically studied. Fig.1 presents the coring structures obtained with and without the effect of internal stresses on the coring structure evolution in two dimensions. The color denotes Ga composition, Red means higher Ga composition while Blue lower Ga composition. The letters "A" and "B" denote two different oriented δ grains. The results demonstrate that the internal stresses speed up the growth in the a-direction, but slow down the growth in the c- direction to minimize the elastic energy, leading to the elongation of the grains as seen in experiments.
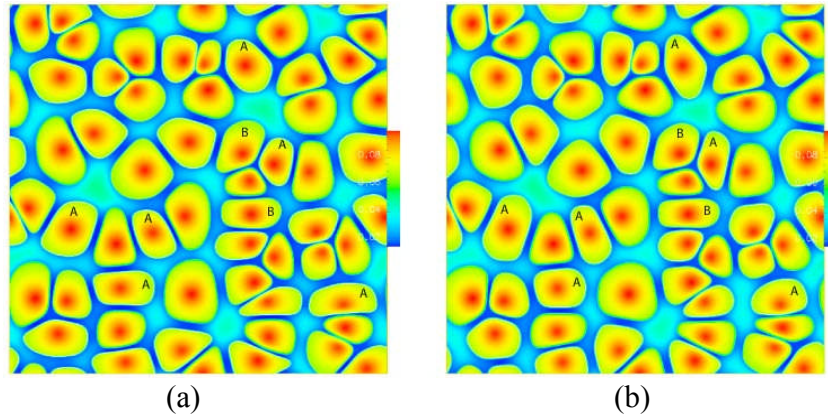

(a)   (b)

Fig 1: Effect of internal stresses on multi-particle growth in 2D, (a) without internal stresses and (b) with internal stresses

Tantalum Corrosion with Pu-Ti alloys

T. Paget, R. Watson, S. Slade

AWE plc. Aldermaston, Reading,RG7 4PR, UK

INTRODUCTION

Reported here are recent observations during the processing of plutonium-titanium alloys. Six runs were conducted, where plutonium metal was treated with ~10 wt% $MgCl_2$ in $CaCl_2$. The metal was introduced into a magnesia crucible and the salt mixture poured on top. The crucible was heated to around 850ºC under an argon atmosphere and stirred for 3.5 hours. The stirrer was removed while the salt and plutonium were still molten and the furnace allowed to cool. The product metal was recovered by breaking away the ceramic crucible and salt.

The flat paddle stirrers were fabricated from tantalum (99.9% pure, ASTM B708-86 GRAIN 5-7). Two stirrers of the same design were studied, both had been used previously to process plutonium of a similar purity, but without added titanium. Stirrer 1 was used on eight previous occasions, Stirrer 2 was used on twenty previous occasions, no signs of corrosion were observed at the end of any of these runs.

Run1/1 was carried out at half batch size using Stirrer 1. Figure 1 shows the stirrer following processing. The corrosion is in the form of pitting and occurred on one face only, close to the salt-metal interface. The lighter grey portion indicates the depth to which the stirrer extended into the molten plutonium during processing. Chemical analysis shows the metal contains between 0.1-0.3 wt% Ta and 0.6 wt% Ti.
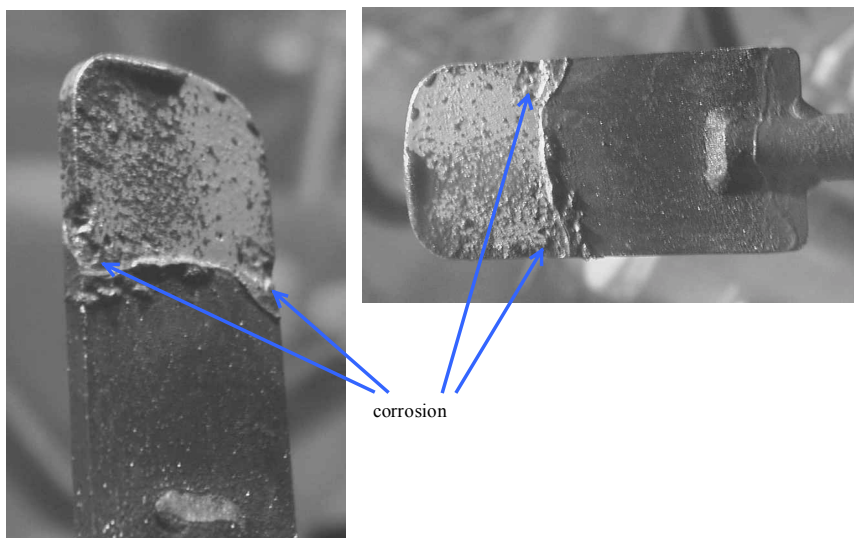

corrosion

Figure 1. Stirrer 1 following Run 1/1

Run 2/1 used similar feed to Run1/1 at the same batch size. There was no sign of corrosion of the stirrer at the end of the run. The product had a similar appearance to the product of Run

1/1 with an apparent surface layer. Chemical analysis shows the Ti content was between 0.3 and 0.4 wt% and the Ta content was around 100-300 ppm.

Stirrer 2 was re-used in Run 2/2 which processed metal that did not contain Ti. A full batch was treated in this run, the salt-metal interface being close to the top of the stirrer blade during processing. Corrosion of the stirrer, similar to that in Run1/1, was observed approximately halfway up the blade. The location of the corrosion is consistent with the depth of the metal during the previous run, Run 2/1.
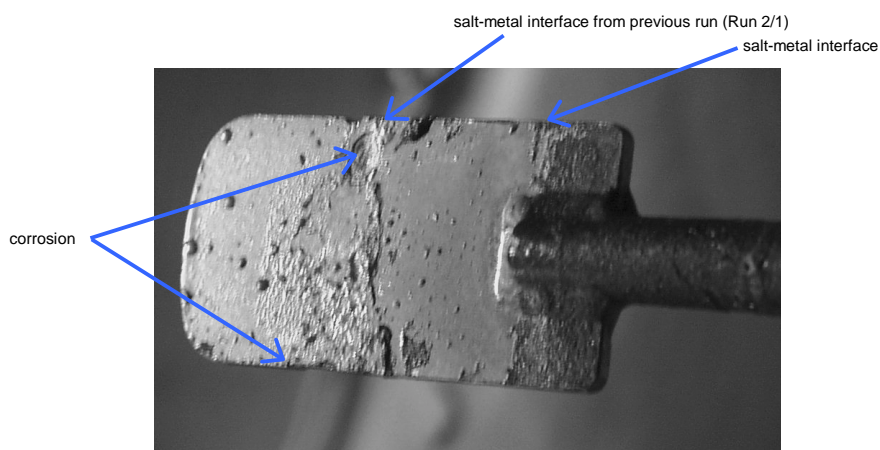

Figure 2. Stirrer 2 following Run 2/2

The Stirrer 2 was subsequently used in Run 2/3 and Run 2/4 without further corrosion. Run 2/5 processed a full size batch of Pu-Ti alloy and used Stirrer 2. Noticeable corrosion of the stirrer blade occurred at a location consistent with the upper surface of the molten metal during processing (Figure 4). No further corrosion was observed at the earlier sites from Run 2/2. Chemical analysis show the product contains between 0.3 and 0.6 wt% Ti and between 0.02 and 0.2 wt% Ta.

Unusual Appearance of Plutonium Metal in Electrorefining Product

R Campbell-Kelly, R Watson

AWE plc, Aldermaston, Reading, RG7 4PR, UK

INTRODUCTION

The electrorefining process is used to produce high purity plutonium metal. The product usually forms a well coalesced uniform ring in the outer annulus of the ceramic process crucible. In a small number of cases the process has operated with reduced current efficiency at the anode and cathode and a lower process yield. In two instances the process electrolyte, $CaCl_2$, has been significantly depleted in plutonium. In these runs the product metal is not uniform but exhibits an area with a most unusual structure. The majority of the product is well formed, but there is a ~ 90° sector of the annulus which appears to comprise two vertical layers of plutonium. An example is shown in Figure 1. The cathode was withdrawn from the crucible while the contents were at 850°C and the crucible held at this temperature for 1 hour before cooling started. The vertical face of the metal bears the impression of the rivets used in the construction of the cathode. This area corresponds to a gap in the cathode and reduction of Pu(III) may be taking place on both surfaces.
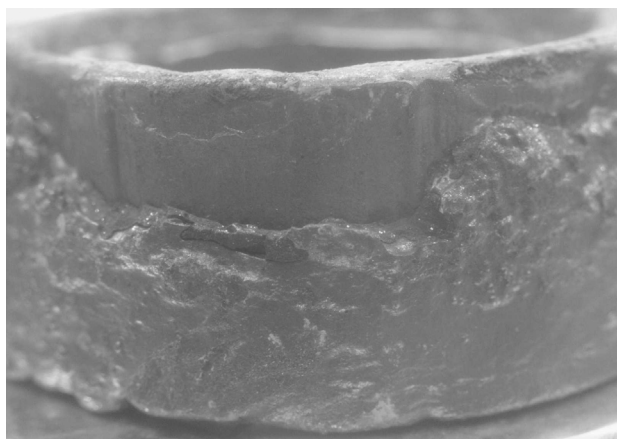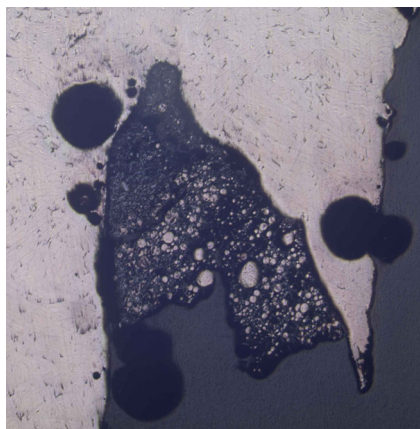

Figure 1. Unusual electrorefining product

Figure 2. Metallographic image of recast material

As the salt was depleted in plutonium it was thought possible that reduction of the $CaCl_2$ salt may have taken place to generate calcium. Examination of the applied potential in these runs does not show an increase to potentials where calcium could form. Chemical analysis is inconclusive in showing if calcium metal is formed. Metallography of recast material shows the bulk metal is alpha phase, but there are also metal spheres suspended in a salt matrix. The large globules have a two phase structure which may indicate the presence of calcium, Figure 2.

Possible explanations for this unusual behaviour are either a high viscosity of liquid plutonium or surface effects. A number of studies have shown that additions of up to 5 at% impurities such as iron, gallium and cerium can result in increases in the viscosity of the metal of more than 25%. Chemical analysis does not show any impurities at levels which could explain a significant increase in the viscosity of the metal. There is very limited data on the surface tension of plutonium and none examining the effect of impurities.

In a number of cases the metal has been drip cast to produce a well formed, uniform, product. About 5% of the metal is retained as a casting skull. Analysis of this material shows high levels of gallium and probably $CaCl_2$ salt to be present.

The cause of the unusual formation of plutonium metal in electrorefining is not fully understood. Detected impurities are not present at high enough concentrations to significantly affect the viscosity of the metal. The influence of solid phases on the surface properties of the metal may be an important factor.

On the fcc → monoclinic Martensitic Transformation in a Pu-1.7 at. % Ga Alloy

T. E. Mitchell[*], J. P. Hirth[*], J. N. Mitchell[†], D. S. Schwartz[†]

Los Alamos National Laboratory, Los Alamos NM 87545 USA
[*]Structure-Property Relations Group, MST-8, Mail Stop G755
[†]Nuclear Materials Science Group, NMT-16, Mail Stop

The face-centered cubic $\delta \rightarrow$ monoclinic α' martensite transformation in a Pu-1.7 at. % Ga alloy is analyzed in terms of the defect-based topological model[1]. The crystallography of the $\delta \rightarrow \alpha'$ transformation, and of twinning, is greatly facilitated by the replacement of the monoclinic phase by a hcp pseudostructure. Both have ABAB stacking and, in spite of the distorted arrangement of atoms in the (010) plane of the monoclinic structure, this structure can be mapped into the hcp structure without changing atom neighbors. After analyzing transformations from δ to the hcp pseudostructure, and the formation of twins therein, the pseudostructure can be transformed to α' by means of shuffles and one shear of 3.2^o. There is also a large volume change of ~20%. Another important feature is the near parallelism of the $\{111\}_\delta$ and $(010)_\alpha$ planes as well as of the $<\bar{1}10>_\delta$ and $[100]_\alpha$ directions. Because of the large strains involved in the transformation, there are significant differences between the predictions of the topological model and the standard phenomenological theory of martensitic transformations.

In the topological model, the Burgers vectors of the disconnections along the terrace planes for the transformation are deduced from the transformation strains. The habit plane is determined from the height and spacing of the disconnections. The predicted habit plane is in good agreement with experimental results. Observed twinning is associated directly with the transformation strain. The lattice invariant deformation due to strain parallel to the disconnection line direction is connected with slip in the α' plates. Implications for hysteresis in the transformation as observed by dilatometry and calorimetry are discussed.

1. J. P. Hirth, J. N. Mitchell, D. S. Schwartz and T. E. Mitchell, Acta Materialia, in press.

NMR Studies of Neptunium and Plutonium Compounds

Y.Tokunaga, S.Kambe, H.Sakai, T.Fujimoto, R.E.Walstedt and H.Yasuoka

ASRC, Japan Atomic Energy Agency, Tokai, Naka, Ibaraki, 319-1195 Japan

Octupole Ordering in NpO$_2$

  Multipolar degrees of freedom in the f-electron shell bring rich and complex physics to rare-earth and actinide compounds. Recently, it has been suggested that the phase transition in NpO$_2$ can be understood as the spontaneous ordering of octupolar degrees of freedom [1]. Soon after, resonant X-ray scattering (RXS) measurements gave evidence for the appearance of a longitudinal triple-q antiferro-quadrupolar (AFQ) structure in the ordered state [2]. This AFQ structure, however, has been regarded as a secondary order parameter driven by a primary longitudinal triple-q antiferro-octupolar (AFO) order, since the AFQ order alone cannot successfully explain the breaking of time reversal invariance suggested by susceptibility [3] and µSR [4] measurements. The longitudinal triple-q AFO ordered ground state has also been corroborated by recent microscopic calculations [5].

  In order to elucidate the nature of the exotic ordered phase of NpO$_2$, we have initiated the first NMR measurements on this system [6]. Figure 1 shows the anglar dependence of the NMR spectrum obtained recently in a single crystal, where θ is the tilting field angle from [110] to [001] through the [111] direction for the cubic crystal axes. From this field-angle dependence, the occurrence of a hyperfine interaction which stems from a field-induced AFO moment has been confirmed. This field-induced AFO moment appears as a result of the longitudinal triple-q AFQ structure in the ordered state. We have also observed characteristic spin echo modulation behavior caused by quadrupole splittings created by the AFQ ordering. This reveals that the AFQ structure is directly observable with NMR.

  In general, multipole order is hard to investigate by conventional means. Although there are several indirect methods, recent identification of multipole order parameters can be credited mostly to RXS, which can directly probe the anisotropy of the f-electron shell. In the present work, we show that direct observation of multipole order parameters is also possible by means of NMR. Our NMR results provide further insight into the microscopic nature of
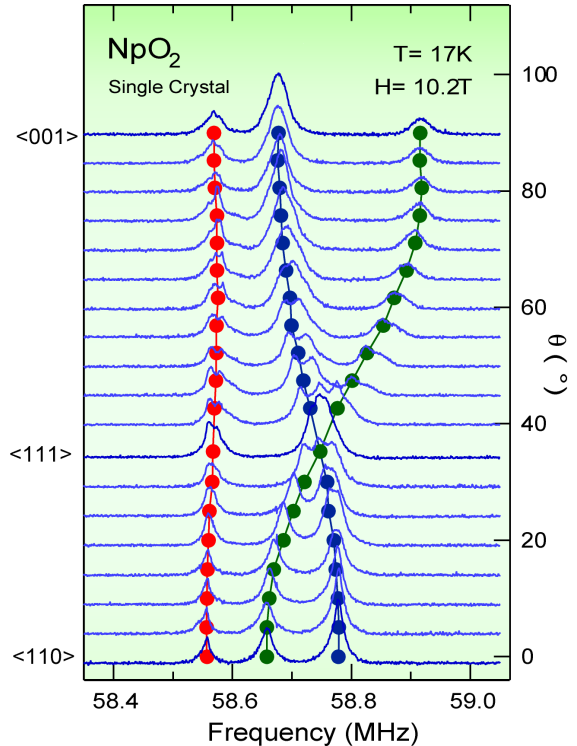

Figure 1: The field-angle dependence of the NMR spectrum at T= 17 K.

multipole phase transitions in f-electron systems.

Unconventional Superconductivity in PuRhGa$_5$

In 2002, the Los Alamos group reported that PuCoGa$_5$ exhibited superconductivity with a transition temperature T$_c$ =18K [7]. A few months after that discovery, the ITU group at Karlsruhe reported that its sister compound PuRhGa$_5$ also exhibits superconductivity below 9K [8]. The relatively high T$_c$ values of these PuTGa$_5$ compounds has stimulated interest in the mechanism of their superconductivity. It has been suggested that the superconducting (SC) state may be unconventional, similar to other classes of strongly correlated electron systems.

To investigate the SC pairing symmetry, we have performed $^{69;71}$Ga NMR/NQR studies on a single crystal of PuRhGa$_5$ [9]. We have observed a ^{69}Ga NQR line at 29.15 MHz, and have assigned it to the 4i Ga site (Ga(2) site) using NMR data. The spin-lattice relaxation rate 1/T$_1$ shows no coherence peak just below T$_c$ and obeys T^3 behavior below T$_c$, as seen in Fig. 2. This result strongly suggests that PuRhGa$_5$ is an unconventional superconductor having an anisotropic SC gap. We have obtained the gap amplitude 2Δ(0) =5k$_B$T$_c$ and found the residual density of states to be N$_{res}$(0)/N$_{res}$(T$_c$) ≅0.25, assuming a simple polar function. For PuCoGa$_5$, Curro, *et al.,* have obtained 2Δ(0) =8k$_B$T$_c$ [10].

Recently, we have also measured the Knight shift at the Ga(2) site. The Knight shift has been confirmed to decrease below T$_c$. This gives strong evidence for spin singlet SC pairing in PuRhGa$_5$. Together with the NQR results for 1/T$_1$, it is entirely plausible that the d-wave SC pairing is realized in PuRhGa$_5$.
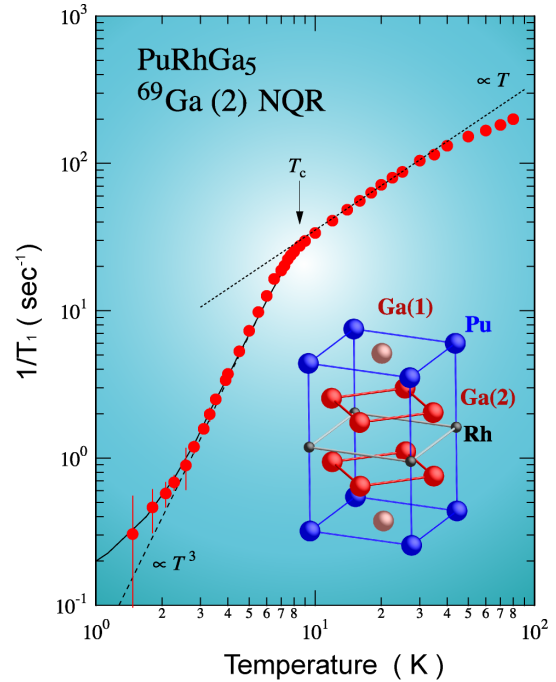

Figure 2: Temperature dependence of 1/T$_1$ in PuRhGa$_5$.

1   P. Santini and G. Amoretti, Phys. Rev. Lett. **85**, 2188 (2000).
2   J. A. Paixão *et al.*, Phys. Rev. Lett. **89**, 187202 (2002).
3   P. Erdös *et al.*, Physica B **102**, 164 (1980).
4   W. Kopmann *et al.*, J. Alloys Compd. **271**, 463 (1998).
5   K. Kubo and T. Hotta, Phys. Rev. B **71**, 140404(R) (2005).
6   Y. Tokunaga *et al.*, Phys. Rev. Lett. **94**, 137209 (2005).
7   L. J. Sarrao *et al.*, Nature **420**, 297 (2002).
8   F. Wastin *et al.*, J. Phys.:Condens. Matter. **15**, S2279 (2003).
9   H.Sakai *et al*, J.Phys.Soc. Jpn. **74**, 1710 (2005).
10   N. J. Curro et al., Nature **434**, 622 (2005).

GGA and LDA+U calcalutions of Pu phases and Pu-Ga system

J. Bouchet[*], R.C. Albers[†], G. Jomard[*]

[*]CEA-DAM, DPTA, Bruyères-le-Châtel, 92690 France

[†]Theoretical Division, Los Alamos National Laboratory, Los Alamos NM 87545, USA

INTRODUCTION

It is well known that the unique position of Pu in the periodic table is responsible for its unusual physical properties. Before its melting point Pu passes through six different phases, where the low temperatures distorted structures, α or β (monoclinic with 16 and 34 atoms/cell respectively) contrast with the high-temperature simple structures δ (fcc) or ε (bcc). This crystallographic sequence is surprisingly very close to the crystallographic sequence of the actinide series with open structures for the light actinides (Ac-Np) and close-packed structures for the heavy actinides. This transition, directly related to the delocalized (light actinides) and the localized (heavy actinides) behaviour of the f electrons, places Pu in the middle of a discontinuity and indicates that the delicate balance between itinerant and localized states must be responsible for its anomalous properties and for its structural diversity.

Söderlind[1] used density functional theory (DFT) and the generalized gradient approximation (GGA) to study the α phase. They found a good agreement with experiment, confirming α as the most favourable structure for Pu, and explained the presence of this structure by a narrow $5f$ bands with approximatively 5 electrons. On the other hand, in despite of the simplicity of the δ phase, DFT with GGA completely failed to describe this structure. Recently a new understanding has emerged, with the assumption of δ-Pu as a strongly correlated system, that requires going beyond GGA in order to take into account the Coulomb interaction between the f electrons. The LDA+U approach[2,3] reproduces the experimental equilibrium volume and the stability of the fcc structure for plutonium. Söderlind[4] included an energy shift of the $5f$ orbital via the Racah parameter to reproduce the volume of the six phases of Pu. But the problem of all these approaches is that they predict a long-range magnetic order for δ-Pu, not observed experimentally, despite a compensation between the orbital and the spin magnetic moments. Recently Savrasov[5] combined dynamical mean field theory (DMFT) with density functional methods to obtain the total energy of a correlated system. They showed the possibility of a double well for the total energy of δ-Pu as a function of volume, with one minimum assigned to the α phase and the other one, at high volume, assigned to the δ phase. But a major problem with DMFT is the complexity of the calculation and the computational time, which makes it very difficult to treat structures with more than one atom per primitive cell, such as the α, β and γ phases of Pu.

RESULTS AND DISCUSSION

We have recently proposed a pseudo-structure to model α plutonium[6], which is an orthorhombic structure with two atoms per unit cell. We found a surprisingly simple path between α and γ phases. Here we have used this pseudo-structure to study the complete phase diagram of Pu and supercells of Pu with Ga, using the GGA, and LDA+U approximations. We use the simplicity of the pseudo phase to understand the main differences between low and high temperatures phases of Pu. We have compared the total energies of the α, pseudo-α, γ, δ, ε phases, using different functionals and magnetic order. The total energies of pseudo-α and α phase are very similar for a long range of volumes and are much lower than for the other phases. This gives us confidence to use the pseudo structure instead of the real α in more computationally intensive techniques. The volumes of the different structures are well reproduced, compared to the experiments, as found in Ref.[4]. To see the effects of the correlations, we have performed calculations with LDA+U, allowing U to vary between 0 and 4 eV. As U increases, the γ, δ, ε phases rapidly develop a magnetic and high-volume solution, whereas the pseudo-α stays non-magnetic and at low volume. These two kinds of behavior are interpreted in terms of the interatomic distances of the different phases, and we show that the short bonds in the pseudo phase suppress correlations effects. Moreover, since the pseudo-α and the γ structures are orthorhombic but with different b/a and c/a ratios, we can easily simulate a transition path between low and high volume structures and follow the effects of the correlations. This would be, of course, impossible

without the pseudo phase. We show a threshold in the nearest-neighbor distance, independent of structure, which controls the occurrence of magnetism and the high volume solution. Finally, we have included a Ga atom in supercells of Pu. This allows us to study the influence of an alloying element of the surrounding Pu atoms, and to see its effect on the phase stability. We show that Ga stabilizes the high volume structures as found experimentally.

1   P. Söderlind, J. Wills, B. Johansson and O. Eriksson, Phys Rev B **55**, (1997)
2   J. Bouchet, B. Siberchicot, F. Jollet and A. Pasturel, J Phys : Condens Matter, **12**, (2000)
3   S. Y. Savrasov and G. Kotliar, Phys Rev Lett, **84**, (2000).
4   P. Söderlind, and B. Sadigh, Phys Rev Lett **92**, (2004).
5   S. Y. Savrasov, G. Kotliar and E. Abrahams, Nature, **410**, (2001).
6   P. Söderlind, and B. Sadigh, Phys Rev Lett **92**, (2004).

Hysteresis of the δ ↔ α´ Transformation in Pu-Ga alloys

J.N. Mitchell, D.S. Schwartz, and T.E. Mitchell

Los Alamos National Laboratory, Los Alamos NM 87545 USA

BACKGROUND

Face-centered cubic δ-phase plutonium stabilized with <2 at. % Ga will undergo a transformation to monoclinic α´ Pu at temperatures of ~-100 C or less. This transformation is martensitic, meaning that it appears to be diffusionless and that there is a shear-induced change in the shape of the unit cell. A variety of factors can affect the onset of the δ → α´ transformation, including the concentration and distribution of the stabilizing solute, grain size, cooling rate, and possibly age. This transformation has several unusual characteristics, including its incompleteness, a >20% volume contraction, and a 150-200 °C reversion hysteresis. A second type of hysteresis is also found where thermal cycling displaces the transformation to lower temperatures and decreases the amount of transformation. In this presentation, we will explore in detail these two types of hysteresis.

EXPERIMENTS

All experiments were performed on well homogenized δ-phase Pu alloys stabilized with 1.7 to 2 at. % Ga. Measurements were made using a Netzsch 402C dilatometer with cooling and heating rates of 1-10 C/min and in a ultra-high purity He gas environment. Two types of experiments were performed: (1) single-cycle cooling to induce the transformation followed by heating to induce the reversion and (2) multiple-cycle cooling and heating to observe the effect of these cycles on the transformation behavior. Typical minimum temperatures were -165 °C; maximum temperatures ranged from 200-375 °C. In one experiment, the sample was held at room temperature following the high temperature phase for 2-5 hours before beginning the next cryogenic cycle.

RESULTS

A typical single-cycle hysteresis loop is shown in Figure 1. In this experiment, the sample was heated to 200 °C prior to cooling and holding at -155 °C. Several interesting features are present in this hysteresis loop, including the very sharp transformation onset and distinctive steps during the reversion. The latter feature is best represented in the dL/dt curve, where they appear as bursts [1, 2].

In the experiment shown in Figure 2, the sample was cycled three times between RT, -155 °C, and 200 °C. After the first 200 °C segment (second cycle), the sample was held at RT for 2 hours prior to cooling to -155 °C. After the second 200 °C segment (third cycle), the sample was held at RT for 5 hours before cooling to -155 °C. This experiment shows that although cycling reduces the amount of transformation, a RT rest stage will inhibit further hysteresis of the transformation.

We have also studied the effects of the maximum temperature on thermal cycling hysteresis. In Figure 3, the sample was cycled twice through the transformation up to 200 °C and once up to
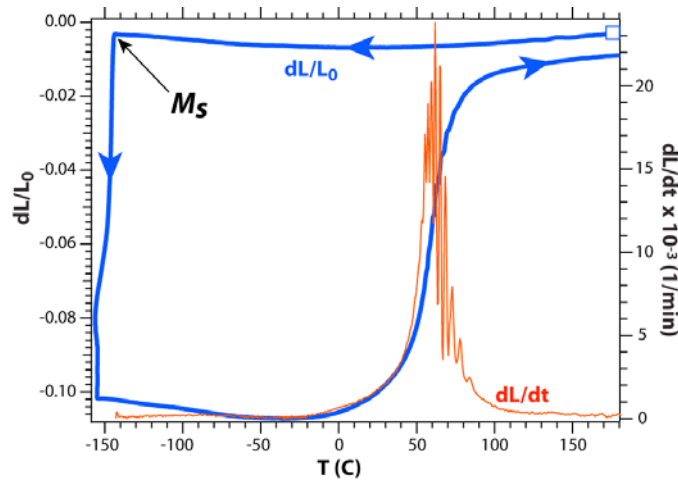
Fig. 1: Hysteresis loop of the δ ↔ α′ transformation.

375 °C. The curves show that the transformation was displaced to lower T and resulted in less alpha prime, but that the 375 °C anneal produced more alpha prime during the subsequent cryogenic stage.

These experiments show that there are several factors that can influence the transformation behavior during thermal cycling. Resting at RT for as little as two hours limits and heating to temperatures well above the reversion temperature range limits hysteresis. We will discuss in detail the role that microstructure plays in these phenomena.
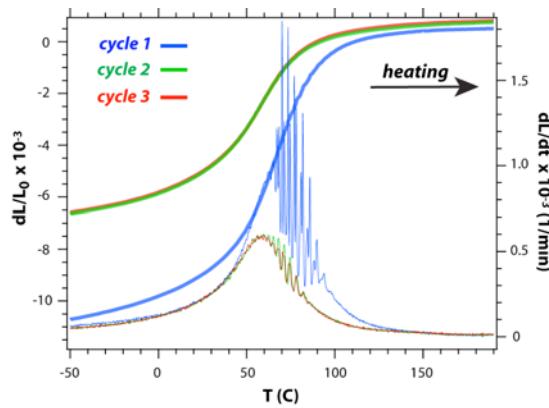

Fig. 2: Detail of the α′ → δ reversion during separate heating phases of a three-stage thermal cycle. Cycle 2 and 3 include 2 and 5 hour rests, respectively, at RT before cooling. The thin lines are the dL/dt curves.
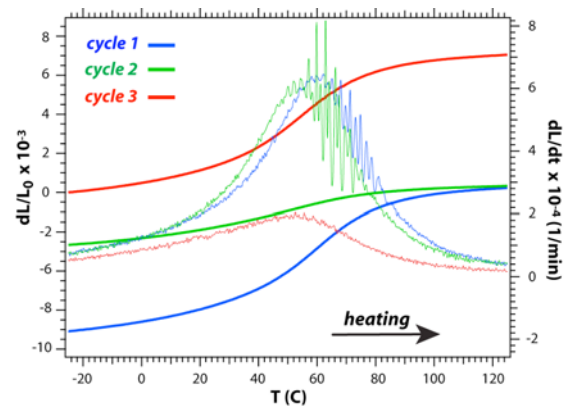

Fig. 3: Detail of the α′ → δ reversion during separate heating phases of a three-stage thermal cycle. Cycle 2 finished with a 375 °C anneal, allowing more transformation in Cycle 3. The thin lines are the dL/dt curves.

1   J. N, Mitchell *et al.*, Metall. Mater. Trans. 35A, 2267 (2004).
2.   K.J. Blobaum *et al.,* Metall. Mater. Trans. 37A, 567 (2006).